ADDITIONAL MATERIALS AVAILABLE ON THE HEI WEBSITE

Research Report 202

Enhancing Models and Measurements of Traffic-Related Air Pollutants for Health Studies Using Dispersion Modeling and Bayesian Data Fusion

Batterman et al.

Additional Materials. Supplementary Information.

These Additional Materials were not formatted or edited by HEI. This document was part of the HEI Review Committee's review process.

Correspondence may be addressed to Dr. Stuart Batterman, 109 Observatory St., Ann Arbor, MI 48109-2029; e-mail: *stuartb@umich.edu*.

Although this document was produced with partial funding by the United States Environmental Protection Agency under Assistance Award CR–83467701 to the Health Effects Institute, it has not been subjected to the Agency's peer and administrative review and therefore may not necessarily reflect the views of the Agency, and no official endorsement by it should be inferred. The contents of this document also have not been reviewed by private party institutions, including those that support the Health Effects Institute; therefore, it may not reflect the views or policies of these parties, and no endorsement by them should be inferred.

RESEARCH REPORT APPENDICES

Enhancing Models and Measurements of Traffic-Related Air Pollutants for Health Studies Using Dispersion Modeling and Bayesian Data Fusion

Stuart Batterman, Veronica Berrocal, Chad Milando, Owais Gilani, Saravanan Arunachalam, K. Max Zhang

Table of Contents

Tables and Figures

APPENDIX 1 - CHARACTERISTICS OF TRAFFIC-RELATED AIR POLLUTION

COMPOSITION

Traffic-related air pollution (TRAP) is a complex and dynamic mixture. It includes engine exhaust emissions, which consists of particulate matter ($PM_{2.5}$), carbon monoxide (CO), nitrogen dioxide (NO_2), VOCs, e.g., benzene and formaldehyde, carbonaceous compounds (e.g., polycyclic aromatic hydrocarbons (PAHs) and elemental carbon), metals (e.g., copper and zinc), sulfate, and other components. The composition and quantity of exhaust emissions depend upon the engine (e.g., type, age, and maintenance), emission control systems, fuel sulfur content and other fuel properties, engine power, load, temperature, and other factors. These "primary" tailpipe exhaust emissions can undergo physical and chemical changes in the atmosphere to form "secondary" pollutants, three important examples of which are the oxidation of NO emissions to NO_2 (Wang et al. 2011), the evolution of nanoparticle emissions by nucleation, coagulation, deposition and condensation processes into larger particles (Canagaratna et al. 2010; Kumar et al. 2011; Myung and Park 2011), and the reaction of gas-phase organic compounds into secondary organic aerosol (SOA) (Gentner et al. 2017). Thus, "fresh" TRAP differs from "aged" TRAP. TRAPs also includes emissions from the wear of tire, brake and pavement materials, and the resuspension of materials deposited or placed on the road, e.g., silt and salt (Grigoratos and Martini 2015; Pant and Harrison 2013; Thorpe and Harrison 2008).

Concentrations of TRAPs vary spatially and temporally. These variations are important because they provide the *exposure contrasts* needed to elucidate health effects in epidemiological studies. Unfortunately, this variation makes the estimation of exposures challenging.

TEMPORAL VARIABILITY

Surprisingly few analyses apportion the sources of temporal variability of TRAPs. Traffic volume may dominate the temporal variation of some TRAPs, e.g., particle number concentration (PNC), CO, NO_x and black carbon; regional sources and meteorological factors may dominate other pollutants, e.g., $PM_{2.5}$ (Kendrick et al. 2015; Padró-Martínez et al. 2012; Patel et al. 2009; Yu et al. 2016; Zhang and Batterman 2010). Interestingly, hourly, daily and seasonal variability may have comparable magnitude as spatial variability, e.g., as demonstrated for PNC measured near an urban arterial in Somerville, MA (Kendrick et al. 2015).

SPATIAL VARATION

Spatial patterns of ambient pollutant concentrations at the urban scale may vary from nearly homogeneous to quite heterogeneous; small-scale (or intra-urban) variation may be large for CO, NO, NO_2, elemental carbon, and black carbon (Özkaynak et al. 2013; Sarnat et al. 2010; Turner and Allen 2008), but typically small for pollutants such as O_3 and $PM_{2.5}$. Strong small scale variation implies that central monitoring sites may not accurately characterize spatial patterns (Wilson et al. 2005) due to "small-area" variation in concentrations (Jerrett et al. 2007) resulting in exposure measurement error. For analysis and exposure purposes, the spatial variation may be characterized into compartments or zones, specifically "tailpipe-to-road", "on-road," "near-field" and "far-field" categories (S. Batterman et al. 2014b). The tailpipe-to-road compartment represents the zone of elevated concentrations where chemical conversion may be rapid, e.g., NO $\rightarrow$ NO_2. On-road applies to commuters, pedestrians, cyclists, and workers such as police and truck drivers who travel and work on high traffic roads. The near-field environment is the region lying from curbside to several hundred meters of major roads; this can include some commuting and outdoor exposures, but mainly applies to indoor exposures in homes, schools, and workplaces. The far-field applies to areas more distant from major roads, where TRAP becomes part of the "urban plume" and spatial and temporal gradients may be present but blurred. The physical and chemical changes undergone by TRAP, as well as the concentrations in these different zones, are important for understanding the ability to monitor and quantify exposure. This report focuses on the near-field or near-road environment.

SPATIAL RESOLUTION

Given that concentrations of TRAP can exhibit dramatic changes with modest changes in distance, especially in directions perpendicular to major roads (Figures 1 and 2, shown later), exposure metrics for TRAP are prone to spatial errors. This section discusses several issues pertaining to spatial resolution and dispersion modeling.

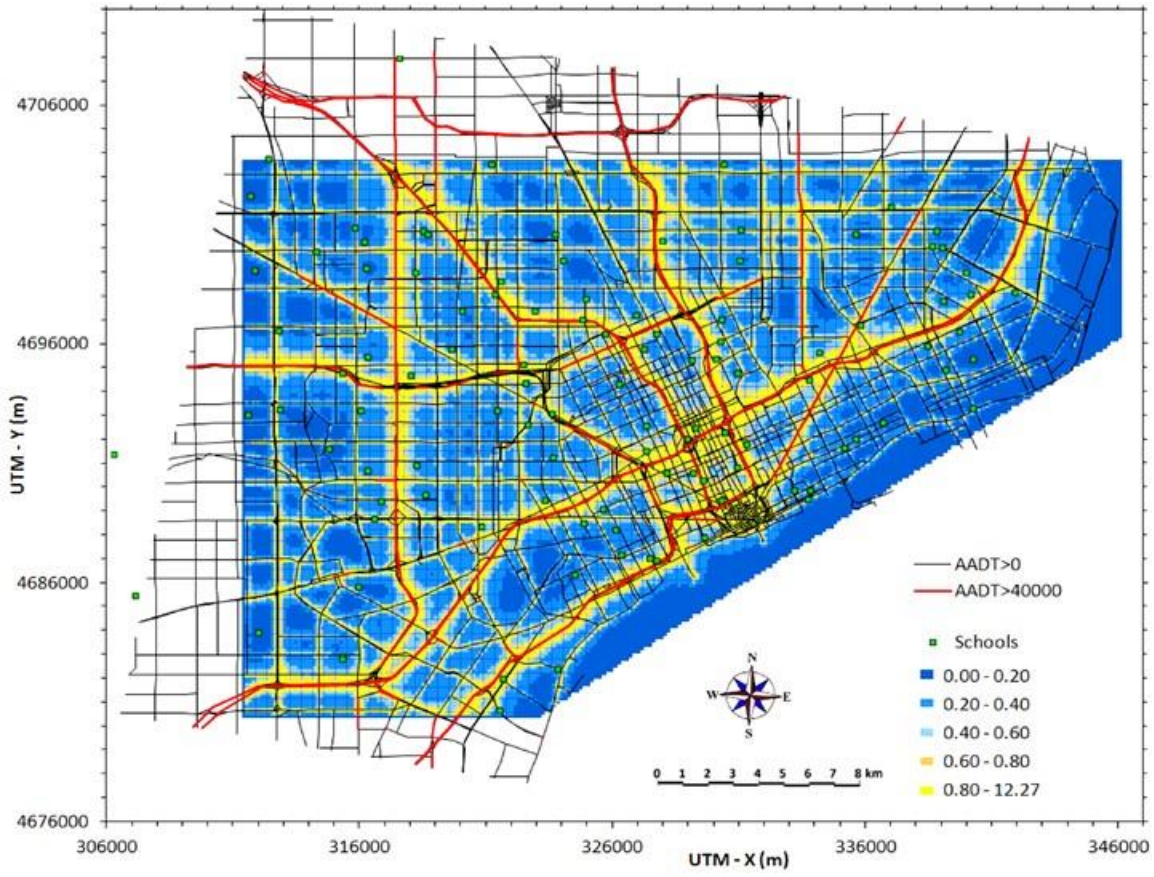

Figure 1. Predictions of maximum daily average $PM_{2.5}$ due to on-road mobile sources in Detroit/Wayne County. Based on EPA MOVES, RLINE, 9701 road links, 2010 meteorology, and 150 m receptor grid (27,000 receptors). Also shows homes and schools in the NEXUS study. From (S. Batterman et al. 2015b).

First, link-based emission inventories involve simplification and potentially misalignment of the road network as discussed in Appendix 5.

Second, dispersion model receptors must be appropriately placed to adequately represent gradients of TRAP and not compromise the accuracy of estimated concentrations. We ran detailed simulations for the NEXUS study using receptor grids with spacing as fine as 10 m (rectangular grid on 10 m centers). Figure 1 depicts the nature of concentration gradients due to on-road emissions in Detroit. The highest concentrations occur near major roads, e.g., I75, I96, I94, M10 and M39, especially at the intersections of major roads. Several arterials also have relatively high concentrations, e.g., 8-Mile Road. Because HDDVs produce a disproportionate share of $PM_{2.5}$, the highest concentrations tend to be near high diesel-traffic roads like I94 and I75. Based on analyses investigating concentrations at NEXUS participant homes, we estimated that interpolations between receptors and locations of interest should not exceed about 40 m for locations near major roads (like those discussed), and 100 m at larger distances (S. Batterman et al. 2015b). This is considerably smaller than earlier estimates of appropriate spatial scales, however, these used annual average concentrations and have not used line-source models like RLINE (Stroh et al. 2007).

Third, when estimating exposures at specific locations like homes or schools, dispersion model receptors may be placed at the location of interest, thus, localization is potentially exact. However, automated geocoding methods widely used to estimate locations using street addresses can introduce additional spatial errors. In NEXUS, we found average and maximum positional errors using automated geocoders were 35 and 196 m, respectively, and errors in residence locations to highway edge house-to-highway distances averaged 23 m (Ganguly and Batterman 2014). These errors were mostly attributable to errors in the geocoders, as well as in representing road curvature, road width, and the presence of ramps. More broadly, in health studies using link-based inventories and automated geocoding of residence locations, 5% to 20% of residences are expected to have positional errors that exceeds 100 m. Such errors can substantially alter exposure estimates for residences near roads, thus, confirmation of geocoordinates is recommended. Potentially, a "mini-grid" approach can be used in which a home or other location of interest is represented using a small receptor grid itself, providing a degree of local spatial averaging rather than a point estimate (Isakov et al. 2014).

Fourth, health and dispersion modeling studies using standard geographical units like census tracts and blocks encounter can issues of *exposure measurement error*, including those called the *modifiable areal unit problem* and other issues related to the aggregation of receptor concentrations. Use of the larger units can involve significant errors: average exposure estimates may be overestimated since few individuals live very near major roads; the range of concentrations among units will be compressed; and high concentrations near roads will be omitted as they are "averaged" out. Smaller geographic units can reduce errors, but even block-level data can misclassify exposures of many individuals based on an analysis of Detroit data (S. Batterman et al. 2014b).

APPENDIX 2 - EXPOSURE METRICS AND METHODS FOR TRAP

The purpose of exposure metrics, in general, has been stated by a recent NAS panel:

> "Ideally, exposure metrics … will provide the information needed for evaluating the overall health and resilience of humans and ecosystems, identifying vulnerable populations, assessing the impact of cumulative exposures, and addressing exposure disparities. It could also be used to assess environmental improvements and to provide early warnings of emerging problems. More data on exposures will allow us to forecast, prevent, and mitigate the impacts of such major societal challenges as climate change, security threats, and urbanization" (Lippmann 2013).

For TRAP, the basic challenge is that the true exposure cannot be measured at each location and time of interest, and that air pollution measurements collected at central monitoring sites may not reflect spatial and temporal variability of pollutants from local sources and their relationship to true personal exposures (Dionisio et al. 2016; Özkaynak et al. 2013). Said differently, environmental epidemiological studies examining air pollution exposures suffer from *spatial misalignment* between the available monitor locations and the subjects' locations. Direct measurement of TRAP using personal, home or biomarker measurements in large scale health studies is rarely practicable due to cost and logistical issues (Rioux et al. 2010). As recognized in many epidemiological studies, monitoring at central sites may not provide the spatial coverage needed to estimate neighborhood exposure, much less near-road exposures (Batterman 2013). While improved exposure estimates are needed for epidemiological, health impact, environmental justice and other applications described below (Brauer 2010; Dionisio et al. 2016; Health Effects Institute 2010; Jerrett et al. 2005; Sheppard et al. 2012; U.S. Environmental Protection Agency 2013), exposure assessment remains a recognized weakness of many TRAP studies (S. Batterman et al. 2014a).

The choice of an appropriate exposure metric for a study depends on the study design and the conceptual framework, including the spatial and temporal dimensions, biologic considerations, and available resources

(National Research et al. 1997). Exposure assessments for epidemiological studies can be guided by five key issues: the definition and characterization of the potentially exposed population; the collection of quantitative information on population exposure, temporal characteristics, and dose-response relations; the medium and the microenvironment of principal concern; the use of information collected in one population in assessing potential risk to others; and the biologic plausibility of any hypotheses based on mechanistic considerations (National Research et al. 1997).

TRAP exposure estimates are needed for several types of health effect studies. *Epidemiological studies* of TRAP, which are mostly observational in nature, use longitudinal (or time-series) designs that examine temporal variability of aggregated outcomes (often at the urban scale), cohort designs that examine individual-level data and spatial and/or temporal variability, and (sometimes) case-control designs that contrast groups on the basis of disease status using retrospective exposure estimates. Spatially- and temporally-resolved exposures are especially needed for urban-scale cohort and panel studies (Dionisio et al. 2016). Other types of health-related studies also needing exposure estimates include *health risk, health impact, burden of disease, environmental justice, cumulative impact, regulatory impact assessment (RIA), integrated science assessments (ISA), and accountability studies* (Chart-asa and Gibson 2015; Gurram et al. 2015; Health Effects Institute 2010; Isakov et al. 2009; Lobdell et al. 2011; Molitor et al. 2007). Often, these studies emphasize the spatial variability in exposures, use long-term exposure estimates, and employ simplified dose-response or concentration-outcome relationships compiled from the epidemiological literature to explain or predict health outcomes at the population level. However, short-term pollutant exposures are sometimes used, e.g., RIA, ISA, and some HIA applications have used 24-hr (daily) average pollutant concentrations. For these study types, the form of exposure metrics ideally would correspond to those used in the underlying epidemiological studies. While beyond the scope of this report, methods to estimate TRAP exposure also can be used to identify pollutant "hotspots", facilitate "project-level" analyses of transportation options, and identify vulnerable and susceptible populations (S. Batterman et al. 2015b).

Table 1 summarizes several approaches for developing exposure measures; additional background on the most important approaches follows.

AIR QUALITY MONITORING

Potentially, health effect studies can use personal, in-vehicle cabin, mobile, indoor and ambient air quality monitoring to estimate TRAP exposure. Ambient air quality monitoring data from central sites may be sufficient for air pollution epidemiology studies using time-series and case-crossover designs, especially for pollutants that tend to be fairly homogenous over broad areas, e.g., O3, but central site monitoring may not provide the spatial coverage needed to estimate near-road exposures and the small scale (or intra-urban) variation of TRAP, especially important in cohort and panel studies (Batterman 2013; S. Batterman et al. 2014b; Dionisio et al. 2016; Özkaynak et al. 2013). Personal or home measurements are rarely feasible in large-scale health studies due to cost and logistical issues (Rioux et al. 2010). A potentially promising development is the recent evolution of miniature, low-cost and wireless sensors, which is improving the feasibility of personal and other types of air quality monitoring, although many data quality issues remain to be addressed

Table 1. Summary of metrics used for exposure to traffic-related air pollutants. From (S. Batterman et al. 2014a)

Type	Exposure Metric as defined for NEXUS	Strengths	Limitations	Results in Detroit
1. Distance to major road	Distance from home to road edge, and distance from home to road centerline, using GPS home location.	Simple to construct. Low data needs. Can potentially distinguish roads with varying traffic volume, vehicle mix, or other characteristics.	Distance limit used as cutoffs for classifying homes/receptors is arbitrary. May not consider traffic volume, vehicle mix, and other factors. Sensitivity to distance calculation, e.g., using road edge or centerline.	HDHT and LDHT roads had comparable distances to homes. LDLT distances considerably exceeded HDHT and LDHT groups, by design and recruitment approach.
2. Total traffic volume on nearby roads	AADT roads within 200 m of homes, using nearest road edge and GPS home location.	Relatively simple to construct. Reasonably good volume estimates on major roads. Can select period of day, e.g., rush hour.	Traffic volume estimates needed. Distance criterion used to determine road is arbitrary. Does not provide metric for low traffic groups.	HDHT and LDHT groups largely indistinguishable. HDHT group had considerable range.
3. Diesel (or truck or commercial) traffic volume n nearby roads	Roads within 200 m of homes using road edge and GPS home location.	Relatively simple to construct. May relate to PM emissions from diesel traffic. Can select period of day.	Difficult to estimate diesel traffic volume accurately. Does not account for type of diesel vehicles and emissions. Otherwise as 2 above.	HDHT and LDHT groups were largely indistinguishable. HDHT group had roughly 10%–20% higher diesel volumes than LDHT group, but about 2/3 of the values overlapped.
4. Local traffic density	AADT on road segments with 300 m distance (buffer) around each home, based on distance to road centerline, GPS home location, and traffic-demand model estimates of AADT.	Includes local traffic emissions that might affect receptor. Result (VKT/day) is easily interpretable and possibly generalizable. Large range across sites. Can be applied to irregular shaped sources and receptors. Can select period of day. Relevant to traffic analysis zones used by planners.	Moderately high data needs. Computationally intensive. Sensitive to distance criterion, which is somewhat arbitrary. Uncertainty of traffic estimates on all but major roads. Excludes smaller roads.	LDHT group had slightly greater exposure than the HDHT group. All but a few LDLT homes had low values.
5. Emissions on local roads	As 4 above with addition of annual average road-link emissions estimates for $PM_{2.5}$, NO_x and CO.	Incorporates vehicle emissions of pollutants of interest. Reflects vehicle mix on roads. Also as 4 above.	Results depend on pollutant, to an extent. High data needs. Computationally intensive. Difficult to estimate emissions accurately.	For $PM_{2.5}$ and NO_x, HDHT had slightly higher exposure than LDLT. For CO, results are reversed but very similar All but a few LDLT homes had much lower values.
6. Pollutant concentration predictions	$PM_{2.5}$ predictions at homes used road-link emissions inventory and RLINE dispersion model; area and point sources using AERMOD and regional sources handled using CMAQ and kriging interpolations of monitoring data.	Incorporates effects of emissions, meteorology, and location in physically based approach. Quantifies and apportions concentrations due to each sources, e.g., traffic. Can be derived for specific periods of day, season or year, e.g., daily predictions at rush hour periods. Inter-study comparisons are possible and meaningful.	Results depend on pollutant, averaging time, and statistic. High data needs. Computationally intensive. Uncertainty not well characterized. Results potentially sensitive to many factors, including home placement.	For $PM_{2.5}$, HDHT and LDHT distributions were similar although some dependence on averaging time and statistic. $PM_{2.5}$ contributions from local traffic at HDHT and LDHT homes were about twice those at LDLT homes. Regional sources provide much (80%) of total $PM_{2.5}$, but smaller contributions of NO_x and CO.

Abbreviations: AADT: Annual average daily traffic; HDHT: high diesel/high traffic; LDHT: low diesel/high traffic; LDLT: low diesel/low traffic; VKT: vehicle kilometers traveled

Typical urban air quality monitoring have reasonable temporal coverage (e.g., observations are captured at hourly, daily, 1 in 3 day to 1 in 12 day schedules, depending on site and pollutant), but spatially, sites are

sparse and near-road sites are few. For example, considering active $PM_{2.5}$ monitors in cities in the U.S. and their surrounding suburbs, Los Angeles has 11 monitoring sites, Washington DC has 4, and Detroit has 9 (U.S. Environmental Protection Agency 2017). Considering near-road monitoring stations, these cities have only one or two sites each, and a total of only 72 near-road sites currently operate across the U.S.A. as of 2015 (U.S. Environmental Protection Agency). Typical approaches to assign pollutant concentrations to participants in a health study includes using measurements from the nearest monitoring site or averages of measurements from the closest sites (Escamilla-Nuñez et al. 2008; Michelle and Beate 2005; Naeher et al. 1999), or applying interpolation techniques, e.g., inverse distance weighting, weighted averages of the monitoring results near homes and workplaces, and ordinary kriging (Hoek et al. 2002; Jerrett et al. 2009). Still, given the limited spatial coverage, urban networks do not represent local scale variation or intra-urban gradients of TRAP concentrations, and these techniques may provide little, if any, additional information regarding especially the spatial variation of TRAP exposure.

SURROGATE MEASURES

Surrogate exposure measures that correlate well with exposure can be used when there is insufficient exposure data; surrogates also can improve spatial-temporal models (Woodruff et al. 2009). As noted, proximity to major roads and specifically the distance between a subject's residence and the nearest major road has been extensively used as an exposure surrogate to reflect the elevated concentrations found near busy roads (Baldauf et al. 2008; Barzyk et al. 2009; English et al. 1999; Hagler et al. 2009; Health Effects Institute 2010; Hitchins et al. 2000; Hu et al. 2009; Karner et al. 2010; Reponen et al. 2003; Zhu et al. 2006). The use of such simple measures is encouraged by the availability of geocoded information and the widespread use of geographical information systems (GIS) in environmental and epidemiological applications. Residence location reflects the portion of exposure received at home, an important and potentially dominant share since most individuals spend the majority of their time at home (YL Huang and S Batterman 2000). Other surrogates include traffic intensity, traffic-use patterns and land-use patterns (English et al. 1999; Jerrett et al. 2005; Michelle and Beate 2005; Rémy et al. 2007; Woodruff et al. 2009).

Surrogate measures have drawbacks. These include the potential for exposure measurement error since effects of meteorology, vehicle emissions, time-activity patterns of the study subjects (e.g., time spent away) and other factors are not considered. In addition, in most cases, surrogate measures do not portray short-or long-term temporal variation, quantify exposure in concentration or exposure units, account for geographic or regional differences, and appropriately account for small scale variation in pollutant concentrations (S. Batterman et al. 2014a; Y-L Huang and S Batterman 2000; Ward and Wartenberg 2006; Woodruff et al. 2009).

LAND USE REGRESSION

Land use regression (LUR), which has become widely used in epidemiological studies, expresses a pollutant concentration at a given site as a function of local geographic information system (GIS) covariates, e.g., surrounding land use, traffic characteristics and other spatial data, through a multivariate regression framework, which then is used to predict pollutant concentrations at other sites (Aguilera et al. 2007; Allen et al. 2011; Beelen et al. 2007; Briggs et al. 2000; Brook et al. 2008; Dons et al. 2013; Gehring et al. 2002; Henderson et al. 2007; Hoek et al. 2008a; Hoek et al. 2008b; Jerrett et al. 2005; Jerrett et al. 2007; Jerrett et al. 2009; Madsen et al. 2007; Montagne et al. 2015; Morgenstern et al. 2007; Puett et al. 2009; Rémy et al. 2007; Ryan and LeMasters 2007; Shi et al. 1999; Stedman et al. 1997; Wang et al. 2013; Wilton et al. 2010). The primary advantage of LUR models is their ability to characterize small-scale variations in urban settings without the need for detailed and accurate emission information. However, LUR models are area-specific and cannot be reliably extrapolated to areas with different topography, land uses, emission types, etc. In addition, since monitored pollutant levels are used as the dependent variable in the regression model, a network of air monitoring sites and historical data are required. Typically, these models have been developed using 2-week integrated NO or NO_2 measurements measured using passive samplers in seasonal field campaigns and "saturated" sampling designs (e.g., 40 or more locations measured simultaneously in

an urban setting); recent developments include the use of satellite data and applications at national scales (Stieb et al. 2016). Originally, LUR models estimate only long-term or seasonal concentrations, but temporal adjustments have been added to estimate temporal variability (Hannam et al. 2013). Data quality and comparability issues for the satellite and various types of ground-based measurements can be important.

Performance evaluations of LUR models include comparisons examining temporal stability (Wang et al. 2013), and comparisons to dispersion models (using the URBIS system, and Calculation of Air pollution from Road/CAR traffic model), which indicated moderate to high correlations for NO_2 but lower correlations for $PM_{2.5}$ and PM_{10} in Dutch studies (Beelen et al. 2009; de Hoogh et al. 2014; Wang et al. 2015). While LUR has relative good ability to capture the mean pollution trend in an intra-urban setting, being based on a multivariate linear regression framework, it implicitly assumes that concentrations at different sites are independent. This assumption might not be realistic, particularly in the near-road environment where typical land use covariates do not exhibit much variability.

DISPERSION MODELING

Dispersion models relevant to TRAPs have a long history, with the original line source formulations used to represent a road or road "link" dating back to the 1950s or possibly earlier. These physically based simulation models utilize emission and dispersion components, the latter often based on a Gaussian plume formulation. Samson (in (Kennedy and Bates 1987)) reviews the formulation and development of these models. The U.S. Environmental Protection Agency supports the development of a number of dispersion models relevant to TRAPs, including the recently-developed Research LINE-source model (RLINE) (MG Snyder et al. 2013), which can predict near-road exposures with high spatial and temporal resolution. (This model and others for near-road applications are detailed in Appendix 4).

With appropriate input data, including detailed information regarding traffic activity and emissions (Lindhjem et al. 2012), dispersion models can predict short- and long-term air pollution concentrations at desired locations called "receptors," including locations without monitors (Sheppard et al. 2012). Spatial gradients at regional, urban and smaller scales can be represented using multiple receptors. Source-oriented emission, dispersion and exposure models, which estimate near-road pollutant concentrations and individual exposures based on first principles, and in particular high fidelity models, provide great flexibility and theoretical strength, and can represent the spatial variability of TRAP concentrations that is not measured by conventional (and spatially sparse) air quality monitoring networks. Dispersion models have been used to evaluate near-roadway impacts of TRAP in a number of regulatory and health studies (S. Batterman et al. 2015b; Beevers et al. 2012; S. D. Beevers et al. 2013; Sean D. Beevers et al. 2013; Bell et al. 2011; Isakov et al. 2009; Isakov et al. 2014; Lobdell et al. 2011; Pachón et al. 2016; Van Den Hooven et al. 2012; Vette et al. 2013; Wang et al. 2015[Beevers, 2012 #1708; Wu et al. 2011; Zhai et al. 2016). Urban scale applications of dispersion models require extensive input data, and computational demands can be high.

So-called "*hybrid models*" combine several types of dispersion and/or exposure models. For example, modeling of emissions from on-road vehicles, point (industrial) and area sources can be accomplished by combining a near-road model (e.g., RLINE or ADMS) with a longer range model, e.g., the Community Multi-scale Air Quality Model (CMAQ) or AERMOD (Beelen et al. 2010; Beevers et al. 2012; Chang et al. 2015a; Isakov et al. 2009). A second type of hybrid model combines dispersion model predictions with *space-time activity data* to quantify exposures of individuals. This approach has been used for NO_x and PM in London with reasonable agreement to personal monitoring observations (Sean D. Beevers et al. 2013). Other recent applications of hybrid models for TRAPs (volatile organic compounds and NO_x) have combined CALPUFF, CMAQ and travel survey data to model the Tampa area (Gurram et al. 2015; Yu and Stuart 2016).

Another type of process-based modeling uses *computational fluid dynamic* (CFD) *models* (Wang and Zhang 2009) [Yang, 2017 #2000]. Based on the Navier-Stokes equations, such models are useful for estimating short-term dispersion of plumes, especially in areas containing obstacles like large buildings and complex

terrain, and with calm or very light winds, situations when Gaussian plume models are not applicable or perform poorly. CFD models have demanding data and computational requirements. The CFD models, as well as models for street canyons and reactive pollutants, are beyond the scope of the present report.

The ability of dispersion models to accurately predict concentrations is evaluated using a number of statistical *performance metrics* (Chang and Hanna 2004; Hanna and Chang 2012) in several types of evaluations (Dennis et al. 2010). *Operational evaluations* include statistical and graphical analyses to determine whether model estimates agree with observations in an overall sense, and utilize routine observations of pollutant concentrations, emissions, meteorology and other variables with the goal of characterizing prediction uncertainties and limitations of models for particular applications. *Diagnostic evaluations* test the ability to predict pollutant concentrations by correctly capturing physical and chemical processes. *Dynamic evaluations* examine the ability to predict air quality changes in response to changes in source emissions and meteorological conditions. Finally, the rare *probabilistic evaluation* looks at statistical properties of model performance, including uncertainty. This report employs both operational and diagnostic evaluations. Overall, prediction accuracy and uncertainty of dispersion models applied to urban settings are not well characterized (Jerrett et al. 2005). However, approximately half of a small set of model applications did meet performance criteria suggested for model performance (Chang and Hanna 2004; Hanna and Chang 2012).

SPATIO-TEMPORAL MODELING

The geostatistical method of *universal kriging* can address some limitations of LUR and spatial interpolation methods (Cressie 1993). Universal kriging models pollutant concentrations as a spatial process whose mean trend is expressed as a function of covariates, for example, the same GIS covariates used in LUR, with a covariance function that accounts for the spatial dependence in concentrations at different sites (Calder 2008; De Iaco and Posa 2012; Fanshawe et al. 2008; Finkelstein et al. 2003; Künzli et al. 2005; Lindstrom et al. 2014; Paciorek et al. 2009; Pikhart et al. 2001; Sahu et al. 2006; Smith et al. 2003; Son et al. 2010).

Another strategy to estimate pollutant concentrations at unsampled locations uses *data fusion* approaches that leverage the information contained in the output of deterministic numerical models that estimate concentrations, e.g., dispersion models (Berrocal et al. 2010a, b; Choi et al. 2009; Crooks and Özkaynak 2014; Fuentes and Raftery 2005; Gilani et al. 2016; Hystad et al. 2012; McMillan et al. 2010; Reich et al. 2014; Rundel et al. 2015; Zidek et al. 2012). While such models explicitly incorporate the physical and chemical processes related to pollutant emissions and transport with the ability to estimate concentrations at the desired spatial and temporal resolution, they often display systematic biases for several reasons, e.g., numerical approximations and uncertain model inputs. Data fusion models have been developed and successfully applied to a number of pollutants, e.g., NO_2 (Gilani et al. 2016), PM (Choi et al. 2009; Crooks and Özkaynak 2014; McMillan et al. 2010; Rundel et al. 2015), and ground-level O_3 (Berrocal et al. 2010a, b; Fuentes and Raftery 2005; Reich et al. 2014; Zidek et al. 2012).

Typically, both universal kriging models and data fusion approaches used for air pollutants in the literature have assumed that the spatial dependence in pollutant concentrations is stationary (Bliznyuk et al. 2014; Gryparis et al. 2007; Schmidt and Gelfand 2003), implying that the correlation between concentrations at two locations is only a function of their separation distance. Although computationally convenient and widely used, the assumption of stationarity might be untenable for TRAP concentrations as characteristics of the locations might affect the covariance between pollution levels at any two sites.

Non-stationary spatial modeling, and specifically non-stationary covariance functions, have been an active area of research in spatial statistics for the past 20 years. The most used and cited methods include: the "deformation" approach (Sampson and Guttorp 1992) that was initially presented in a frequentist non-parametric setting and later extended to a Bayesian framework by Damian (Damian et al. 2001) and Schmidt and O'Hagan (Schmidt and O'Hagan 2003); process convolution (Calder et al. 2002; Higdon 1998; Higdon et al. 1999; Paciorek and Schervish 2006); basis function expansions (Holland et al. 1999; Katzfuss 2013;

Matsuo et al. 2011; Nychka et al. 2002; Pintore and Holmes 2005); kernel mixing (Banerjee et al. 2004; Fuentes 2001; Fuentes and Smith 2001; Fuentes et al. 2005); Markov random field models using stochastic partial differential equations (Lindgren et al. 2011), and dimension expansion (Bornn et al. 2012). More recently, in the past 10 years, efforts have increased to develop models for non-stationary covariance functions that incorporate spatial covariates in the covariance function to help identify the factors that drive the non-stationarity. Working within the convolution approach framework of Higdon (Higdon 1998), Calder (Calder 2008) used covariate information to determine and fix the kernel parameters, Neto (Neto et al. 2014) proposed a method that included directional variables in spatially varying kernels, and Risser and Calder (Risser and Calder 2015) included covariates in the kernels through covariance regression-based methods. On the other hand, starting with the kernel mixing approach of Fuentes (Fuentes 2001), Reich (Reich et al. 2011) showed how covariates could be included in the weights of the kernels, while building on the Bayesian deformation approach (Schmidt and O'Hagan 2003), Schmidt (Schmidt et al. 2011) included covariate information in the covariance function of the spatial process. Finally, Ingebrigtsen (Ingebrigtsen et al. 2014) added covariates to the method proposed by Lindgren (Lindgren et al. 2011). Applications of these methods for non-stationary covariance functions generally have been applied to environmental processes for which data are available over a large geographic region (Calder 2007; Fuentes and Smith 2001; Higdon 1998; Higdon 2002; Paciorek and Schervish 2006) that might include natural boundaries such as land and oceans (Fuentes et al. 2005). However, non-stationary covariance functions may be needed for processes within a localized spatial domain, e.g., near-road exposures of TRAPs in urban settings. For example, due to the configuration of emission sources, meteorological effects, and possibly other factors, concentration gradients of TRAPs are more prominent with distance from highways at downwind sites, and thus the covariance at these sites is expected to have a larger effective range as compared to the covariance between upwind sites. These ideas are explored in this project.

APPENDIX 3 – NEAR ROAD DISPERSION MODELS

Dispersion models estimate near-road pollutant concentrations based on first principles and can offer great flexibility and theoretical strength. Dispersion models relevant to TRAPs date using line source formulations to represent a road or road "link" date back to the 1950s or possibly earlier. These physically based simulation models utilize emission and dispersion components, the latter often based on a Gaussian plume formulation. Samson (in (Kennedy and Bates 1987)) reviews the formulation and development of these models. The U.S. Environmental Protection Agency supports the development of a number of dispersion models relevant to TRAPs. This appendix summarizes models widely used in the U.S.

CALINE

CALINE is a line-source Gaussian plume dispersion model originally developed by the California Department of Transportation in 1972 to predict 1- and 8-hr CO concentrations at pre-determined receptor positions near roadways (Benson 1989). CALINE2 added the ability to model depressed (below-grade) roads and winds parallel to the road. CALINE3 used new vertical and horizontal dispersion curves modified for the effects of surface roughness, averaging time and vehicle-induced turbulence, replaced the virtual point source formulation with a finite line source formulation, and added multiple link capabilities. The latest version, CALINE4, used a different method to estimate dispersion parameters and improved input/output handling. Historically, the CALINE series of models required relatively minimal input from the use. Inputs include roadway geometry, hourly surface meteorology, traffic volume, and emission rates. Individual highway links are divided into a series of elements, each modeled as an "equivalent" finite line source, from which incremental concentrations are computed and summed to predict concentrations at designated receptors. The CALINE4 documentation includes sensitivity analyses for several model inputs, including wind direction variability, surface roughness, deposition velocity, highway geometry (including width, height, length) (Benson 1989). These models have been widely used.

EARLY EPA MODELS AND AERMOD

HIWAY and HIWAY-2 were early models (1980s) developed by U.S. Environmental Protection Agency (EPA) for emissions associated with roads. The Industrial Source Complex (ISC) models of the 1970s through 1990s and AERMOD in the 2000s also allowed modeling of road sources, which were represented as a "string" of volume sources or as elongated area sources. U.S. EPA calculated performance statistics comparing CALINE, AERMOD, ADMS and RLINE (described below) to observations collected in two short-term field studies. This evaluation concluded that AERMOD appeared to perform best, particularly for the highest concentrations relevant to "regulatory" models used to demonstrate compliance with the National Ambient Air Quality Standards, i.e., "hot-spot" modeling for mobile source conformity analyses of CO, PM_{10} and $PM_{2.5}$ (D. Heist et al. 2013; U.S. Environmental Protection Agency 2015a). AERMOD is being updated to incorporate line sources and newer algorithms.

RLINE

Due to growing concern about TRAP exposure and associated health effects, U.S. EPA initiated efforts to reexamine the dispersion of TRAP with the goal of developing a dispersion model that could capture the temporal and spatial variability of TRAP in the near-road environment (https://www.cmascenter.org/r-line/). Wind tunnel and field studies were undertaken to measure transport and dispersion of near-surface pollutant releases; these studies provided new datasets for the development and evaluation of improved line source algorithms. RLINE, the initial product of this development program, is considered a research grade dispersion model primarily designed to support risk assessments and health studies related to near-road pollutants. At present, U.S. EPA does not consider that RLINE is appropriate for regulatory applications because it has not undergone the extensive testing and comprehensive evaluation for such applications (https://www.cmascenter.org/r-line/).

Like its predecessors, RLINE is based upon a steady-state Gaussian formulation that simulates line type emission sources (e.g., mobile sources on roadways) by numerically integrating point source emissions along the line source. RLINE was designed to simulate impacts from line source emissions at receptors positioned very near the line source; i.e., in the road's near-field environment. It utilizes the AERMET meteorological data preprocessor surface to process meteorology. RLINE requires hourly values of sensible heat flux, surface friction velocity, convective velocity, convective stable planetary boundary layer heights, Monin-Obukhov length, surface roughness, wind speed, and wind direction. The current version (RLINE 1.2) was formulated for near-surface releases in flat terrain ("simple" terrain without surrounding complexities), and it contains new formulations of vertical and lateral dispersion rates based on the field and wind tunnel studies noted earlier. In addition, the model simulates low wind meander conditions, includes Monin-Obukhov similarity profiling of winds near the surface, and selects plume-weighted winds for transport and dispersion calculations (https://www.cmascenter.org/r-line/). The current version includes beta-option algorithms for simulating several complex near-source effects, e.g., effects of noise and vegetative barriers and depressed roadways; these features have not been evaluated in the peer-reviewed literature. RLINE version 1.2 also provides an analytical approximation (an option to the default numerical integration), which can dramatically speed calculations, although the current guidance notes that "this solution includes some simplifying assumptions that lead to slightly different results than the numerical solution, especially for receptors close to the source, or for sources and/or receptors significantly off the ground."

RLINE has been documented in a report, book chapters, and journal articles that describe its formulation (MG Snyder et al. 2013), plume spread (Venkatram et al. 2013) and upwind plume meander algorithms (David Heist et al. 2013). RLINE has undergone several performance evaluations (Chang et al. 2015b; David Heist et al. 2013; MG Snyder et al. 2013; Venkatram et al. 2013), which show generally comparable results as other "line" source models that simulate dispersion from on-road traffic emissions (Ganguly and Broderick 2008; Levitin et al. 2005; Oettl et al. 2001; Patton et al. 2017; Rao et al. 1980). RLINE has been used in a number of applications. In a hybrid modeling application involving RLINE, AERMOD and

estimates of background concentrations provided by space-time ordinary kriging, RLINE was used to contrast indoor and outdoor community-scale exposures at the Census block level in North Carolina (Chang et al. 2015b). Using a similar hybrid structure, TRAP exposures (daily and annual average $PM_{2.5}$ concentrations) were predicted at homes and schools of children in the NEXUS epidemiological study in Detroit, Michigan (Stuart Batterman et al. 2014; Vette et al. 2013). RLINE has been applied to studies examining pollutant hotspots (S. Batterman et al. 2015b), effects of receptor grid resolution on prediction errors (S. Batterman et al. 2014b), and a novel "mini-grid" receptor placement scheme to characterize concentration gradients around receptors and anonymize residence locations (Isakov et al. 2014). Recently, the model was incorporated into a C-PORT, a community-scale tool for modelling emissions related to port-related activities, including ships, trucks and cranes (Arunachalam et al. 2015; Isakov et al. 2016).

(MG Snyder et al. 2013)illustrated effects of four distinct and representative meteorological conditions found in Detroit, namely, convective, neutral, stable and very stable conditions, using RLINE to simulate concentration gradients perpendicular to a road (also using winds perpendicular to the road). Figure 2 reproduces the essential results, which shows the effect of upwind plume meander and the large differences in downwind concentrations under the four stability regimes. Under convective and neutral conditions, downwind concentrations rapidly decrease with distance from the road; under stable and especially very stable conditions, downwind concentrations persist at much longer distances, beyond 500 m. Unstable conditions typically occur during the early morning and can last through the morning rush hour. This simple sensitivity analysis indicates that the combination of a very stable atmosphere and high roadway emissions can produce high concentrations at extended downwind distances. Further, differences in dispersion between stability conditions, particularly between stable and very stable conditions, are large, which highlights the importance of using accurate meteorological parameters in dispersion modeling. This topic is explored in Appendix 9.

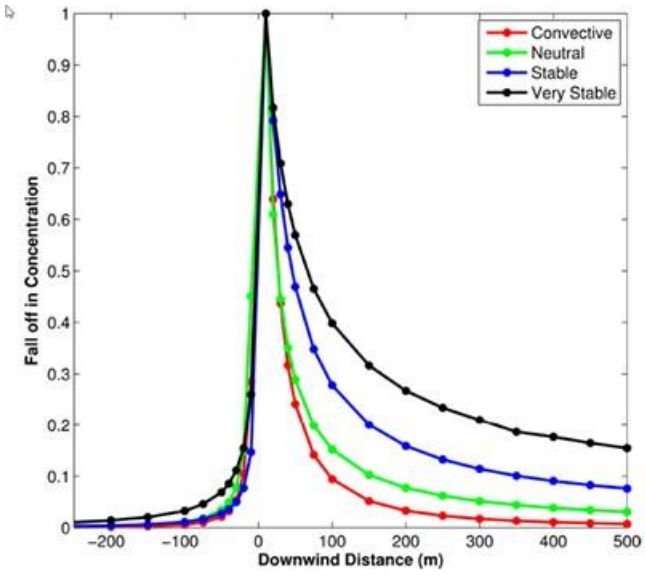

Figure 2. Concentration gradients predicted by RLINE for four representative meteorological conditions in Detroit. Concentrations are normalized by the concentration closest to the roadway. From (M Snyder et al. 2013).

RLINE has undergone several performance evaluations (Chang et al. 2015b; David Heist et al. 2013; M Snyder et al. 2013; MG Snyder et al. 2013; Venkatram et al. 2013), with respect to health studies, however, these evaluations have several limitations: they lack evaluations of daily (and sometimes annual) average concentrations; tracers rather than TRAP are often used; and they rarely are performed at the urban scale corresponding to population-level observations of health outcomes. Instead, most evaluations have examined hourly (sometimes sub-daily) average concentrations, used experimental tracer gases released at controlled rates (and which undergo only limited chemical and physical transformations at the scale of the

study), and examined small (<1 km^2) and simplified domains that contain few sources (Chang et al. 2015b; David Heist et al. 2013; Isakov et al. 2014). While providing valuable diagnostic information that can help improve models, these evaluations do not represent the complexity and scale of urban settings. Studies comparing RLINE predictions to observations of TRAPs have additional limitations: most have used short study periods and single pollutants (Patton et al. 2016; M Snyder et al. 2013) examined only annual average concentrations (Zhai et al. 2016), and provided only a limited discussion of model performance and study methodology (Pachón et al. 2016). Finally, model performance has not been evaluated with respect to season, day-of-week and other potentially exposure-relevant factors that could alter results and lead to exposure measurement errors.

CLINE

Using a simplified modeling approach based on RLINE, U.S. EPA recently developed and currently supports CLINE (Community LINE Source Model), a model designed to inform the community user of local air quality impacts from mobile-sources, and to allow exploration of alterative scenarios, e.g., changes in traffic volume, fleet mix, or vehicle speed. CLINE estimates emissions for road links by combining national database information on traffic volume providing an estimate of the annual average daily traffic (AADT) and the fleet mix with emissions factors from EPA's MOVES-2010b. This web-based tool can model any region of the U.S. (Barzyk et al. 2015).

COMPUTATIONAL FLUID DYNAMICS MODELING

It is worth noting the potential of computational fluid dynamics (CFD) modeling to represent the chemical transformation of NO to NO_2 in the on-road environment, including the very near-field of the "exhaust pipe to road" environment (Yang et al. 2017) as well as transformation in the near-road environment. Both CFD and simpler (empirical) correlations (Valencia et al. 2018) appear promising in preliminary applications and may provide insight regarding the NO/NO_2 relationship.

APPENDIX 4 – MOBILE, POINT AND AREA EMISSION INVENTORIES

This appendix provides some background on emission inventories but mainly describes the mobile, point and area source emission inventories developed for Detroit.

A high-level view of the emissions data is presented in Table 2, which summarizes emissions in Wayne County, Michigan, which includes Detroit, based on 2011 National Emission Inventory data.

Table 2. Summary of CO, NO_X and $PM_{2.5}$ emissions in Wayne Country in 2010. From the National Emission Inventory (2014) in short tons (to the nearest ton), and percent of total emissions in each category.

Emission category	CO	%	NO_X	%	$PM_{2.5}$	%
Non-point	**7,316**	**3**	**6,307**	**10**	**1,930**	**38**
Industrial processes	194	3	4	0	489	25
Miscellaneous area sources	< 1	0	7	0	27	1
Mobile sources†	107	1	872	14	689	36
Natural sources	642	9	167	3	-	-
Stationary source fuel combustion	6,347	87	5,087	81	725	38
Waste disposal, treatment and recovery	27	0	170	3	-	-
Non-road mobile sources	**65,491**	**27**	**6,847**	**11**	**493**	**10**
On-road mobile sources	**129,647**	**54**	**29,767**	**48**	**1,098**	**21**
Highway - Compressed Natural Gas	54	0	42	0	0	0
Highway - Diesel	6,260	5	15,740	53	748	68
Highway – Gasoline	123,332	95	13,985	47	349	32
Point	**36,335**	**15**	**19,489**	**31**	**1,610**	**31**
External combustion	67	0	211	1	18	1
External combustion boilers	7,422	20	10,516	54	246	15
Industrial processes	20,230	56	3,082	16	904	56
Internal combustion engines	3,193	9	1,363	7	260	16
Mobile sources*	4,702	13	2,326	12	85	5
Petroleum and solvent evaporation	13	0	20	0	52	3
Waste disposal	708	2	1,972	10	46	3
Grand Total	**238,788**		**62,411**		**5,131**	

† Railroad equipment and marine vessels; * Aircraft and airport support vehicles

MOBILE SOURCE EMISSIONS

We used a "*link-level*" inventory that provides information for individual road segments or "links," which was assembled using a "bottom-up" approach. As described below, this starts with the *road network configuration* (location, number of lanes, depth above/below grade), adds *traffic activity* information (vehicle volume, speed, acceleration and vehicle mix on each link), and then *emission factors*. Such inventories consolidate data from multiple sources, e.g., GIS shape files representing roads, estimates of total vehicle-kilometers-traveled (VKT) from metropolitan planning organizations, historical traffic measurements and estimates, traffic demand model estimates of vehicle volumes, and other data types.

As the preceding paragraph implies, emissions of TRAPs are determined by many factors and the development of mobile source emission inventories requires extensive data (Wang et al. 2008). Similarly, uncertainty in link-level emissions inventories is contributed by many factors. These include: (1) the representation of the road network geometry; (2) uncertainty in traffic activity, e.g., VKT, volume, vehicle type and age, speed, acceleration, and the number of cold starts; and (3) uncertainty of emission factors, e.g., engine exhaust emissions depend strongly on operating temperature and vehicle operating modes, while non-exhaust emissions depend on siltation loading and other factors (Fujita et al. 2012; Wang et al. 2008; Zheng et al. 2009). Many of these factors vary temporally and spatially, and temporal adjustments can contribute large uncertainties (Lindhjem et al. 2012). Other important factors include a lack of on-road traffic and emission measurements, and discrepancies between fleet classifications and VKT needed by models and the available statistical summaries (Snyder et al. 2014; Zheng et al. 2009). Several of these items are discussed below for the Detroit application.

Road Network

The road network for dispersion modeling is represented using a simplified configuration of straight segments or "links" for major roads (interstates, freeways, major arterials) and many lesser roads (minor arterials and collectors). Typically, the smallest (local) roads are not represented. Emissions (and other characteristics) are assumed uniform along the length of each link, and emissions are quantified in units of g m^{-1} s^{-1}. Curves in the road geometry can be represented using multiple links. Larger roads may be

represented using parallel links, e.g., one for each direction. Roads may be broken into several links if traffic volume or other road characteristics change. Geometrical or spatial errors result from simplifications taken to represent curves and ramps; other errors can result from spatial misalignments or approximations (S. Batterman et al. 2015b; Ganguly and Batterman 2014). For Detroit, we updated a road network consisting of 9,701 links (Figure 3) (Snyder et al. 2014). The network was overlaid with Google Earth maps in specific areas, e.g., near ambient air quality monitoring sites. Generally, links matched actual road configurations, although we noticed (and corrected) a number of geometrical errors.

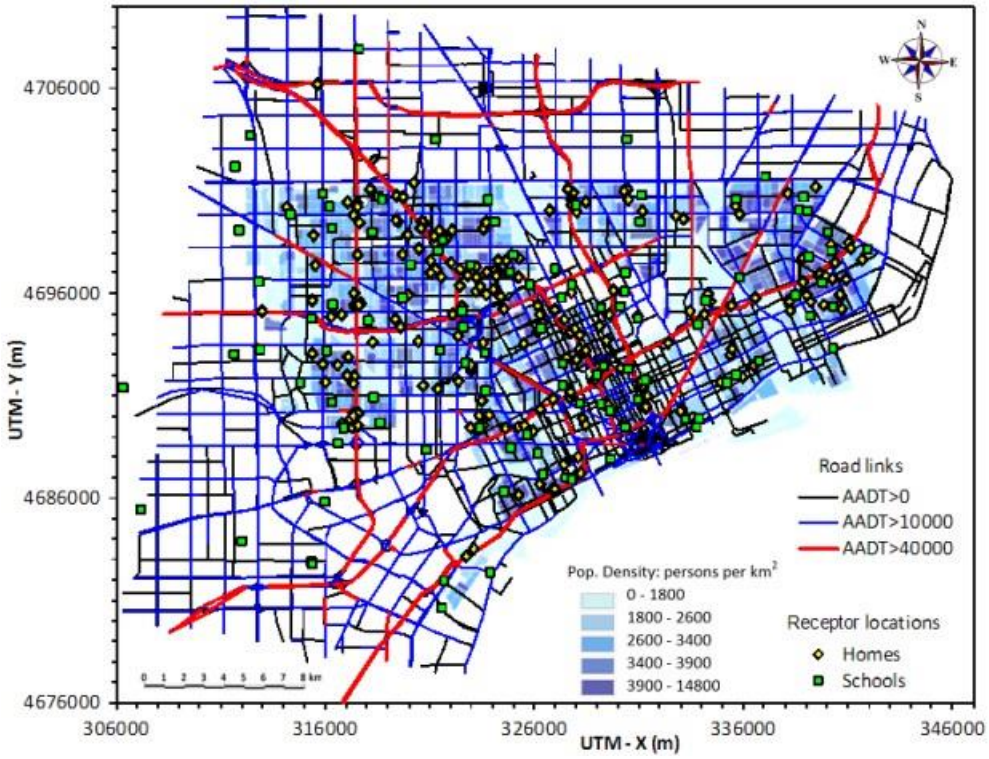

Figure 3. Map of link-based road network used in mobile source emissions inventory for Detroit. Map shows study area, and locations of children residences and schools in NEXUS. Shaded area defines city of Detroit and population by Census Block group. Axis scales are Universal Traverse Mercator coordinates (m). AADT is annual average daily traffic (vehicles/day). Highlighted roads are National Functional Class 11 and 12. From (S. Batterman et al. 2014a).

Traffic Activity and Variability

Traffic activity encompasses the volume (number), mix, speed and acceleration of vehicles on roads. In urban areas, volumes needed for link-based inventories usually are taken from *traffic demand models* (TDMs), which cover major roads (interstates, freeways, major arterials) and most lesser roads (minor arterials and collectors); the smallest roads (local roads) are typically excluded (Lindhjem et al. 2012). TDMs are typically validated or adjusted using data from traffic monitoring stations, e.g., permanent traffic recorders (PTRs), including data collected as part of the Federal Highway Administration (FHWA) Highway Performance Monitoring System (HPMS). Traffic monitoring stations are spatially sparse, and few classify vehicle type (or weight, size, or number of axles), an important omission since a single heavy-duty vehicle (HDDV) can represent many passenger car equivalents (PCEs) in terms on emissions. For example, one HDDV represents about 12 PCEs of NO_x and 50 PCEs of $PM_{2.5}$, based on the emission factor model MOVES 2010a and 2010 scenarios for Detroit, Michigan (Stuart Batterman et al. 2015; Lindhjem et al. 2012). The regional VKT is allocated to the road network using spatial surrogates (e.g., population (Lindhjem et al. 2012)), travel demand models, empirical extrapolations (e.g., the U.S. Highway Performance Monitoring System that consolidates traffic count data (North American Research Strategy for Tropospheric Ozone 2005)), or other methods. Estimated volumes are usually weekday averages.

In Detroit, we used annual average daily traffic (AADT) and commercial AADT (CAADT) volumes reported in the Michigan Trunkline Highway System (including interstates, US and state highways) (Michigan Department of Transportation) and a custom mapping/linking algorithm. Fleet mix (by link) was derived using AADT and CAADT estimates, short-term counts (usually 2-3 days of data, excluding ramps and loop measurements), and PTRs in the Traffic Monitoring Information System (TMIS) (Michigan Department of Transportation 2016). Because count data were sparse, especially on minor roads, fleet mix was estimated by National Function Class (NFC). NFC 12 and 19 links (without traffic count data) were assigned to distributions for NFCs 14 and 17, respectively (Snyder et al. 2014). Hourly data using the 13 Federal Highway Administration (FHWA) classes were averaged across days, road direction and stations, and mapped to the 8 Highway Performance Monitoring System (HMPS) classes (Decker et al. 1996). The average HMPS-by-NFC volume fractions were allocated to commercial and non-commercial traffic, normalized and weighted by average commercial traffic fractions by NFC from the final dataset. Vehicle speeds were assigned to each link for four periods: morning and evening rush hours, and afternoon and evening periods. On major commuting routes, speeds dropped (5 to 20 mph) during rush hour periods, reflecting traffic congestion.

The variability of traffic activity is one reason why on-road vehicle emissions are difficult to quantify (Parrish 2006). Historically, estimates of the VMT mix at the metropolitan level are applied uniformly across all roadway types and hours of the day. More recently, road-type specific VMT mixes have been used, important since HDDVs account for a larger share of VMT on freeways than on surface streets, and since small differences in the fraction or number of HDDVs can yield large changes in emissions, as noted earlier. Locally monitored traffic counter and vehicle classification also can be used to derive temporally varying profiles of vehicle volume mix and volume, as performed for Detroit (Batterman 2015; Stuart Batterman et al. 2015). While continuous and real-time traffic data have been used to estimate road emissions (Samaranayake et al. 2014; Zhang and Batterman 2010), the number and placement of traffic monitoring stations are rarely sufficient for this purpose.

In Detroit, to improve the temporal allocation of vehicle activity, we derived annual, monthly, daily and hourly *temporal allocation factors* (TAFs) that apportion annual average estimates of traffic volume to hourly estimates, using historical data collected in the region. This analysis used four years of hourly traffic activity data recorded at 14 continuous counting stations, including five stations that provided vehicle classification (Batterman 2015; Stuart Batterman et al. 2015). We evaluated the sensitivity of model results to default and Detroit-specific TAFs.

Examples of temporal allocation factors for Detroit are shown in Figures 4 and 5. Passenger and commercial vehicle patterns differ significantly, and separate sets of allocation factors are needed for total and commercial vehicles, and for weekdays, Saturdays, Sundays and observed holidays. It is also apparent that urban-wide TAFs can provide accurate predictions of traffic volume with a few exceptions, e.g., low volume due to adverse weather (Stuart Batterman et al. 2015). This is important because TAFs often do not always separate vehicle types, despite large differences in especially hour-of-day and day-of-week patterns of light and heavy-duty vehicles. In addition, some TAFs that may be used in lieu of site-specific data (including those in the SMOKE modeling system http://www.cmascenter.org/smoke/) can be old and can differ significantly from current traffic patterns. The TAFs derived for Detroit were used to estimate hourly volumes of commercial and non-commercial volumes for each link.

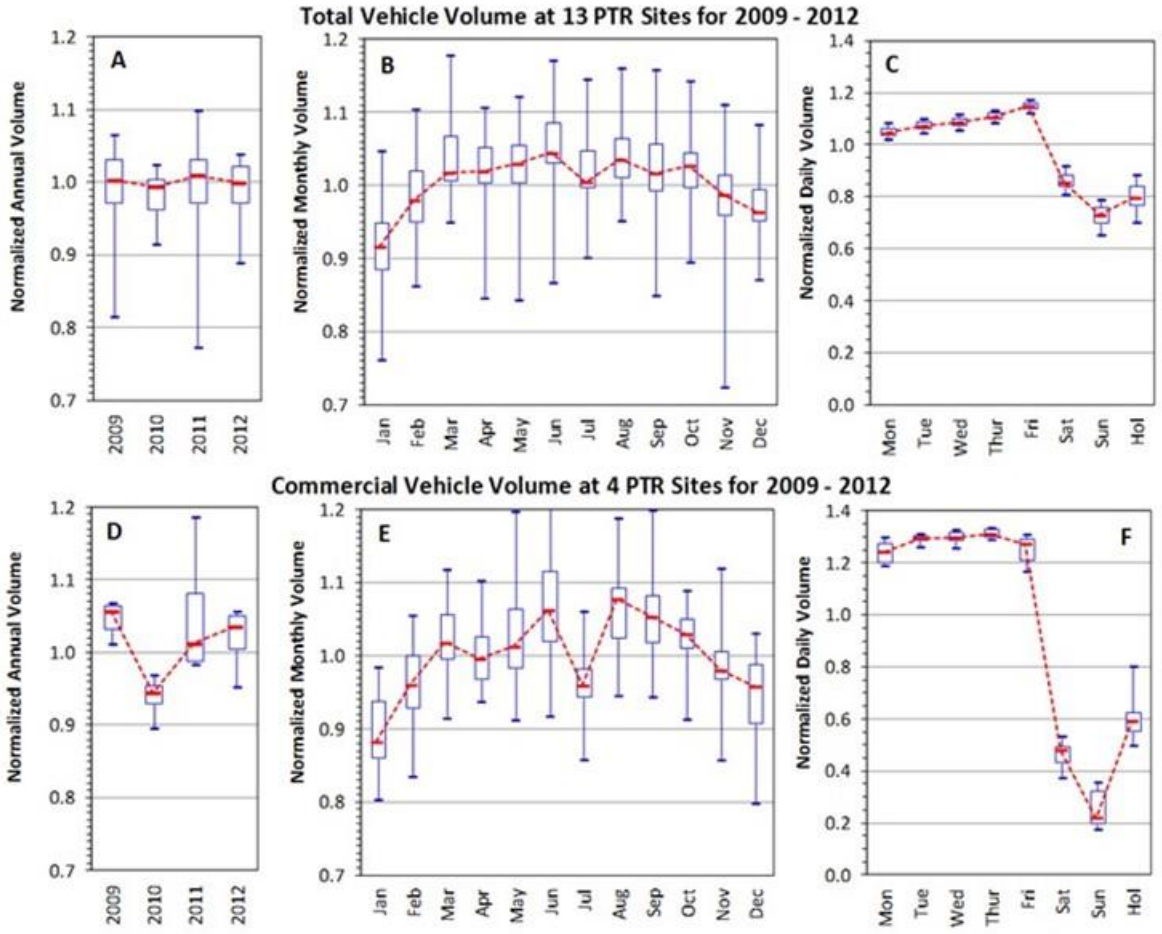

Figure 4. Normalized traffic volumes by year, month and day-of-week and holidays for volumes of total vehicles (A - C) and commercial vehicles (D - F). Plots shows 5th, 25th, 50th (red bar), 75th and 95th percentile values. Scales of panels A, B, D and E differ from plots C and F. Panels C and F consider all 10 federal holidays. (Reprinted from Batterman et al. 2015 by permission of Elsevier.)

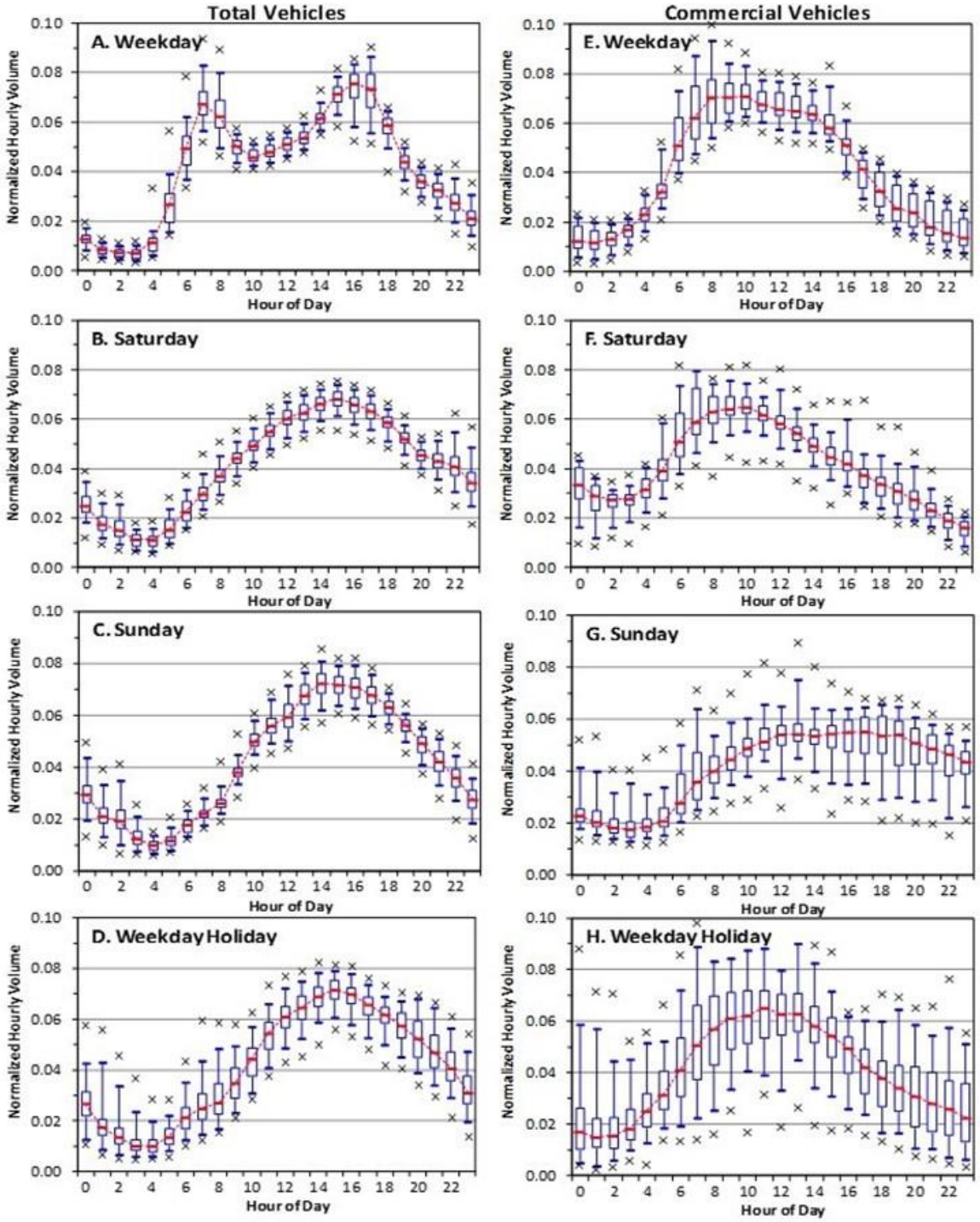

Figure 5. Diurnal trends of total volume for total vehicles across the 14 site and 4 years (panels A-D), and commercial vehicles for four weigh-in-motion sites and 4 years (E-H). Hourly volume is normalized to daily traffic for the same day and site. Weekday, Saturday and Sunday excludes ten holidays plus Friday after Thanksgiving. Weekday Holiday includes six federal holidays plus Friday after Thanksgiving. Plot shows 1st, 5th, 25th, 50th (red bar), 75th, 95th and 99th percentiles. (Reprinted from Batterman et al. 2015 by permission of Elsevier.)

Emission Factors

Emission factors (in units of g vehicle^{-1} mile^{-1}) are multiplied by traffic volumes of each vehicle type to obtain link-based emission rates. Traffic related emissions include engine exhaust and non-exhaust emissions.

Engine exhaust emissions for a given pollutant depend on vehicle type, speed, age, engine power, engine configuration, after-treatment technology, fuel, maintenance, operating temperature, and other factors. Prior to 2010, U.S. EPA supported the MOBILE series of models giving emission factors for hydrocarbons, CO, NO_x, CO_2, PM, and toxics for cars, trucks, buses and motorcycles under various conditions (U.S. Environmental Protection Agency 2003). This model (and the California Air Resources Board's EMission FACtors or EMFAC model) used cycle-average emissions corrected for average speed, derived from emission measurements using standard driving cycles designed to represent typical driving patterns along roads such as freeways, arterials, ramps and local roads. This "macroscopic" approach was widely used in emission inventory and dispersion modeling applications. In 2010, U.S. EPA released the Motor Vehicle Emissions Simulator (MOVES 2010) model, which was developed, in part, to address a National Research Council review that found that although the MOBILE model was suited for aggregate regional and national analyses, it could not be used at temporal and spatial scales relevant to specific transportation projects and control measures; further, the review noted model validation and evaluation issues, e.g., large underestimates of CO and hydrocarbons (Fujita et al. 2012). MOVES provides great flexibility for vehicle operation cycle, and running exhaust emissions based on vehicle-specific power (instantaneous power demand/vehicle mass). The current version, MOVES2014a, provides a number of updates, calculates on-road and non-road emissions, and is considered by U.S. EPA as a state-of-science modeling system (https://www.epa.gov/moves/moves2014a-latest-version-motor-vehicle-emission-simulator-moves).

Non-exhaust emissions arise from brake, tire and clutch wear, pavement surface abrasion, entrainment of re-suspended dust (silt), and certain vehicle "running losses" (primarily applicable to VOCs) (Fujita et al. 2012; Wang et al. 2008; Zheng et al. 2009). There is significant uncertainty regarding the characterization and quantification of non-exhaust emissions (Pant and Harrison 2013). Both the MOBILE and MOVES models include tire and brake wear in their PM_{10} emission factors. In urban environments, brake wear is estimated to account for 16 to 55% of total non-exhaust traffic-related PM_{10} emissions (11 to 21% of total traffic-related PM_{10} emissions), with the greatest contributions in high-density traffic with high braking frequency, and the lowest for freeways where braking frequency is low (Grigoratos and Martini 2015). Brake wear has a unimodal size distribution (maxima between 1 and 6 μm) and thus, a potentially significant fraction is $PM_{2.5}$. The contribution of "road dust," which encompasses pavement surface abrasion and entrainment, is suggested by receptor modeling apportionments, although the "mineral" or "crustal" factor identified in such studies can include demolition, construction and road dust (Querol et al. 2004). Road dust emissions vary greatly by location, vehicle speed, street maintenance, siltation, use of studded tires, climate, and sanding and salting of roads during the winter and spring periods (Milando et al. 2016; Pant and Harrison 2013; Querol et al. 2004).

In Detroit, emission factors were generated using MOVES version 2014a (U.S. Environmental Protection Agency 2015b) and 2015 inputs for the Wayne, Macomb and Oakland Counties (the most populated local areas) provided by the Southeast Michigan Council of Governments (SEMCOG). Other MOVES inputs included monthly average local temperatures in 11 bins (0 to 100 °F in 10 degree increments) (Snyder et al. 2014) and the default barometric pressure, which was similar to local conditions (Southeast Michigan Council of Governments (SEMCOG) 2011). Following previous work(Snyder et al. 2014) , emission factors for running exhaust and running evaporative modes were calculated for CO, NO_X, $PM_{2.5}$ and $PM_{2.5}$ precursors (evaporative hydrocarbon emissions), and for $PM_{2.5}$ tire-wear and brake-wear emissions, and crankcase and other emissions were omitted to reduce computational time (these emissions are small compared to exhaust emissions). Finally, emission factors were consolidated by pollutant type (e.g., tire and brake wear for $PM_{2.5}$), vehicle types mapped to the HPMS vehicle classes, and averages were weighted by vehicle type counts and VMT fraction on major roads and NFC 11 and 12 in the link network and minor roads (NFC 14, 16, 17 and 19), and the number of weekday and weekend days. CO, NO_X and $PM_{2.5}$ emission factors were calculated by vehicle type, speed and ambient temperature. As in most areas, little information was available regarding non-exhaust traffic-related emissions of $PM_{2.5}$.

Hourly commercial and non-commercial emission factors for each NFC and speed bin were calculated for each pollutant. Finally, link emissions were calculated as the product of link-specific volume with the speed-, month-, temperature- and vehicle type-specific emission factor (described below).

POINT SOURCE EMISSIONS INVENTORY

We consolidated stack-level data in the National Emission Inventory (NEI) (2014) with facility and stack-level data in the Michigan Air Emission Reporting System (MAERS) (Michigan Department of Environmental Quality 2014); emission data was available for 564 facilities. Stacks were aggregated to the facility level by assigning emissions to the largest stack (normally the tallest with the greatest emissions and volumetric flow). A subset of 179 facilities were selected based on the 100 highest emitting facilities for each pollutant). Of these, 58 mostly smaller sources had incomplete information and were excluded. Quality checks included extensive comparisons between MAERS and the 2011 NEI data. Facility-level emissions for CO and NO_X were mostly within 5%. However, the PM data, which included condensable PM, $PM_{2.5}$ and PM_{10}, showed larger discrepancies, e.g., MAERS and NEI emissions of $PM_{2.5}$ differed by over 5% at 99 of 121 sources, and filterable $PM_{2.5}$ emissions in MAERS exceeded primary $PM_{2.5}$ emissions (sum of filterable and condensable $PM_{2.5}$) in 23 cases. These discrepancies were resolved following a 3-step procedure (Dorn et al. 2013): quality checking available data; trivial gap filling using available data; and then ranked "best-guess" estimates using, in sequence, data in an NEI year, primary emissions data converted directly using facility-specific SCC conversion factors, the median $PM_{2.5}$ emission estimate generated indirectly, and lastly the $PM_{2.5}$ estimate created by trivial gap-filling of converted values. The final point source inventory contained 121 sources that represented over 90% of countywide point source emissions. Pollutant concentrations were predicted using this inventory, the AERMOD dispersion model (View v8.1.0; AERMOD.exe v12345) (Cimorelli et al. 2004), and the preprocessed meteorological data described later in Appendix 8. Sources in Detroit were classified as "urban" with a reference population of 10^6 and the default surface roughness (Michigan Department of Environmental Quality 2015).

AREA SOURCE EMISSIONS INVENTORY

Earlier work completed for NEXUS modeled local *area sources* in a 30 x 40 km domain over the Detroit area. These sources include on-road emissions from (small) local roads, non-road mobile sources, area sources, port sources, and airport sources. As noted, inventory data for area sources lack spatial and temporal resolution. This effort extracted area source data from NEI data for 2008 (Version 1.5 and 1.7) obtained from the U.S. EPA CHIEF website (http://www.epa.gov/ttn/chief/emch), which was processed for the NEXUS domain using the Sparse Matrix Operator Kernel Emissions (SMOKE) modeling system (Houyoux et al. 2000) to obtain model inputs that were sector-specific, speciated, time varying, and spatially allocated on a 1 km grid. Each of the 1,200 cells was treated as an individual area source in AERMOD.

APPENDIX 5 – AIR QUALITY MONITORING DATA IN DETROIT

CO, NO, NO_2, NO_X and $PM_{2.5}$ data collected at air quality monitoring sites in Wayne County were downloaded from U.S. Environmental Protection Agency (2015). Locations of the five near-road sites emphasized in the present analysis, nearby roads and point sources in the emissions inventory are shown in Figure 6. Periods when measurements were available and data capture rates are shown in Table 3. Quality checks on the monitoring data included screening for concentrations equal to or below zero, comparing measurements to detection limits (DLs), and comparing measurements to trip and field blanks. Modeled NO_x values (in $\mu g\ m^{-3}$) were compared to measured NO_X levels (in ppb) using the measured NO_2:NO_X ratio. $PM_{2.5}$ blanks were collected only at Allen Park and Dearborn for the Chemical Speciation Network monitors, but not the TEOM monitors (Solomon et al.) used in the evaluation, thus, data were not blank-corrected.

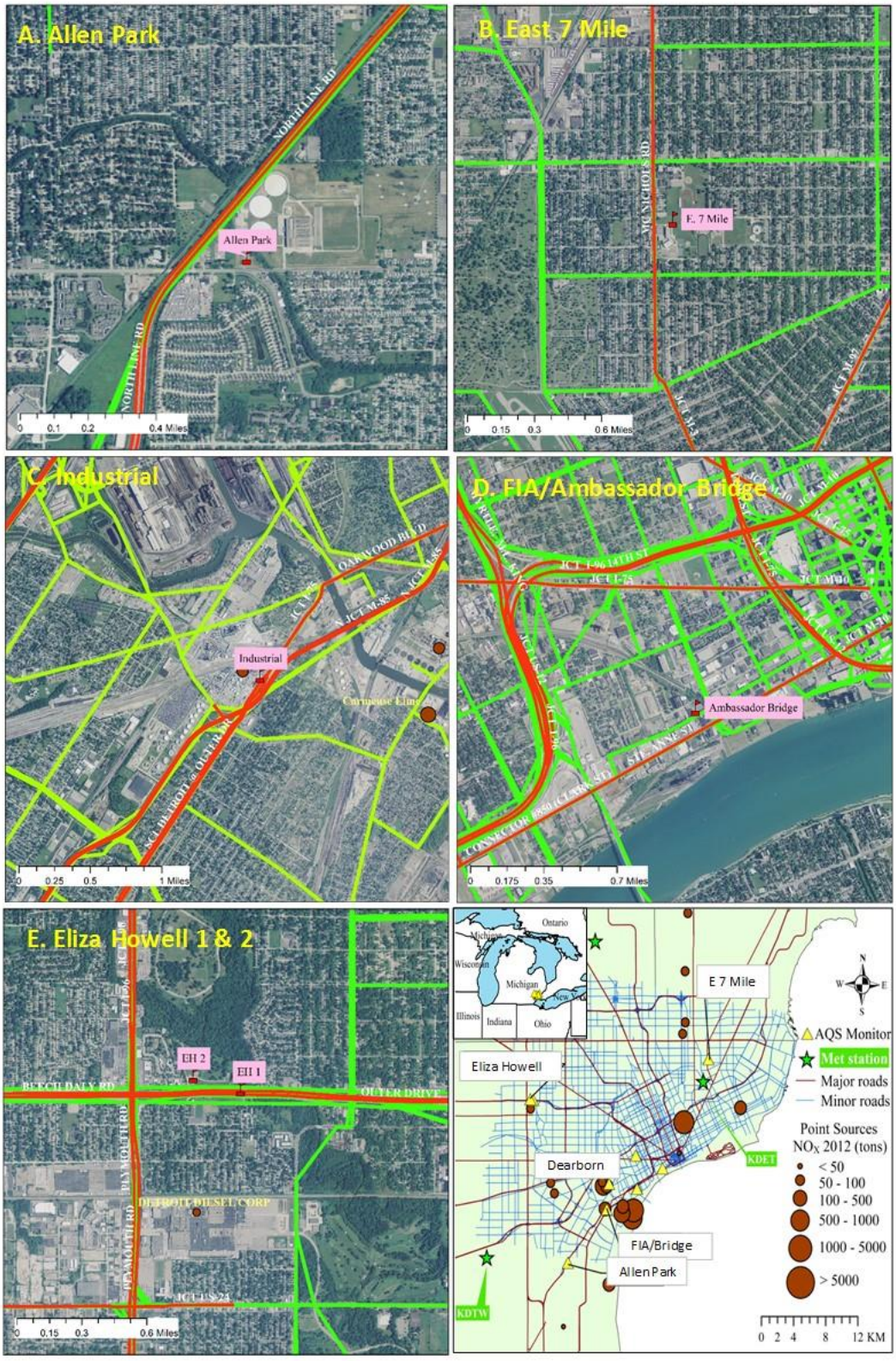

Figure 6. Aerial photographs around six air quality monitoring sites showing roads, point sources, and other features. Red lines are roads in the MDOT Trunkline system, red and green lines are in the Detroit mobile source inventory. Point sources shown with yellow text and brown circles. Map at lower right shows all sites as well as major point sources of NO_x.

Table 3. Five near-road monitoring sites in Detroit area. Starting month-year and percent of measurements above detection limit for hourly data shown. EH is Eliza Howell.

Site location / Name / AQS ID	CO	%	NO	%	NO_2	%	NO_X	%	$PM_{2.5}$	%
Allen Park / "Suburban" / 261630001	Jan-11	(8)	Jan-11	(98)	-		-		Jan-11	(100)
East 7 Mile / "Schools" / 261630019	-		Jan-11	9	Jan-11	95	Jan-11	(51)	-	
Dearborn / "Industrial" / 261631008	Jan-12	(10)	-		-		-		Jan-14	(100)
EH #1 (10 m) / "Near-road" / 261630093	Oct-11	(54)	Oct-11	(63)	Oct-11	(97)	Oct-11	(89)	-	-
EH #2 (100 m) / "Urban" / 261630094	Oct-11	(25)	Oct-11	(18)	Oct-11	(89)	Oct-11	(62)	-	-

BACKGROUND ESTIMATES

For NO_X, most hourly measurements exceeded DLs (51 to 100%, depending on site), and background estimates generated using the conditional selection method fell into a narrow range (15 to 18 ppb). For CO, observations frequently fell below the DL for the less sensitive instruments (IGFC and INDiI), which yielded relatively high background estimates (averaging 519 to 671 ppb); background estimates were much lower (128 ppb) for the more sensitive instrument (EC9830T). Because background estimates reflected DLs of the instrumentation used, datasets were not pooled across sites or instruments. For $PM_{2.5}$, background averaged 8.8 μg m^{-3} at the schools and suburban sites, equivalent to 88 to 92% of observed levels (9.5 and 10 μg m^{-3}, respectively), and day-to-day variability was significant. Predicted contributions from point and on-road mobile sources at the monitoring sites were small (averaging from 0.1 to 0.8 μg m^{-3}), and including these sources in the daily background estimates did not increase the correlation between observed and estimated background levels. Thus, performance evaluations for $PM_{2.5}$ were not attempted, a result of the dominance of regional sources and the small signal remaining from local sources, the gaps and uncertainties of the $PM_{2.5}$ emission inventory, the absence of chemical transformations in RLINE, and the few near-road sites monitoring $PM_{2.5}$.

APPENDIX 6 – EXPLORATORY ANALYSIS OF NEAR-ROAD INCREMENTS

This appendix presents an exploratory analysis of the ambient pollutant data collected using a Mobile Air Pollution Lab (MAPL), a recreational vehicle equipped with a variety of air quality monitoring instruments, along nine transects that crossed major roadways in Detroit, MI, on seven consecutive days (December 14 - 20, 2012). Further details are available elsewhere (Baldwin et al. 2015).

The analysis revealed considerable variability in concentrations of NO, NO_x, and BC between the different areas. Mean pollutant concentrations ranged from 9.9 to 40.7 ppb for NO (areas 7 and 1, respectively), 20.0 to 58.5 ppb for NO_x (again areas 7 and 1), and 0.8 to 2.2 μg m^{-3} for BC (areas 2 and 4). Weekend concentrations tended to be higher than weekday levels: average ± SD concentrations were 21.3 ± 18.9 ppb for NO, 36.3 ±20.0 ppb for NO_x, and 1.6 ± 1.1 μg m^{-3} for BC on weekends, compared to 17.6 ± 16.8 ppb for NO, 31.1 ± 20.5 ppb for NO_x, and 1.2 ± 0.8 μg m^{-3} for BC on weekdays. Mornings had higher mean concentrations than evenings for all three pollutants: average concentrations were 22.8 ± 20.0 ppb for NO, 34.9 ± 23.6 ppb for NO_x, and 1.4 ± 1.0 μg m^{-3} for BC in mornings, compared to 14.0 ± 12.7 ppb for NO, 29.8 ± 16.1 ppb for NO_x, and 1.1 ± 0.7 μg m^{-3} for BC in evenings. Finally, downwind sites experienced higher pollution levels than upwind sites for all three pollutants: mean concentrations were 22.2 ± 19.4 ppb for NO, 36.6 ± 22.2 ppb for NO_x, and 1.4 ± 1.0 μg m^{-3} for BC at downwind sites, compared to 15.1 ± 14.6 ppb for NO, 28.5 ± 17.8 ppb for NO_x, and 1.1 ± 0.7 μg m^{-3} for BC at upwind sites. Histograms of pollutant

concentrations show right-skewed distributions for all three pollutants (Figure 7), which suggests that modeling these pollutant concentrations on the log-scale would be more appropriate.

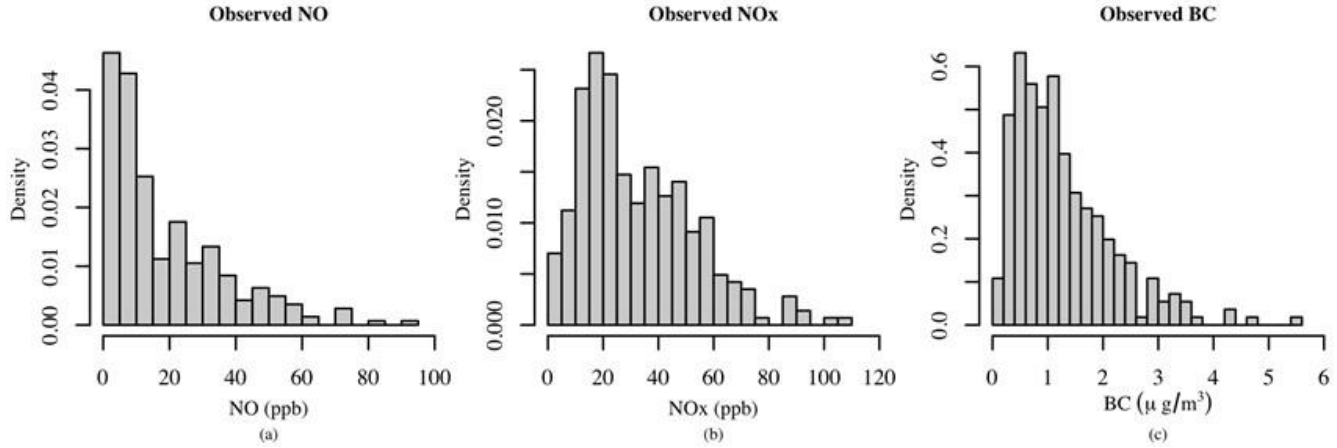

Figure 7. Histograms of NO, NO_x and BC concentrations observed at monitoring sites in the nine transect areas across major highways on December 14 - 20, 2012 in Detroit, Michigan.

The NRI of NO_x and $PM_{2.5}$ concentrations also showed considerable variability between areas. The mean NRI in concentrations of both pollutants was lowest at area 9 (9.6 ± 8.5 ppb for NO_x and 0.5 ± 0.4 μg m^{-3} for $PM_{2.5}$). This was expected since area 9 sites were sampled either just after the morning rush hour or before the afternoon rush hour period, while the other sites were monitored during morning and afternoon rush hour periods. The highest mean NRI concentrations of NOx were recorded at area 5 (21.5 ± 18.7 ppb), and at area 1 for $PM_{2.5}$ (2.2 ± 2.2 μg m^{-3}). Histograms of the NRI concentrations of both pollutants displayed right-skewed distributions (Figure 8**)**, which suggests that also modeling the NRI in on the log-scale would be more appropriate.

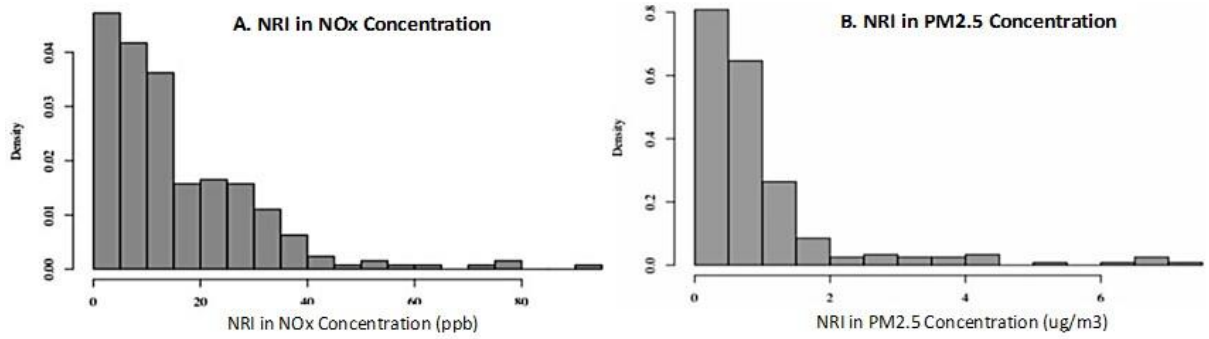

Figure 8. Histograms of (a) NO_x and (b) $PM_{2.5}$ near road increment concentrations, in ppb and μg m^{-3}, respectively, measured at the sites in the 9 transect areas on December 14 – 20, 2012.

APPENDIX 7 – FITTING AND EVALUATION OF SPATIO-TEMPORAL MODELS

This appendix presents prior specification, fitting and evaluation of the non-stationary spatio-temporal statistical models developed for (1) universal kriging and spatial interpolation of observed concentrations

of TRAP and (2) data fusion of observations of near-road-increments of pollutant concentrations with dispersion model outputs. Equation numbers refer to the core report.

PRIOR SPECIFICATION AND MODEL FITTING

Each of the models is specified within a Bayesian framework. Here, we detail the prior distributions used to fit the various models. All models are fit by running an MCMC algorithm with Gibbs sampling for all regression coefficients and variance component parameters, and with Metropolis-Hastings steps to update the remaining spatial covariance parameters. For each model, we developed the MCMC algorithm, writing the sampling functions to generate samples from the joint posterior distribution in R. All parameters were updated at each iteration, conditionally on other parameters, via Gibbs sampling (if the full conditional distribution was available in closed form) or via Metropolis-Hastings (if the full conditional distribution was not available in closed form).

Code to fit the joint Bayesian data fusion model, and the univariate regression-based Bayesian data fusion model will be made available in a github repository. Convergence of each Markov chain and mixing of the sampler was assessed by running multiple MCMC chains with different initial values visually inspecting the trace plots and by computing convergence diagnostics such as Geweke's diagnostic (Geweke, 1992).

Non-Stationary Universal Kriging

For each pollutant, the full non-stationary universal Kriging model contains 17 parameters: 10 regression coefficients $\beta_0, \ldots, \beta_9$, one nugget effect, τ^2, and six spatial covariance parameters, σ_1^2, ϕ_1, φ_1, σ_2^2, ϕ_2, and φ_2. For all of these parameters, we specify non-informative prior distributions. Parameter ψ in the definition of the mixture weights $w_{1,t}(\mathbf{s})$ and $w_{2,t}(\mathbf{s})$ in (5) is kept constant and determined through empirical considerations. Specifically, ψ is chosen such that if a site $\mathbf{s}$ is the furthest downwind site during time period t, the mixture weight $w_{2,t}(\mathbf{s})$ is equal to about 0.05. We assess the sensitivity of the results to the choice of ψ by using different values of ψ.

Priors on the 17-pollutant specific model parameters are specified using an empirical Bayes approach. Specifically, on each of the β_l, $l = 0, \ldots, 9$, we place independent normal priors with large variances and means set equal to the estimates of the regression coefficients obtained by fitting a linear regression model on the monitoring data for the pollutant considered with the 10 variables in (2) as covariates. For variance components parameters, τ^2, σ_1^2 and σ_2^2, we place vague inverse Gamma priors with shape and scale parameters chosen so that the prior variance is infinite (achieved when the scale parameter is equal to 2), and the prior mean is equal to, respectively, 20%, 40% and 40% of the estimated residual variance from the linear regression model fit to get prior means for the regression coefficients $\beta_0, \ldots, \beta_9$. Finally, for parameters ϕ_1, φ_1, ϕ_2, and φ_2 controlling the roughness/smoothness of the covariance function of the underlying spatial processes $\eta_{1,t}$ and $\eta_{2,t}$, $t = 1, \ldots, \mathcal{T}$ in the x - y and signed wind speed direction, respectively, we place Gamma priors with shape and scale parameters chosen so that the variance of the Gamma distribution is large while the prior mean gives a correlation of 0.05 at a distance equal to 3 times the prior mean. This choice reflects that in an exponential correlation function with decay parameter ϕ, the effective range, that is, the distance at which the correlation decays to 0.05, is about 3ϕ. Hence, the prior mean is set to approximately 1/3 of the maximum inter-monitoring site distance and 1/3 of the maximum signed wind-speed "*distance*".

Non-Stationary Joint Modeling Bayesian Data Fusion

The model for the natural log NRI of each pollutant is completely specified when priors are provided on: the coefficients $\hat{\beta}_0, \hat{\beta}_1, \ldots, \hat{\beta}_8$ of the large scale trend $\hat{\mu}_t(\mathbf{s})$ of the unobserved, *true* log NRI field $\hat{Y}_t(\mathbf{s})$, the six covariance parameters $\sigma_1^2, \phi_1, \varphi_1, \sigma_2^2, \phi_2,$ and φ_2 of the true log NRI field $\hat{Y}_t(\mathbf{s})$, the nugget effects, τ_e^2, τ_δ^2, and the additive and multiplicative bias terms, a_0 and b, of the log NRI output, as well as the covariance parameters, σ_a^2, ϕ_a, of the spatial error of the log RLINE output.

Priors are specified using the same strategy as for the non-stationary universal kriging model. Thus, for each model, we use the same prior specifications for coefficients $\hat{\beta}_0, \hat{\beta}_1, \ldots, \hat{\beta}_8$, and inverse Gamma priors are specified for covariance parameters $\tau^2, \sigma_1^2, \sigma_2^2, \sigma_a^2$ with parameters determined as described earlier. Similarly, for covariance parameters $\phi_1, \varphi_1, \phi_2, \varphi_2$ and ϕ_a controlling the rate of decay of the correlation as either the geographical distance or the distance in the signed wind speed space increase, we use Gamma priors analogously as described earlier. Finally, for the overall additive and multiplicative bias terms of the log RLINE output, a_0 and b, we use two vague independent, normal priors with means 0 and 1, respectively, assuming a priori no bias in the log RLINE output. For both pollutants, the MCMC algorithm was run for 70,000 iterations with the first 4,000 discarded for burn-in. To reduce autocorrelation in the posterior samples, we used a thinning of 60, yielding 1,100 posterior samples for each model parameter that were used for posterior inference.

Figures 9, 10, 11, 12, 13, and 14 present trace plots for the two best-performing joint data Bayesian fusion models for NOx and $PM_{2.5}$ NRI, respectively Model 2-JBDF-S for NO_x and Model 2-JBDF-NS for $PM_{2.5}$.

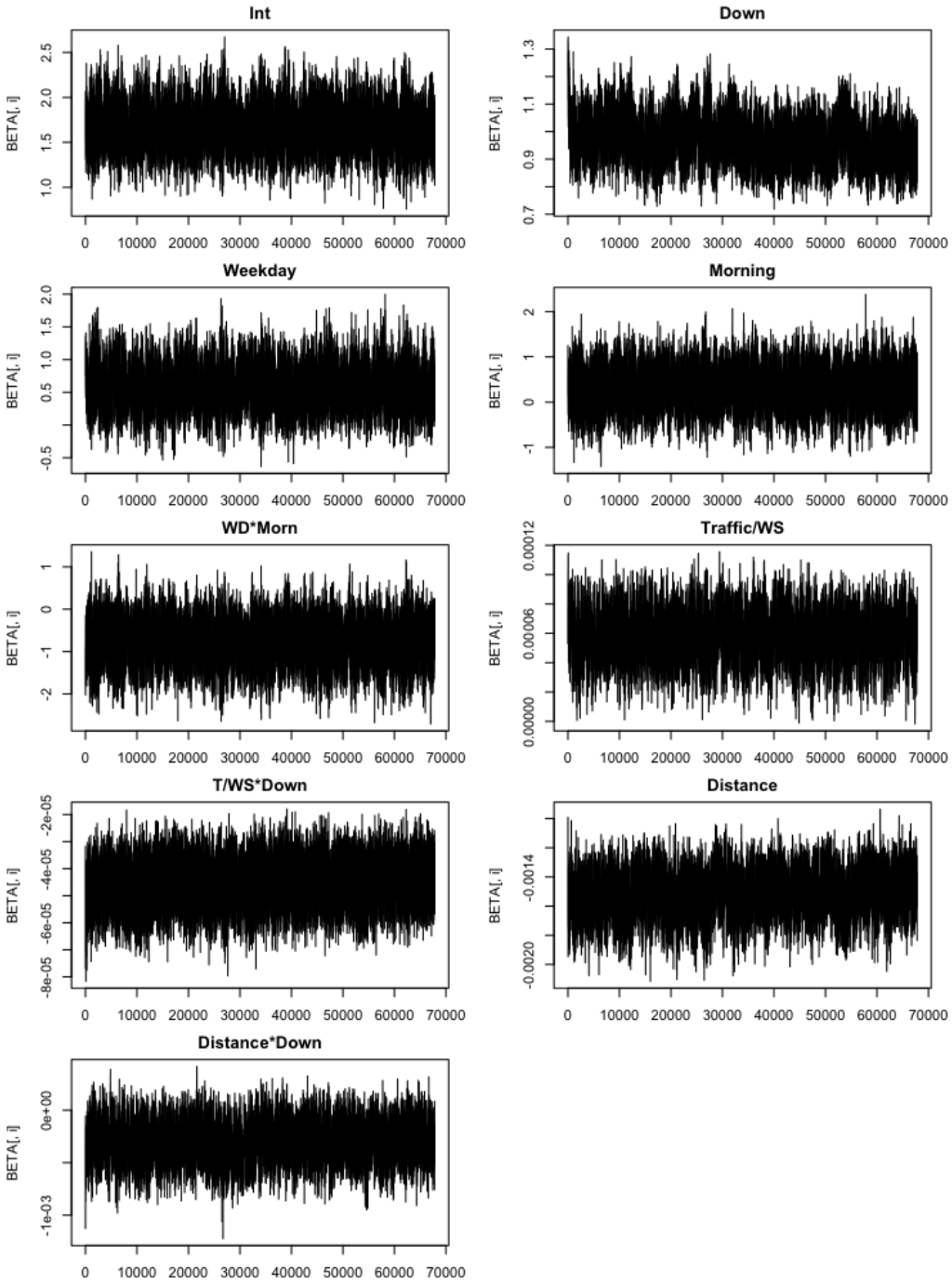

Figure 9. Trace plots for $\boldsymbol{\beta_0}, \ldots, \boldsymbol{\beta_9}$, regression coefficients of the meteorological and traffic covariates in the joint Bayesian data fusion model Model 2-JBDF-S for NO_x NRI concentration.

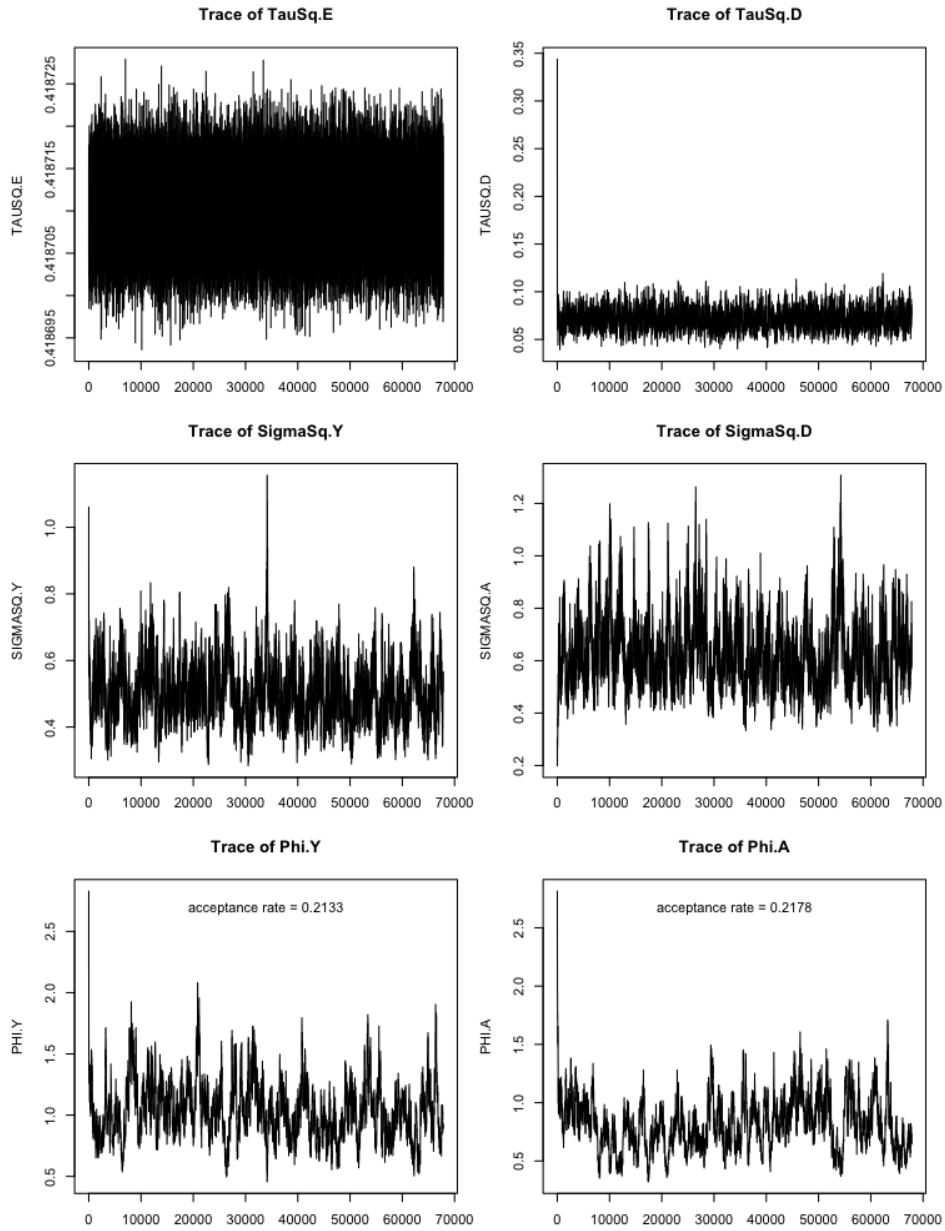

Figure 10. Trace plots of the covariance parameters of the joint Bayesian data fusion model Model 2-JBDF-S for NO_x NRI concentration.

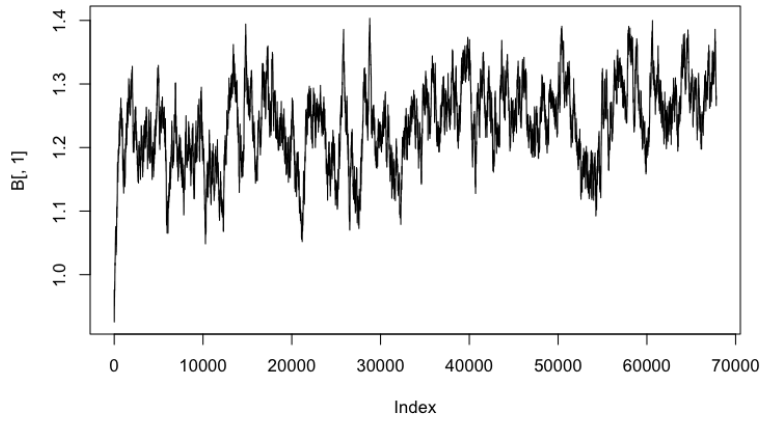

Figure 11. Trace plots of the multiplicative calibration term (*b*) of the RLINE output in the joint Bayesian data fusion model Model 2-JBDF-S for NO_x NRI concentration.

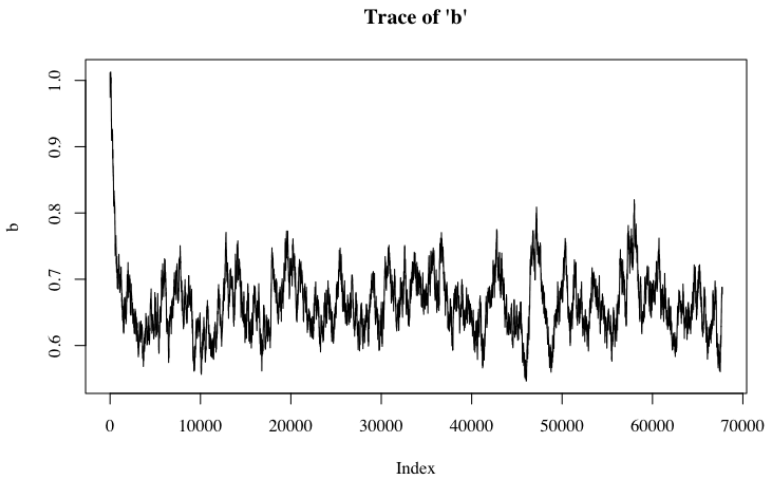

Figure 12. Trace plots of the multiplicative calibration term (*b*) of the RLINE output in the joint Bayesian data fusion model Model 2-JBDF-NS for $PM_{2.5}$ NRI concentration.

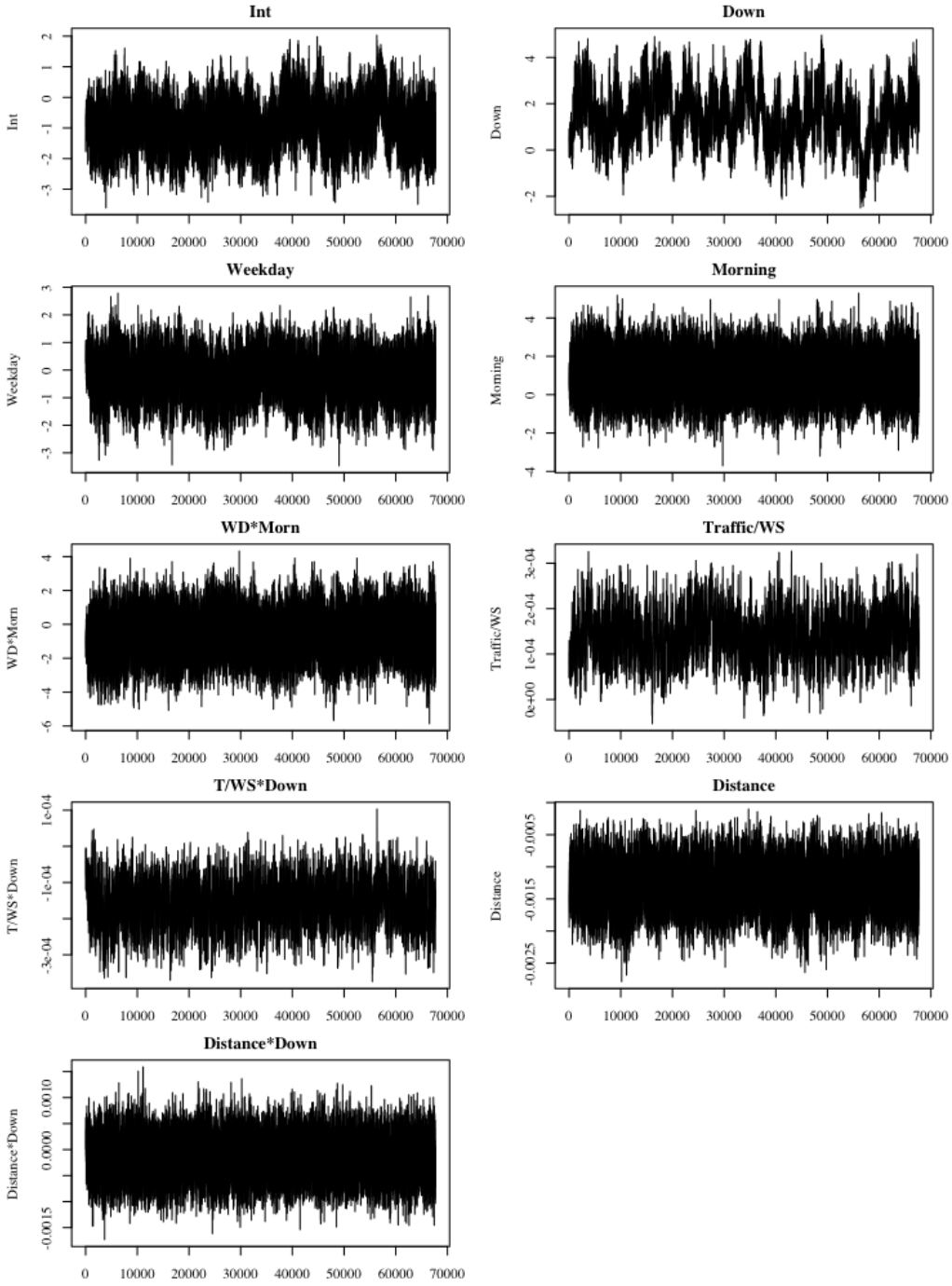

Figure 13. Trace plots for $\boldsymbol{\beta_0}, \ldots, \boldsymbol{\beta_9}$, regression coefficients of the meteorological and traffic covariates in the joint Bayesian data fusion model Model 2-JBDF-NS for $PM_{2.5}$ NRI concentration.

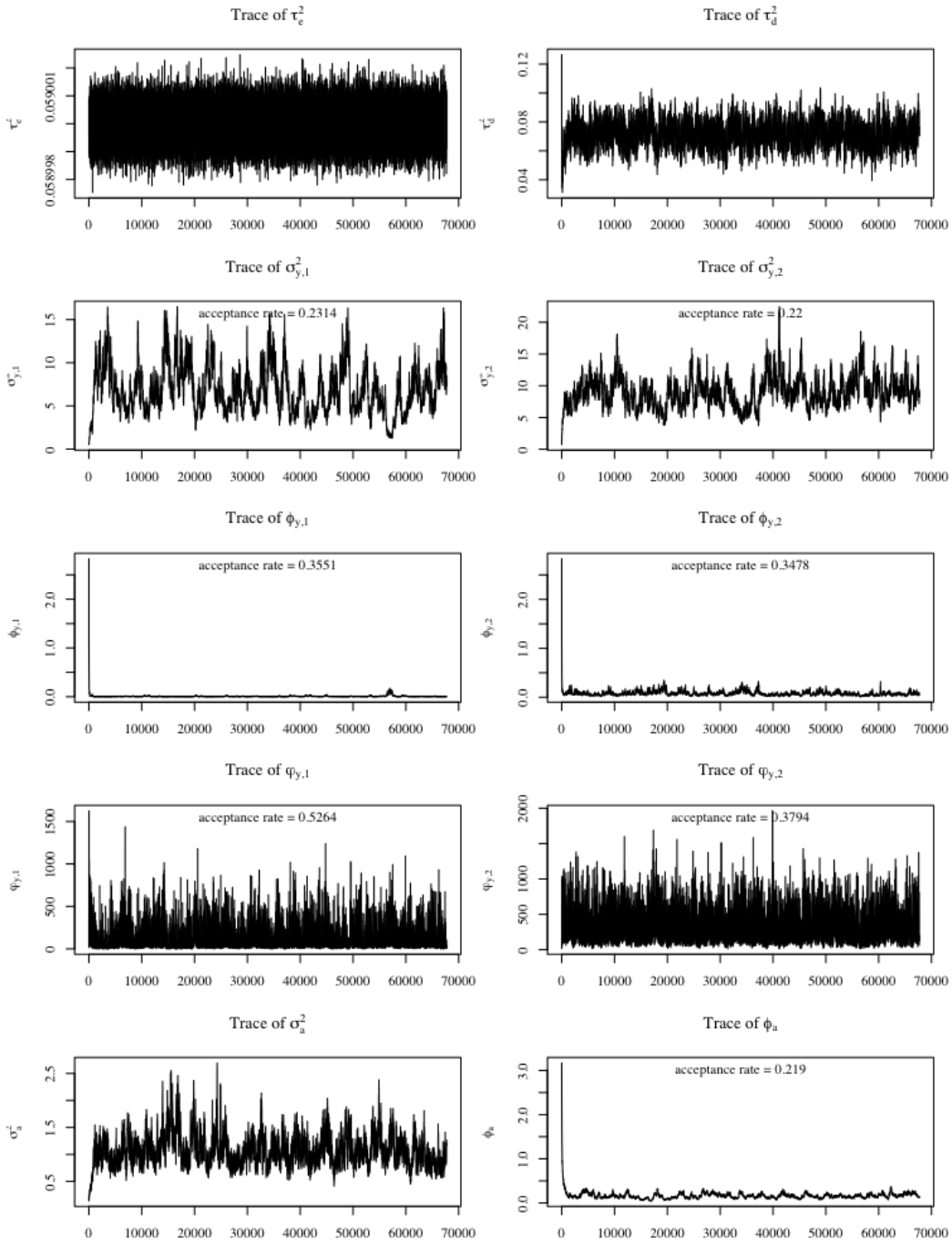

Figure 14. Trace plots of the covariance parameters of the joint Bayesian data fusion model Model 2-JBDF-NS for $PM_{2.5}$ NRI concentration.

Table 4 presents Geweke's diagnostic values to assess convergence of the Markov chains (Geweke 1992). Geweke's diagnostic is obtained by performing a two-sample z-test comparing whether the mean of the first 10% of the Markov chain post burn-in is equal to the mean of the last 50% of the Markov chain post burn-in, with variances adjusted for the lack of independence within the samples. Under the null assumption that the Markov chain has reached its stationary distribution, the mean of the two Markov chain sub-samples should be the same. As the table indicates, Geweke's diagnostic values are indicative of the fact that the Markov chains for each model parameters have reached convergence. The one extremely large value obtained for the regression coefficient of distance in Model 2-JBDF-S for NOx and for the regression coefficient of the interaction of weekday and morning in Model-2-JBDF-NS for PM2.5 could be explained as Type I error.

Table 4. Geweke' diagnostics for the regression coefficients $\boldsymbol{\beta_0}, \ldots, \boldsymbol{\beta_9}$ and covariance parameters of the best fitting models, Model 2-JBDF-S and Model 2-JBDF-NS, for NO_x and $PM_{2.5}$ NRI concentrations respectively.

		NO_x		$PM_{2.5}$	
Parameter		Geweke diagnostic	p-value	Geweke diagnostic	p-value
$\hat{\beta}_0$	Intercept	1.02	0.31	-0.31	0.76
$\hat{\beta}_1$	Downwind [DW]	0.73	0.47	0.21	0.83
$\hat{\beta}_2$	Weekday	1.60	0.11	0.91	0.36
$\hat{\beta}_3$	Morning	-1.43	0.15	1.16	0.25
$\hat{\beta}_4$	Weekday*Morning	0.47	0.63	-4.06	< 0.001
$\hat{\beta}_5$	(Traffic/Wind Speed) x 10^{-5}	0.34	0.73	-0.31	0.76
$\hat{\beta}_6$	(Traffic/WS)*DW x 10^{-5}	-0.88	0.38	-0.63	0.53
$\hat{\beta}_7$	Distance	-5.53	< 0.001	0.97	0.33
$\hat{\beta}_8$	Distance*DW	-0.44	0.66	0.16	0.87
a		–		–	
b		-0.40	0.69	0.34	0.74
τ_e^2	Nugget	-0.92	0.36	1.10	0.27
τ_δ^2		0.09	0.93	-1.77	0.08
σ_1^2	Sill - Downwind	–		1.22	0.22
ϕ_1	Downwind	–		0.52	0.60
φ_1	Downwind, Wind speed	–		-1.22	0.22
σ_2^2	Sill - Upwind	–		-0.27	0.79
ϕ_2	Upwind	–		0.21	0.83
φ_2	Upwind, Wind speed	–		0.32	0.75
$\sigma_{\hat{Y}}^2$		1.25	0.21	—	
$\phi_{\hat{Y}}$		0.70	0.49	—	
σ_α^2		0.25	0.80	-0.21	0.83
ϕ_α		0.67	0.50	1.71	0.09

Non-Stationary Regression-Based Bayesian Data Fusion

The prior specifications used for the regression-based Bayesian data fusion models are analogous to those used for the other two models. The spatial covariance parameters τ^2, σ_1^2, σ_2^2 and τ_1^2, τ_2^2, σ_1^2 and σ_2^2 in the individual and multiple pollutant data fusion models are provided with inverse Gamma priors with shape and scale parameters appropriately chosen. Covariance parameters ϕ_1, φ_1, ϕ_2 and φ_2 in both the individual and multiple pollutant model are provided with Gamma priors, as are the two parameters ψ_1 and ψ_2 that control the weights of the spatially-varying mixture defining $\eta_t^{(1)}(\mathbf{s})$ and $\eta^{(2)}(\mathbf{s})$. Finally, as before, the overall additive and multiplicative bias parameters, α_0 and α_1, and $\alpha_0^{(1)}$,$\alpha_0^{(2)}$ and $\alpha_1^{(1)}$,$\alpha_1^{(2)}$, in the individual and multiple pollutant models, are provided with independent Normal priors with large variances and mean equal to 0 (additive bias, α_0, and $\alpha_0^{(1)}$, $\alpha_0^{(2)}$) and 1 (multiplicative bias, α_1, and $\alpha^{(1)}$, $\alpha_1^{(2)}$), respectively. We perform posterior inference on each model parameter using samples from the joint posterior distribution. Samples are drawn using an MCMC algorithm, consisting of Gibbs sampling and Metropolis-Hasting steps. For each model and each pollutant, we update each parameter conditionally on the other model parameters and we run the MCMC algorithm for 100,000 iteration. We discard the first 50,000 iterations for burn-in and we use a thinning of 10 to reduce autocorrelation in the posterior samples.

Figures 15, 16, 17 and 18 present trace plots of the RLINE calibration terms, and of the covariance parameters for the best-performing regression-based Bayesian data fusion models for NO_x and $PM_{2.5}$ NRI

concentration, e.g. the stationary Bayesian data fusion model with 2012 emissions for NO_x and the non-stationary Bayesian data fusion model with 2010 emissions for $PM_{2.5}$.

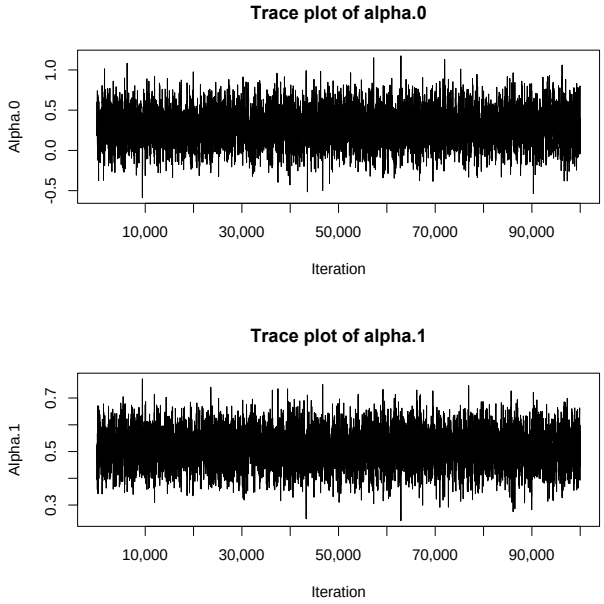

Figure 15. Trace plots of the additive (α_0) and multiplicative calibration term (α_1) for the RLINE output in the regression-based stationary Bayesian data fusion model for NO_x NRI concentration with 2012 emissions.

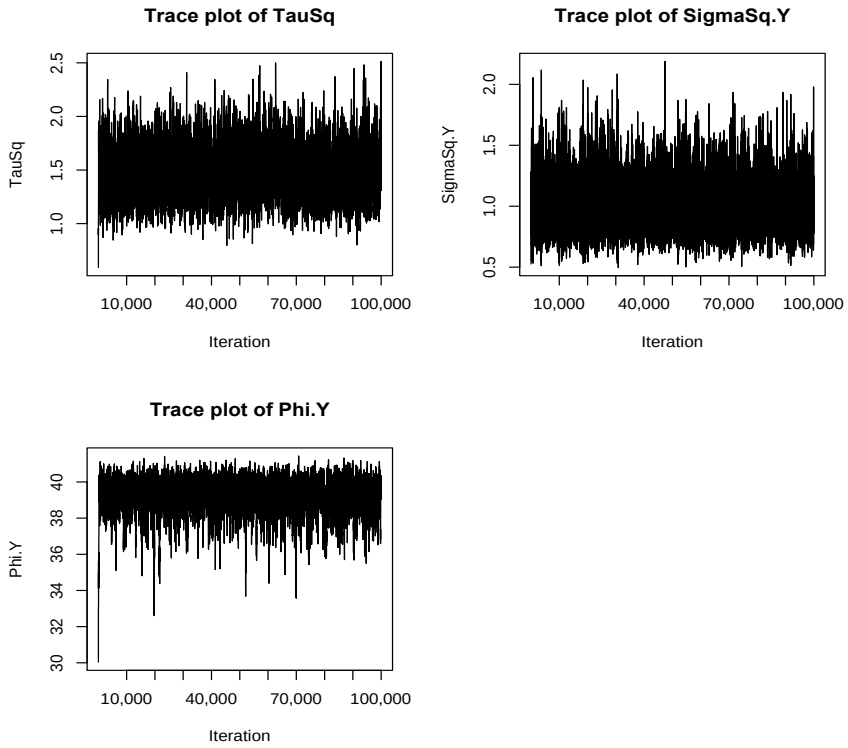

Figure 16. Trace plots of the covariance parameters of the regression-based stationary Bayesian data fusion model for NO_x NRI concentration with 2012 emissions.

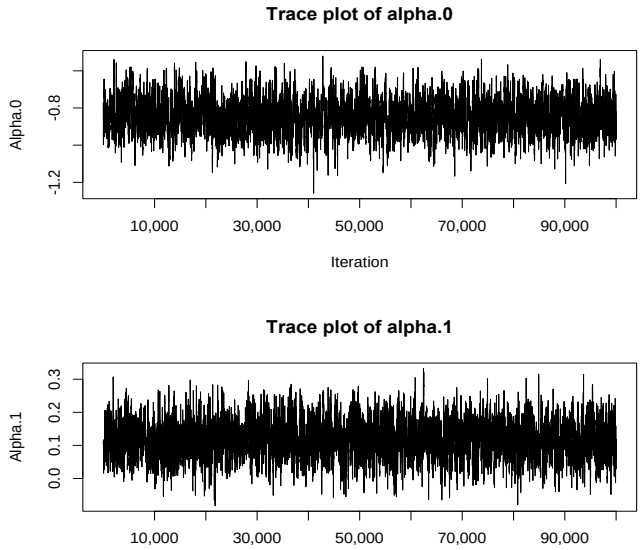

Figure 17. Trace plots of the additive (α_0) and multiplicative calibration term (α_1) for the RLINE output in the regression-based non-stationary Bayesian data fusion model for $PM_{2.5}$ NRI concentration with 2010 emissions.

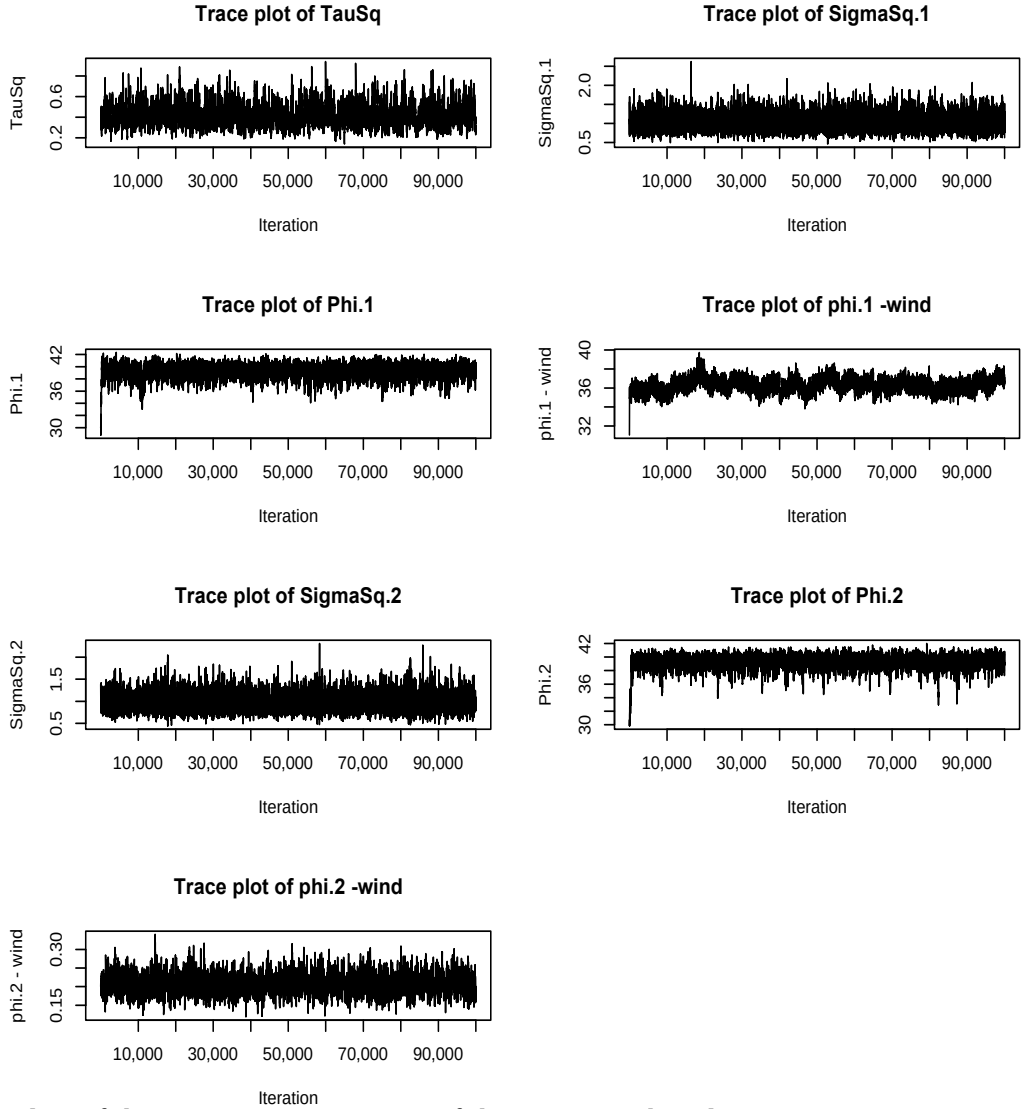

Figure 18. Trace plots of the covariance parameters of the regression-based non-stationary Bayesian data fusion model for $PM_{2.5}$ NRI concentration with 2010 emissions.

Table 5. Geweke diagnostics for the additive and multiplicative bias of the RLINE output, α_0 and α_1, and covariance parameters for the best fitting regression-based Bayesian data fusion model to NO_x and $PM_{2.5}$.

Parameter		NO_x		$PM_{2.5}$	
		Geweke diagnostic	p-value	Geweke diagnostic	p-value
α_0		0.50	0.62	0.21	0.83
α_1		-1.43	0.15	-1.43	0.15
τ^2	Nugget	1.40	0.16	0.31	0.76
σ_1^2	Sill - Downwind	–		0.19	0.85
ϕ_1	Downwind	–		-0.95	0.34
φ_1	Downwind, Wind speed	–		0.24	0.81
σ_2^2	Sill - Upwind	–		-0.12	0.90
ϕ_2	Upwind	–		1.47	0.14
φ_2	Upwind, Wind speed	–		3.77	< 0.001
σ_Y^2		0.44	0.66	—	
ϕ_Y		-0.95	0.35	—	

Analogously to the joint Bayesian data fusion models, Table 5 present Geweke's diagnostics for each model parameters for the best fitting regression-based univariate Bayesian data fusion models for NO_x and $PM_{2.5}$ NRI concentration, respectively. As the table indicates, with the exception of one parameter all Geweke diagnostic are consistent with the null hypothesis that the Markov chains for each model parameter have reached their stationary distributions. The only parameter with a large Geweke diagnostic value refers to the range parameter corresponding to the decay of the spatial correlation for $PM_{2.5}$ NRI as wind speed varies among upwind sites. We interpret the large Geweke diagnostic value for this parameter as an instance of a Type I error, that is, an incorrect rejection of the null hypothesis.

MODEL COMPARISON AND EVALUATION

We compare the predictive performance of the various models to that of other, simpler, counterpart models.

Non-Stationary Universal Kriging

Six models that differed only in the approach used to model the spatial dependence were considered in comparisons of the non-stationary universal kriging model. Table 6 summarizes these models, the combination of weighting schemes, and their covariance functions. The independent model, called model 1, simply models the log concentration $Y_t(\mathbf{s})$ for each pollutant, site $\mathbf{s}$ and time period t as $Y_t(\mathbf{s}) = \mu_t(\mathbf{s}) + \epsilon_t(\mathbf{s})$, where $\mu_t(\mathbf{s})$ is given by (2) and $\epsilon_t(\mathbf{s}) \overset{iid}{\sim} N(0, \tau^2)$. To determine whether it is necessary to model the non-stationarity in the spatial dependence of the log concentrations, a stationary model or "model 2" is fitted for each pollutant with $Y_t(\mathbf{s})$ and $\mu_t(\mathbf{s})$ defined as in (1) and (2), respectively, but with $\eta_t(\mathbf{s})$, $t = 1, \ldots, \mathcal{T}$ modeled as independent realizations over time periods t, $t = 1, \ldots, \mathcal{T}$, of a stationary mean-zero Gaussian process with an exponential covariance function. The definition of the weights in (5) is such that neither $w_{1,t}(\mathbf{s})$ nor $w_{2,t}(\mathbf{s})$ is identically equal to 0 at any time period t or site $\mathbf{s}$, implying that $\eta_t(\mathbf{s})$ is a mixture of two spatial processes. To determine whether the specification of $\eta_t(\mathbf{s})$ as a mixture of two non-stationary spatial processes improved predictive performance compared to a model that employs two different spatial processes for log concentration, one defined on the upwind region, and the second defined on the downwind region, we consider an additional weighting scheme: $w_{1,t}(\mathbf{s}) = 1$ if site $\mathbf{s}$ is downwind at time period t and 0 otherwise, and vice versa for $w_{2,t}(\mathbf{s})$. Using this simple binary weighting scheme, two additional models are fitted for each pollutant. "Model 3" uses the binary upwind-downwind weighting scheme and does not include the signed wind speed in the covariance functions of the two underlying spatial processes $\eta_{1,t}(\mathbf{s})$ and $\eta_{2,t}(\mathbf{s})$, hence these are modeled as mutually independent stationary spatial processes for each time period t with an exponential covariance function. "Model 4" uses the binary upwind-downwind weighting scheme

and includes the covariate signed wind speed in the covariance functions of $\eta_{1,t}(\mathbf{s})$ and $\eta_{2,t}(\mathbf{s})$ defined in (6). The final two models are the full model introduced earlier, as well as a simplification of the full model that investigate whether the signed wind speed is needed to explain the non-stationarity of the covariance function. "Model 5" uses (1), (2), (3) and (5), but the two underlying processes are modeled to be stationary with exponential covariance functions (i.e., without the covariate signed wind speed). Lastly, "model 6" is the full model.

Table 6. Description of the Kriging models. For each model, the trend term $\mu_t(\mathbf{s})$ is modeled according to (2). For each model, we report the type of weighting scheme used in the mixture, and the covariance functions used for $\eta_{1,t}(\mathbf{s})$ and $\eta_{2,t}(\mathbf{s})$. Models 1 and 2 do not express $\eta_t(\mathbf{s})$ as a mixture, thus the covariance function in the table refers to the covariance function of $\eta_t(\mathbf{s})$.

Model name	Weighting scheme	Covariance function
Model 1: Independence	None	Independence
Model 2: Stationary	None	Exponential covariance function
Model 3	Binary upwind-	Exponential covariance function
Model 4	Binary upwind-	Covariates in covariance function as in (6)
Model 5	As in (5)	Exponential covariance function
Model 6	As in (5)	Covariates in covariance function as in (6)

Joint-Modeling Bayesian Data Fusion Models

The predictive performance of the Bayesian data fusion models was evaluated using six models (Table 7) that differ in the approach used to model the bias of the log RLINE output (e.g., constant in space and time versus not) and for the type of spatial dependence structure hypothesized for the two latent processes, $\hat{\eta}_{1,t}(\mathbf{s})$ and $\hat{\eta}_{2,t}(\mathbf{s})$. Each model represents the large-scale spatial trend term $\hat{\mu}^{t}(\mathbf{s})$ according to (2). The simplest model, called "model 1-JBDF," assumes that the error of the RLINE output in representing the true, unobserved field is constant in space, thus $a_t(\mathbf{s})$ is equal to 0. "Model 2-JBDF" postulates that even though the RLINE output has a spatially additive error with mean 0, overall, the RLINE output does not have an additive bias, e.g., $a_0 \equiv 0$. "Model 3-JBDF" is the full model introduced (whether the small-scale spatial structure, $\hat{\eta}_t(\mathbf{s})$, of the unobserved true pollution field, $\hat{Y}_t(\mathbf{s})$, is stationary or not). For each of these three models, we contrast two cases: the first assumes that $\hat{\eta}_t(\mathbf{s})$ is a Gaussian process independent in time with mean 0 and with an exponential covariance function; the second assumes $\hat{\eta}_t(\mathbf{s})$ is equipped with the non-stationary covariance function described in (7). These cases are distinguished by appending "S" or "NS."

Table 7. Summary of the joint Bayesian data fusion models for log NRI of NO_x and $PM_{2.5}$.

Model name	Form of additive bias for RLINE	Covariance structure of $\hat{\eta}_t(\mathbf{s})$
Model 1-JBDF-S	$\delta_t(\mathbf{s}) \equiv 0$	Stationary: exponential
Model 2-JBDF-S	$a_0 \equiv 0$	Stationary: exponential
Model 3-JBDF-S	Full	Stationary: exponential
Model 1-JBDF-NS	$\delta_t(\mathbf{s}) \equiv 0$	Non-stationary, as in (7)
Model 2-JBDF-NS	$a_0 \equiv 0$	Non-stationary, as in (7)
Model 3-JBDF-NS	Full	Non-stationary

Regression-based Bayesian Data Fusion models

The second set of Bayesian data fusion models builds upon findings drawn after fitting the non-stationary universal kriging model. Two sets of models are explored for each pollutant. In the first model, the spatially-varying additive bias $\eta_t(\mathbf{s})$ of RLINE, which also accounts for the small scale residual spatial structure of the observed NRI field $Y_t(\mathbf{s})$, is modeled as a spatially and temporally-varying mixture of two independent in time, stationary, spatio-temporal processes $\eta_{1,t}(\mathbf{s})$ and $\eta_{2,t}(\mathbf{s})$, each equipped with an exponential covariate structure. The second model is the full model. Each set of models is used with the RLINE output derived from the 2010 or 2012 emissions inventory. The predictive performance of these regression-based Bayesian data fusion models is compared to that of the non-stationary universal kriging model.

PREDICTIVE PERFORMANCE

For each pollutant and for measurement type (concentration or NRI), the various models are compared with respect to their out of sample predictive performance. For the non-stationary universal kriging models, of the 286 observed NO and NO_x concentrations, we randomly selected 252 observations for model fitting, and held out 33 observations for model validation. The held-out sites were chosen so that at each time-period about 10-15% of the data was withheld for predictive performance evaluation, leading to holdout samples made of 1-3 observations per time-period, randomly drawn from the original complete dataset. One extreme outlying observation was removed from the analysis. Similarly, for BC, 245 observed concentrations were selected for model fitting, and 31 observations were held out for model validation. Again, one extreme observation was removed. For the Bayesian data fusion models, 254 observations were available for the NO_x NRI and 226 for $PM_{2.5}$. Of these, we used 221 randomly chosen NRI NOx observations for fitting and held out 33 observations for validation; for $PM_{2.5}$, 196 observations were used for fitting and 30 observations were held out for validation. In each case, the held out observations were sampled so that 1-3 observations were held out per time period.

Because the models were developed for log concentration, predictive performance was assessed by back transforming predictions to the original scale. Using the median of the posterior predictive distribution as the predicted value at each site, the predictive performance of each model was evaluated in terms of mean absolute prediction error (MAPE), root mean squared error (RMSE), Pearson correlation between the predicted values and the held-out data, average length of the 90% prediction interval (PI), and empirical coverage of the 90% PI. The latter statistic reveals whether the uncertainty in the prediction is correctly quantified: if empirical coverage is below the nominal level, assuming no bias in the predictions, the model is underestimating the variability/uncertainty in the predictions. Vice-versa, empirical coverage of the prediction intervals above the nominal level signifies that the model overestimates the variability/uncertainty.

APPENDIX 8 - EMISSION FACTORS

SENSITIVITY TO TEMPERATURE AND TIME-OF-DAY

Emission factors depend on operating temperature, vehicle-operating mode, and many other variables. Some broad trends can be generalized, e.g., $PM_{2.5}$ emission factors for gasoline vehicles using MOVES increase at low ambient temperatures. However, on-road (e.g., link-based) emission rates depend on variables that affect both emission factors and traffic activity, e.g., month, hour-of-day, speed, mix, vehicle mix, road type, and ambient temperature. Here sensitivity analyses are employed to evaluate several features that can affect on-road emissions. These analyses employ the models and data described earlier for Detroit, but use a simplified scenario and/or averaged results.

Figure 19 demonstrates the variation in emission rates by hour-of-day associated with ambient temperatures and weekday/weekend periods. This scenario considers an interstate highway (NFC 11) with an AADT of

165,000 and vehicle speed averaging 60 mph, which approximates I-96 near the Eliza Howell monitoring stations in the Detroit area. Emission rates are based on the models used for NEXUS and the 2010 calendar year (Snyder et al. 2014), which used TAFs from SMOKE and did not separate Saturday and Sunday periods. With respect to hour-of-day, Figure 19 shows that $PM_{2.5}$ and CO emissions are highest during the morning and evening rush hours on weekdays; emissions can be high during weekend midday periods. NO_x emissions follow similar trends, although the variation is smaller and levels tend to stay elevated during the midday. With respect to temperature, the highest emissions of CO occur with hours when ambient temperatures are elevated, and the highest emissions of $PM_{2.5}$ can occur on hours with low temperatures and high traffic volumes. Overall, this analysis shows that hour-to-hour variability of emission rates is large, as expected from diurnal pattern of traffic activity. It also shows that $PM_{2.5}$ and CO emissions have significant day-to-day variability (as compared to NO_x), which results from varying traffic activity as well as temperature and other effects.

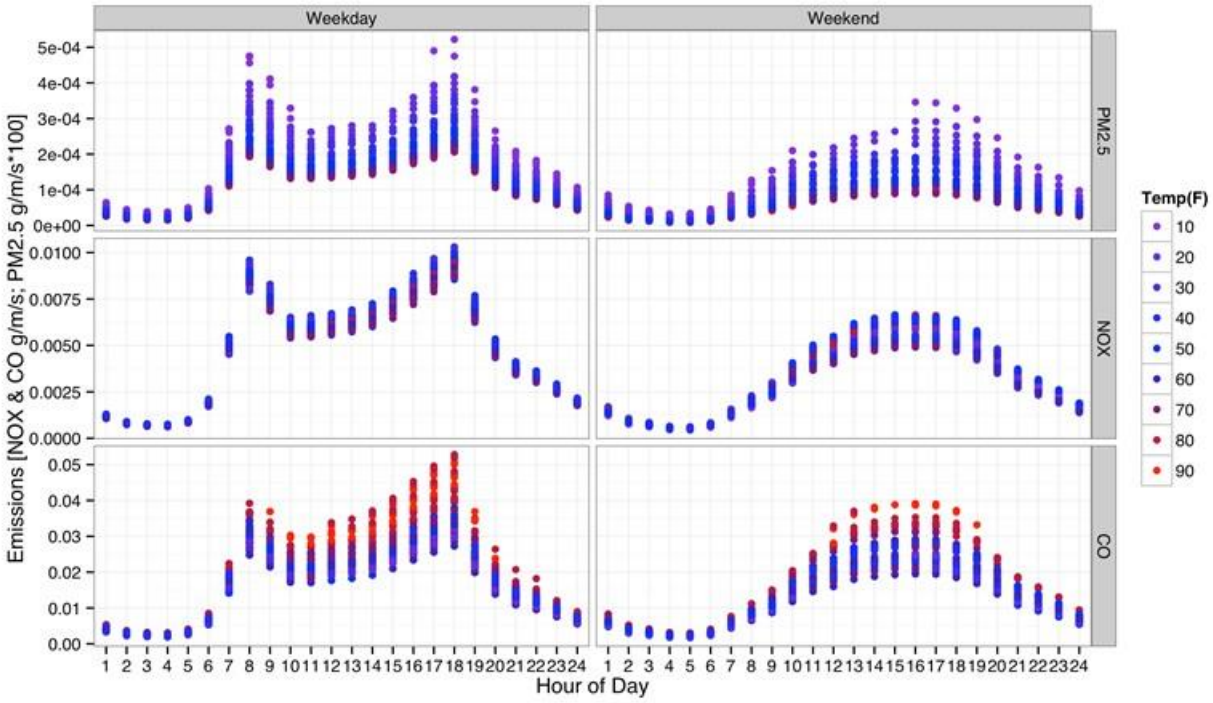

Figure 19. Diurnal emission rates of $PM_{2.5}$, NO_x and CO emissions for the highway scenario described in the text, showing hour-of-day and ambient temperature trends.

SENSITIVITY TO VEHICLE TYPE

A sensitivity analysis examines effects of vehicle type by comparing the variation of emission factors using the ratio of emissions of heavy-duty diesel vehicles (HDDV) to light-duty gasoline vehicles (LDGV) (Table 8). This ratio represents the passenger car equivalents (PCEs) for a HDDV, discussed earlier. Relatively modest changes in vehicle speeds or ambient temperatures can significantly alter the PCEs, e.g., as speeds decrease to zero for HDDVs; also, temperature and speed have the opposite effect on $PM_{2.5}$ as compared to CO and NO_x.

Overall, these examples demonstrate the uncertainty of emission rates used in dispersion modeling. Uncertainties in both emission factors and emission rates, among other factors, have been identified as important issues for mobile source inventories (Fujita et al. 2012; Huo et al. 2009; Wang et al. 2008; Zhang et al. 2010; Zhang et al. 2016; Zheng et al. 2009). The full-scale evaluations of emission factors presented later in the core report (which compare model predictions to observed concentrations) show several impacts, although the operational evaluation contrasting 2010 and 2015 emission factors did not yield significant differences.

Table 8. Ratio between HDDV and LDGV emissions of CO, NO_x and $PM_{2.5}$ by ambient temperature and speed bin. Averaged across months, based on 2015 MOVES with Wayne county parameters.

	Temperature (°F)										
Speed (mph)	0	10	20	30	40	50	60	70	80	90	100
	Carbon Monoxide (CO)										
2.5	1.3	1.3	1.3	1.3	1.3	1.3	1.3	1.3	1.0	0.8	0.7
5	1.2	1.2	1.2	1.2	1.2	1.2	1.2	1.2	0.9	0.8	0.7
10	1.1	1.1	1.1	1.1	1.1	1.1	1.1	1.0	0.8	0.6	0.6
15	1.0	1.0	1.0	1.0	1.0	1.0	1.0	0.9	0.7	0.6	0.5
20	0.9	0.9	0.9	0.9	0.9	0.9	0.9	0.9	0.7	0.5	0.5
25	1.0	1.0	1.0	1.0	1.0	1.0	1.0	0.9	0.7	0.6	0.5
30	0.9	0.9	0.9	0.9	0.9	0.9	0.9	0.8	0.6	0.5	0.5
35	0.8	0.8	0.8	0.8	0.8	0.8	0.8	0.8	0.6	0.5	0.4
40	0.8	0.8	0.8	0.8	0.8	0.8	0.8	0.7	0.5	0.4	0.4
45	0.7	0.7	0.7	0.7	0.7	0.7	0.7	0.7	0.5	0.4	0.4
50	0.7	0.7	0.7	0.7	0.7	0.7	0.7	0.7	0.5	0.4	0.4
55	0.7	0.7	0.7	0.7	0.7	0.7	0.7	0.6	0.5	0.4	0.3
60	0.7	0.7	0.7	0.7	0.7	0.7	0.7	0.6	0.5	0.4	0.3
65	0.6	0.6	0.6	0.6	0.6	0.6	0.6	0.6	0.4	0.4	0.3
70	0.5	0.5	0.5	0.5	0.5	0.5	0.5	0.5	0.4	0.3	0.3
75	0.4	0.4	0.4	0.4	0.4	0.4	0.4	0.4	0.3	0.2	0.2
	Nitrogen Oxides (NO_X)										
2.5	63	63	63	63	63	64	64	58	42	34	30
5	41	41	41	41	41	42	42	39	31	26	24
10	29	29	29	29	29	29	30	29	24	22	20
15	26	26	26	26	26	26	26	26	23	21	20
20	24	24	24	24	24	24	24	24	22	20	19
25	22	22	22	22	22	22	22	22	20	19	18
30	22	22	22	22	22	22	22	22	20	19	18
35	19	19	19	19	19	19	19	19	18	17	16
40	18	18	18	18	18	18	18	18	17	16	15
45	17	17	17	17	17	17	17	17	16	15	14
50	16	16	16	16	16	16	16	16	15	14	13
55	15	15	15	15	15	15	15	15	14	13	13
60	14	14	14	14	14	15	15	15	13	13	12
65	15	15	15	15	15	15	15	15	14	13	13
70	15	15	15	15	15	15	15	15	14	13	12
75	14	14	14	14	14	14	15	14	13	13	12
	Particulate Matter ($PM_{2.5}$)										
2.5	18	23	27	32	37	42	46	50	51	51	51
5	15	19	23	28	33	38	42	46	47	47	47
10	12	16	19	24	28	33	37	41	41	41	41
15	12	15	19	23	27	32	36	40	41	41	41
20	12	15	19	23	27	32	36	41	41	41	41
25	12	15	19	23	28	33	38	42	43	43	43
30	11	15	19	23	28	33	39	44	45	45	45
35	9	11	15	19	23	28	33	38	39	39	39
40	8	10	14	17	22	26	32	37	38	38	38
45	7	10	13	16	20	25	31	36	37	37	37
50	7	9	12	15	20	24	30	35	36	36	36
55	7	9	12	15	19	24	29	35	36	36	36
60	6	8	11	15	19	23	29	34	35	35	35
65	7	9	11	15	19	24	29	35	37	37	37
70	6	9	11	15	19	24	29	35	36	36	36
75	6	8	11	14	18	22	28	33	34	34	34

OPERATIONAL EVALUATION OF UPDATED EMISSION FACTORS

The updated (2015) emission factors mostly did not change R_{SP} for NO_x, though FB and V_G were lowered in three cases (at the near-road/ICHEM and urban sites; Table 9). CO showed similar but less consistent effects. Results for downwind and parallel winds at near-road and urban sites suggested improvements for

NO_x using the updated emission factors, e.g., R_{SP} increased and bias decreased at the near-road/ICHEM and urban sites, V_G increased at the same sites, and % Red decreased at the near-road/IGpCHEM site. For CO, the updated dataset did not change R_{SP} for downwind and parallel winds, but % Red was lowered at the near-road/EC9830T site, and bias and V_G were lowered at the other sites.

Day-of-week analyses for NO_x showed that the updated emission factors improved R_{SP}, bias and V_G on weekdays (all sites) and Saturdays and Sundays (most sites). Day-of-week analysis for CO gave similar trends, e.g., the updated emission factors lowered bias and V_G at the near-road/INDiI site across all day types. Seasonal trends were less consistent. For NO_x, the updated emission factors improved R_{SP} at the near-road and urban/IGpCHEM sites, and lowered bias and V_G at the urban site in winter; effects in other seasons were less consistent. For CO, investigations were hampered by missing data, but results with the updated inventory showed some improvements, e.g., in winter and fall, % Red decreased at the near-road site, and bias and V_G were lowered in most cases, and in spring and summer, bias and V_G were lowered at the near-road/INDiI and industrial sites.

Table 9. Summary of sensitivity analysis for emission factor inputs, comparing results of performance evaluation for original (2010) and updated (2015) emission inventory.

		NO_X					CO			
Metric	Supporting argument	Schools ICHEM	Near-road ICHEM	Near-road IGpCHEM	Urban ICHEM	Urban IGpCHEM	Suburban IGFC	Near-road EC9830T	Near-road INDiI	Urban INDiI
R_{SP}	2015 inventory highest?	~	~	~	~	~	~	~	○	
FB	2015 inventory lowest?	~	●	○	●	●	~	○	●	~
V_G	2015 inventory lowest?	~	●	~	●	●	~	○	●	~
% Red	2015 inventory lowest?	~	○	●	○	○	~	●	○	○

Acronyms: F2 = % of model + background within a factor of 2 of observed; FB = Fractional bias; ICHEM = Instrumental Chemiluminescence; IGpCHEM = Instrumental Gas-Phase Chemiluminescence; R_{SP} = Spearman's correlation coefficient; Red = reducible or random component of VG; VG = geometric variance.

The performance analysis suggested that RLINE performed slightly better using the updated emission factors. The updated inputs substantially changed emission factors for several vehicle classes, e.g., overall emissions from light duty gas vehicle (LDGV) and heavy-duty diesel vehicle (HDDV) classes increased by 48 and 30% for NO_x and CO respectively, and changes at certain speeds and temperatures could be larger.

To help interpret these changes as well as traffic activity estimates, which are frequently reduced to vehicle counts (see next section), emission factor differences among vehicle classes can be expressed as passenger car equivalents (PCEs) (S. Batterman et al. 2015a; Watkins and Baldauf 2012). As examples, using LDGV emissions as a base: NO_x emissions from a single HDDV represent 12 to 63 PCEs; CO emissions represent only 0.2 to 1.3 PCEs; and both NO_x and CO PCEs increase at lower speeds and colder temperatures (Table 8). The large changes in NO_x emission factors suggest that emission estimates can be very sensitive to the estimated traffic activity (e.g., commercial traffic counts), especially during cold weather and congestion when speeds are lower and the PCEs are high. However, impacts of emission factor changes also depend on the fleet mix. Our fleet mix estimates for commercial vehicles (which are mostly diesel) in Detroit range from 3 to 5% on most roads to 9% on portions of major roads like I-75 and I-94. Considering a NO_x PCE of 20 and 5% HDDVs, emissions from HDDVs and LDVs are equivalent, which shows the need to obtain accurate traffic activity data.

Uncertainty in mobile source emission inventories can arise from many sources, e.g., the representation of the road network geometry, uncertainty in traffic activity (e.g., vehicle-kilometers traveled or VKT, volume, vehicle type and age, speed, acceleration, and the number of cold starts), uncertainty in emission factors estimates for engine exhaust noted above and, for PM, uncertainty in emission factors for non-exhaust emissions (Fujita et al. 2012; Wang et al. 2008; Zheng et al. 2009). Other notable factors include a lack of traffic counts and on-road emission measurements, and discrepancies between fleet classifications and VKT needed by models and the available statistical summaries (Snyder et al. 2014; Zheng et al. 2009). Because fleet mix and VKT data usually are collected and aggregated at the county level, data may not be representative of the city or the roads of interest. As noted above, even modest changes in the commercial fraction of traffic may significantly affect emissions since one HDDV can emit the equivalent of many passenger cars for NO_x and $PM_{2.5}$ (PCE for PM ranged from 6 to 51, depending on temperature and speed). This may be especially important in Detroit given the considerable through traffic of commercial vehicles (mostly HDDVs) crossing the Ambassador Bridge to or from Canada via along I-75 and I-94, which may have the effect of increasing the HDDV fraction among these roads and boosting NO_x emissions. NO_x also may have been underestimated since the simplified emission factors averaged out higher emissions from cold starts. While these issues may be less important for mobile source inventories when aggregated to the annual average and city-wide level, these issues may be important for estimating spatially- and temporally resolved exposures.

APPENDIX 9 – TEMPORAL ALLOCATION FACTORS

SENSITIVITY ANALYSIS

A sensitivity analysis compared RLINE results using the Detroit-specific TAFs to those in the original Detroit inventory, which were generated from SMOKE using a combination of vehicle and road types to allocate annual traffic activity. The SMOKE TAFs also lumped Saturday and Sunday together into a single weekend profile, and did not treat holidays separately. RLINE was used to predict NO_x and $PM_{2.5}$ concentrations near an idealized road configuration with two road types (NFC 11 and 12) and 2010-2012 Detroit City Airport meteorology. The modeling used a receptor placed 10 m north of an east-west road (like the near-road Eliza Howell site). We also evaluated the sensitivity of switching from NFC 11 (interstate) to NFC 12 (limited access primary highway) which has a lower fraction of HDDVs. As shown in Figure 20, the Detroit-based TAFs increase concentrations by approximately 20% (NFC 12) to 40% (NFC 11), which is consistent with a higher proportion of commercial traffic activity allocated to the overnight hours when meteorological conditions are more stable and unfavorable for dispersion. The figure also shows that switching the road type from NFC 11 to NFC 12 significantly reduced concentrations, a result of fewer heavy-duty diesel vehicles. These results suggest that differences in the treatment of commercial traffic activity can significantly affect emissions. However, these differences also are affected by the classification of vehicle types, which is only approximated by the NFC categories and the TAFs, and a full-scale sensitivity analysis of TAFs presented below shows small and potentially negligible changes.

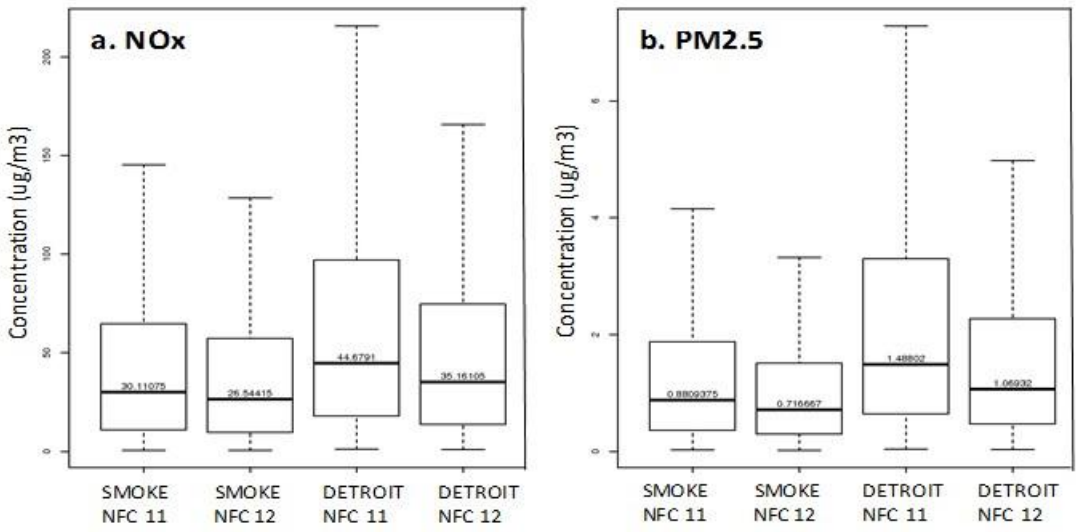

Figure 20. Distribution of predicted NO_x and $PM_{2.5}$ concentrations at the Eliza Howell near-road site using NFC11 and NFC 12 road types and SMOKE and Detroit-based TAFs. Outliers are omitted.

OPERATIONAL VALIDATION

The three sets of TAFs yielded few differences in either NO_x and CO predictions that exceeded the significance thresholds. Thus, the Detroit-specific TAFs that separated commercial and non-commercial traffic did not perform better than the simpler and default TAFs. This result was unanticipated, especially for NO_x, given the differences between commercial and non-commercial vehicles, and the differences seen in the simplified analyses (discussed previously). The fairly large hour-to-hour differences in TAFs at the hourly level may be "washed out" at the daily level or just not observable given other errors and uncertainties. In addition, the local TAFs were based on only the larger Detroit area roads equipped with permanent traffic monitoring recorders. Smaller roads can account for a sizable fraction of TRAP emissions, e.g., based on the Detroit link-based inventory (Snyder et al. 2014), the smaller (non-trunkline) roads accounted for 60% of total VKT in 2010. The use of local TAFs might improve modeling at the hourly level, which was beyond the present scope, as has been suggested elsewhere (Lindhjem et al. 2012).

APPENDIX 10 - METEOROLOGY

COMPARISON OF AIRPORT AND NEAR-ROAD DATASETS

As of May 2015, 79 near-road sites in the U.S. monitored NO_2 and often other pollutants (https://www3.epa.gov/ttnamti1/nearroad.html). Of the 72 sites with listed latitude and longitude coordinates, the distance to the nearest NWS station averaged 18.5 km, and a NWS station was within 5 km of six of the sites, and within 10 km of 28 of the sites. These distances suggest that the meteorological data inputs for dispersion modeling may not be representative of near-road settings.

We compared the meteorological data collected at the five airport sites. All sites have relatively good data completeness (at least 97% valid hours for the 2010-2012 period). Several differences between sites are noted. Hour-of-day average wind speeds varied by 0.5-1.0 m s^{-1} across the sites (annual average is ~ 4 m s^{-1}), and the variation was greatest during nighttime hours. The highest average wind speeds were observed at Willow Run and the lowest at Ann Arbor. Detroit Metro had the fewest calm hours (209 hours) and Ann Arbor the most (653 hours). Detroit City tended to have fewer least stable conditions, higher frictional velocities (U*), higher roughness lengths (Z_o), and larger positive values of Monin-Obukhov length (MO)

during nighttime hours, which would indicate less stable conditions. In contrast, Willow Run had the most stable conditions of the five sites. This analysis, as well as that conducted by the U.S. Environmental Protection Agency for NEXUS (Isakov et al. 2014), indicated that the Detroit City Airport, which is fairly centrally located in the region, was likely the most representative site among the airport datasets for modeling TRAPs.

We also confirmed that the SFC files generated using AERMET and the NWS data similar or identical to those distributed by the Michigan Department of Environmental Quality (MDEQ) for air quality modeling purposes (Michigan Department of Environmental Quality).

SENSITIVITY TO WIND SPEED AND DIRECTION

Wind speeds below 2 m s^{-1} are considered low wind conditions or "calms." The latest version of AERMET includes a minimum wind speed threshold; wind speeds below this threshold are labeled as "calm" and dispersion is not calculated for these hours. (This threshold was introduced after 1-min data became available, which averaged multiple instantaneous measurements throughout the hour to determine hourly average wind speed and direction. Previously, measurements were taken only once during the hour.) AERMOD documentation recommends a minimum wind speed threshold of 0.5 m s^{-1}. Using 2010 Detroit City Airport meteorology, 56 hours (<0.75%) would be labeled as "calm" and no dispersion would be calculated. As noted above, the number of hours of calms varied three-fold at the five NWS sites (209 to 653 hours for the 2010 to 2102 period).

Because high concentrations can be produced under calm and low wind speed conditions, we undertook a diagnostic evaluation using RLINE modeling (Snyder et al. 2014) and data from the I-96 Federal Highways Administration (FHWA)/EPA field study campaign in Detroit. This field study utilized four monitoring sites near Interstate 96, an east-west highway with 8 to 10 lanes at this location. Sites were located 10, 100, and 300 m north and 100 m south of the highway. (Figure 6 shows aerial views of the study sites.) Measurements of air pollutant concentrations, traffic counts, and meteorological parameters were collected from September 26, 2010 through June 20, 2011 (Kimbrough et al. 2013).

Modeled and observed hourly data, matched in time, are shown in Figure 21. The scatterplots show some overprediction at the 10 m roadside site, but underpredictions at the other sites; these results apply for both NO_x and CO. Stratification by wind speed showed that the highest overpredictions occur at the lower windspeeds (<2 m s^{-1}). However, underprediction also occurs at low wind speeds. Figure 22 examines low wind speed conditions and shows that while the geometric means of both pollutants generally increased, changes were not significant. The effect of wind direction is examined in Figure 23, which shows ratios of modeled to measured concentrations as a function of wind direction, again for the same low wind speed conditions. Winds from the south tend to result in overpredictions at the (downwind) 10, 100 and 300 m sites, and similarly, winds from the north tend to result in overpredictions at the (downwind) sites. Winds from the east and west, which represent winds "parallel" to the road, typically resulted in underpredictions. (Several obvious outliers, including both over and underestimation, at the 10 m CO site appear related to a non-roadway related sources.) The potential errors during downwind and parallel conditions are further explored in the operational validation and additional sensitivity analyses.

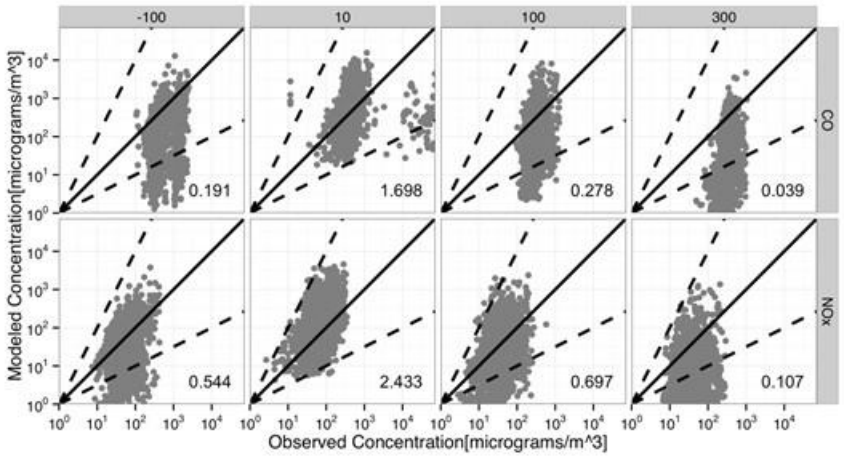

Figure 21. Scatterplots of measured and modeled hourly CO and NO_x concentrations at the four near-road Eliza Howell monitoring sites for 2010. The solid line represents the 1:1 line, dashed lines represents the factor of two range. Number inset is the geometric mean bias (MG Snyder et al. 2013)

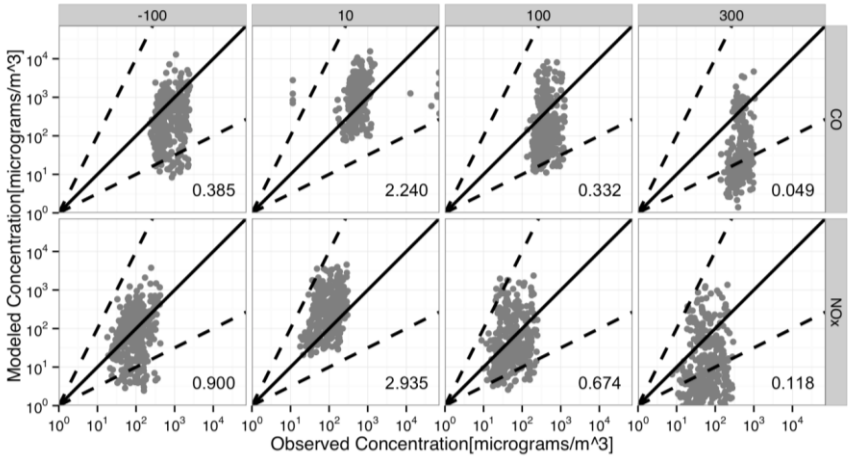

Figure 22. Scatterplots of measured and modeled hourly CO and NO_x concentrations at low wind speeds (<2 m s^{-1}). Otherwise at Figure 21.

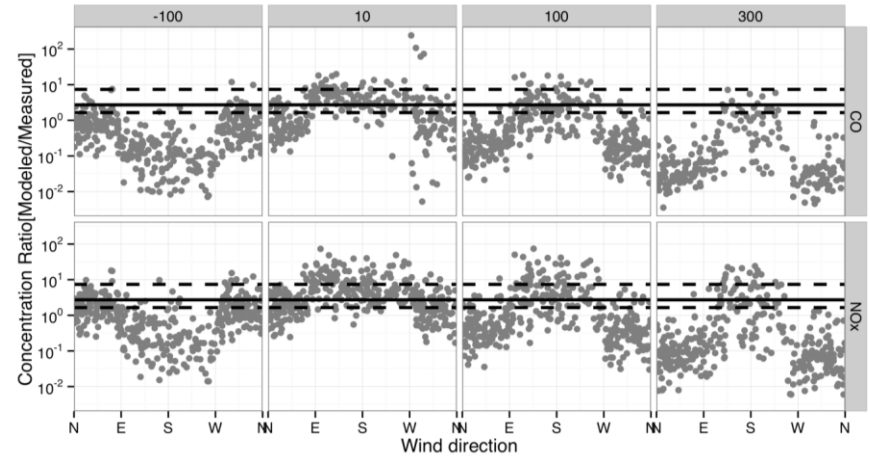

Figure 23. Scatterplots of the ratio of modeled to measured hourly CO and NO_x concentrations at the four near road monitring sites for low wind speeds (<2 m s^{-1}) conditions versus wind direction. The solid horizontal line represents the 1:1 line, the horizontal dashed lines represents the factor of two range.

WRF METEOROLOGICAL DATA

A potential source of meteorological inputs for dispersion modeling is the *Weather Research and Forecasting (WRF) Model*, a mesoscale numerical weather prediction system designed to serve both atmospheric research and operational forecasting needs (http://www.wrf-model.org/). WRF data is continuous in space and time, and can serve as a diagnostic reference providing spatial information (typically at 12 km intervals). The latest version (V3.0) of the Meteorological Model Interface tool (www.epa.gov/ttn/scram/models/relat/mmif/MMIFv3.1_Users_Manual.pdf) was used to extract the meteorological fields from WRF for the months of January and July 2010 for grid cell containing downtown Detroit files, and key meteorological variables were compared to AERMET-generated SFC files based on Detroit City (KDET) airport data for the same periods. (This analysis was feasible given data availability of WRF data from other projects.)

Diurnal hourly-averaged plots comparing these variables show several differences (Figure 24). Wind speeds from MMIF-generated meteorology were lower during January, especially at night; wind speeds are more similar during July. Frictional velocity (U*) had a more pronounced diurnal range in MMIF than in AERMET, e.g., MMIF frictional velocity was higher during daytime and lower during night hours. Wind directions rotated up to 20 degrees, depending on season and time of day. The surface heat flux was higher using MMIF, especially during January. Finally, the MMIF surface roughness length (Zo ~ 0.8 m) is significantly higher than AERMET (Zo ~ 0.2 m). Overall, these differences lead to more stable conditions for Detroit when using WRF/MMIF data as compared to AERMET, which would elevate near-road concentrations as shown earlier for representative conditions in Figure 2.

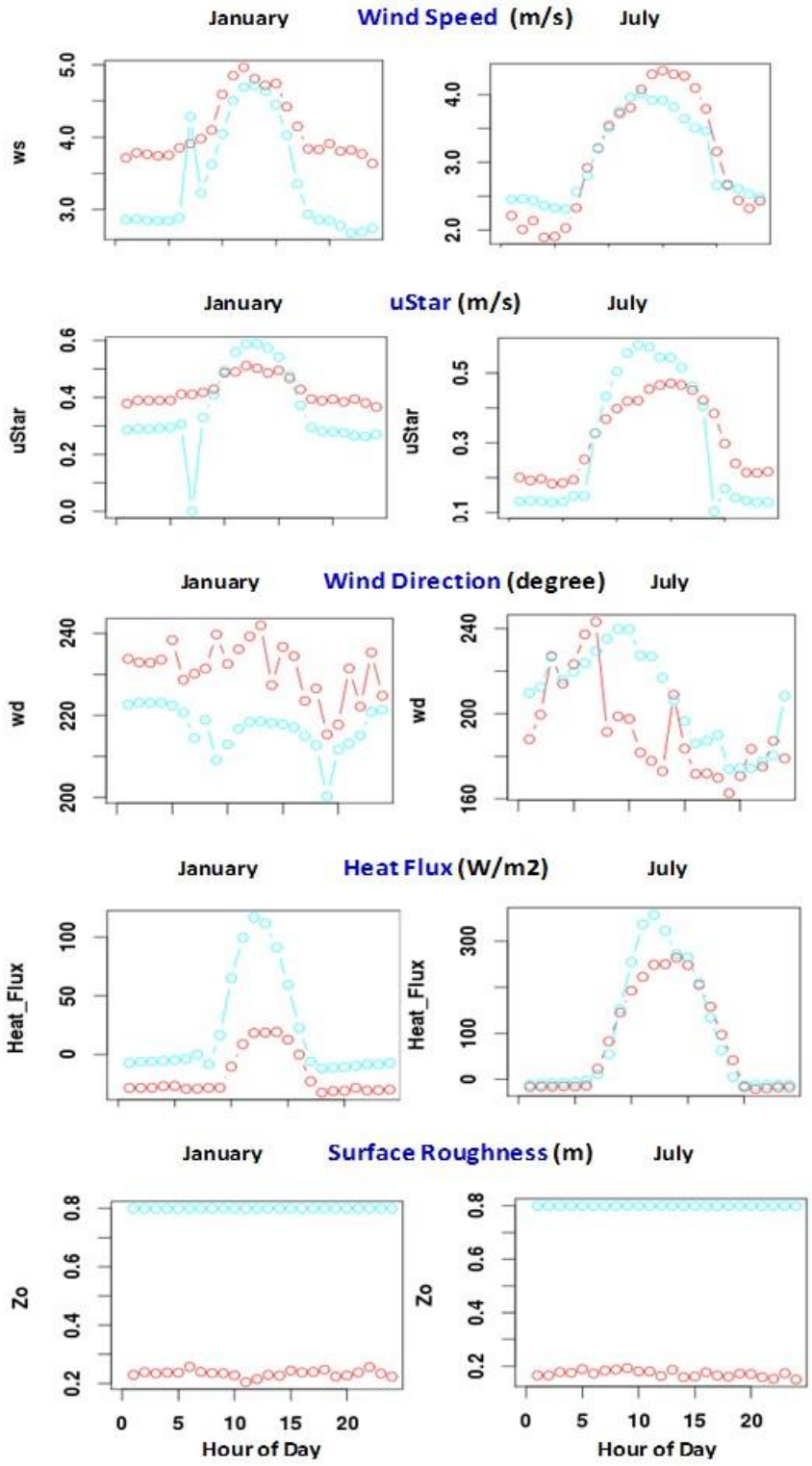

Figure 24. Comparison between hourly-averaged AERMET (KDET, pink) and WRF/MMIF (blue) meteorological parameters. Plots show wind speed, friction velocity, wind direction, heat flux and surface roughness, for hour of day and months of January and July, 2010.

OPERATIONAL EVALAUTION

As expected, RLINE predictions were sensitive to the selection of the meteorological inputs (Table 10). Generally, the best match to monitored data was obtained using on-site/KDET meteorology. For example,

for NO_x at the near-road and urban sites, on-site/KDET meteorology gave the highest R_{SP} (0.57 to 0.74) among the lowest bias, and the lowest V_G (at these plus the other sites). The best performing case (NO_x at the near-road site using the IGpCHEM instrument) also had the lowest % Red with the on-site/KDET data. While the schools site performed better with the NWS data, R_{SP} was low (0.32 to 0.43). Comparing the NWS data both with and without the on-site data, KDET obtained better performance in most cases. CO results were similar, e.g., on-site/KDET data attained among the highest R_{SP} at near-road and urban sites, the best performing case (near-road site, EC9830T method) had the only improvement seen in % Red (although higher bias), and V_G was generally lowered. At sites more distant from roads, performance trends for CO were less clear and often comparable for the four meteorological datasets due to the variation and overlap of R_{SP} and FB across the sites, while V_G and % Red were very similar at most sites.

Analyses by wind direction, weekday and season, while not definitive, again suggested that best performance for data subsets was attained using on-site/KDET meteorology. For NO_x, weekday results largely mirrored results discussed earlier, but Saturday and Sunday results were improved (e.g., higher R_{SP}) at only the near-road site (IGpCHEM instrument). By season, only the near-road site followed the overall trend. Interestingly, results by wind direction show better performance using KDTW rather than KDET meteorology at the near-road site. This site is at the western part of the study area and, unlike the other monitoring sites, is about the same distance to the two sites (20 km to KDTW, 22 km to KDET). Nevertheless, both NWS datasets gave relatively high R_{SP} at this site (0.57 – 0.70; IGpCHEM monitor). For CO, missing data hampered analyses, but on-site/KDET sometimes improved performance, e.g., this dataset obtained the highest R_{SP} at the near-road (EC9308T method) and urban sites during weekdays and during downwind conditions, and during winter at the near-road site (EC9830T) other site had lower bias and V_G using on-site/KDET. However, other CO results were inconsistent, e.g., on-site/KDET meteorology increased bias and V_G during downwind conditions at the near-road and urban sites, and parallel winds lowered R_{SP} at the urban site. Changes at the suburban mostly fell below the significance threshold (e.g., 0.05 for R_{SP}).

The sensitivity of RLINE results to meteorological inputs highlights the importance of appropriate input data. Some results tended to differ by site. For the sites nearest roads, on-site/KDET followed by KDET performed best, e.g., attaining the highest R_{SP}. At the suburban and urban sites, performance with KDET data also was better than with KDTW, but NWS data performed better than on-site. These sites are farther from major roads, and monitored concentrations likely result from multiple emission sources and not just traffic on the nearby road. In these cases, on-site meteorological measurements may be less representative for dispersion modeling than airport data, at least under some source and meteorological conditions, e.g., ground level emissions during calms, and NWS data may better represent the conditions affecting dispersion. Prior dispersion modeling in Detroit has judged both NWS sites to be representative, e.g., modeling of SO_2 emitted from mostly elevated point sources used KDTW (Michigan Department of Environmental Quality 2015), while TRAP modeling used KDET (Stuart Batterman et al. 2014). As noted, individual meteorological parameters, e.g., wind speed or direction, typically are highly correlated between sites, although some differences were identified, especially at the suburban site (Allen Park). However, the combined effect of different meteorological datasets is best determined by sensitivity analyses examining pollutant predictions.

We next compared the impact of using KDET versus KDTW meteorology for receptor sets 2 (NEXUS) and 3 (Detroit residences). These two sets of impact show high correlation ($R_{SP} > 0.85$) on most days (Figure 25), although somewhat lower correlations on a few days (e.g., 3/1/2011 and 12/2/2011) occurred due to relatively large changes at a subset of receptors located across the area; otherwise no systematic spatial or other pattern was observed. The most striking observation, however, of this comparison are the large day-to-day shifts in the bias between predictions using KDET and KDTW meteorology. Of the 28 days modeled, predictions using KDTW meteorology were biased upwards on 16 days, downwards on 3 days (4/6/2011, 5/12/2011, 9/21/2011), and similar on the remaining 11 days. These results, which include weekdays and weekends, are attributable solely to the meteorological inputs. (Stratification by season, day

type and other factors was not attempted due to the limited sample size.) These changes appear to be driven by wind speed and stability effects, and receptors clustered within about 100 m of M-10 and I-94 were especially affected. These large changes were unexpected since daily averages and meteorological parameters at the two NWS sites were highly correlated.

Table 10. Summary of sensitivity analysis for meteorology inputs, showing results of performance evaluation for NO_x and CO for three comparisons. Symbols: ● = improved/supporting, ○ = diminished/contrary, ~ = comparable, ' ' indeterminate (sets overlap by more than the minimum of 0.05 and 50% of the smaller within-set range).

		NO_X					CO			
Metric	Supporting argument	Schools ICHEM	Near-road ICHEM	Near-road IGpCHEM	Urban ICHEM	Urban IGpCHEM	Suburban [illegible]	Near-road EC9830T	Near-road INDiI	Urban INDiI
R_{SP}	On-site/KDET highest?	○	~	●	~	~	○	~	~	~
	KDET > KDTW?		●	●	●	●	●	●	●	●
	On-site > NWS?	○		●		●	○			
FB	|On-site/KDET| lowest?	○	●	○	●	●	~	○	●	●
	|KDET| < |KDTW|?									
	|On-site| < |NWS|?	○		○				○		
V_G	On-site/KDET lowest?	~	●	~	~	~	~	○	~	~
	KDET < KDTW?						●			
	On-site < NWS?	○	●	●	●	●	●	○	●	●
% Red	On-site/KDET lowest?	○	○	●	○	○	○	●	○	○
	KDET < KDTW?							●		
	On-site < NWS?	●	○		○	○	○	●	○	○

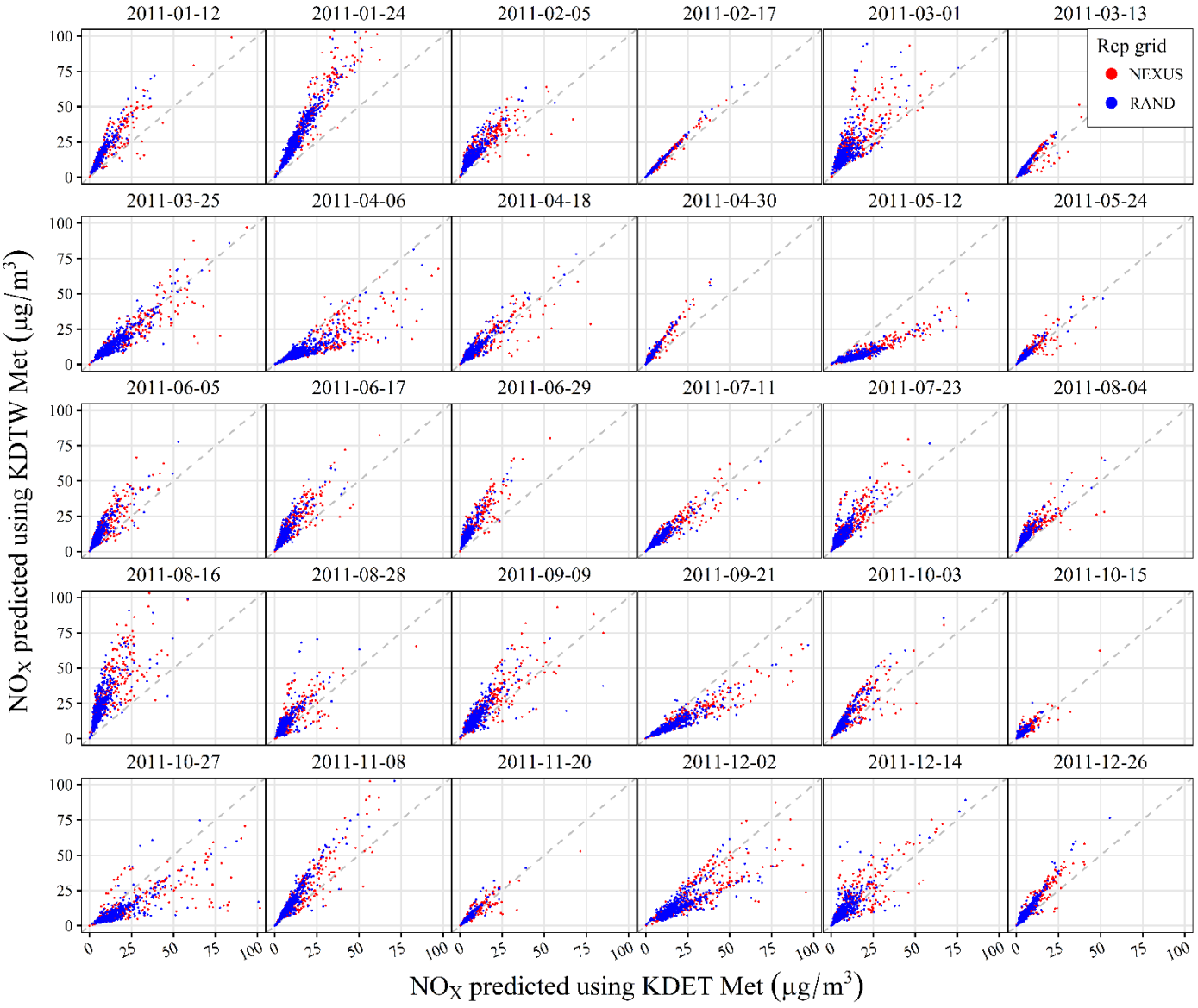

Figure 25. Scatterplots of NO_X predicted using KDET or KDTW meteorology at NEXUS (n=346) and Detroit residences (n=543) by days. Each plot shows the 1:1 line and is truncated at 100 µg m^{-3}.

Application to the NEXUS and Detroit residences receptor sets showed that meteorological datasets obtained at NWS stations 18 km or more apart can make large differences in daily concentration predictions on some days, which supports findings from comparisons at the monitoring sites. Both NWS are at airports, and the surrounding terrain is flat and mostly urban, commercial, wooded, or agricultural. The differences in predicted concentrations seem are likely to result mainly from changes in atmospheric stability that alters near-road concentration gradients, possibly due to very stable conditions which can cause the highest concentrations (MG Snyder et al. 2013). This suggests the possibility of significant exposure measurement error if the meteorological data is not representative, e.g., as measured at a distant site. Moreover, errors may be higher for more vulnerable populations, as portrayed by the NEXUS receptors for children who lived close to major roads.

Due to siting and instrumentation limitations, relatively few air quality monitoring sites, including the near-road sites, measure all of the meteorological parameters required for dispersion modeling. Thus, local measurements were blended together with NWS (or other) observations. While this approach is workable, incorporated in the AERMET processor, and generally obtained the best performance in the Detroit

application, a full set of local measurements may be preferable for obtaining wind fields that are the most representative of near-road environments. This option, which could not be fully tested in Detroit, leads to a recommendation to collect as full set of local meteorological measurements for dispersion modeling when practicable (including factors such as ground cover, surface roughness, and other factors that affect the spatial variation in wind fields). This reinforces long standing model guidance that recognizes the increased heat flux and surface roughness in urban areas and the general need for multiple monitoring sites in large urban areas (Giambini et al. 2012; U.S. Environmental Protection Agency 2000). However, no specific guidance is yet provided for near-road modeling. For larger roads in urban settings, such modeling involves winds, emissions and pollutant dispersion transitioning from the road "microenvironment," often large paved areas (e.g., portions of the right-of-way for I-96 in Detroit exceeds 150 m in width as each traffic direction includes three local and three express lanes, a two lane service road, multiple shoulders, and some vegetated buffers), to the adjacent populated "microenvironment," which can be mostly suburban in nature, dominated by buildings and trees and with relatively little flat paved surfaces. Guidance defining the most representative meteorological data for traffic-related emissions in such settings, which differs from the general urban environment, would helpful for improving near-road modeling.

APPENDIX 11 – RECEPTOR SETS

This Appendix describes three receptor sets used to evaluate RLINE and to show the sensitivity of exposure estimates produced by dispersion models to meteorological, emission and traffic allocation inputs. The modeling system described in Appendices 4 through 8 is used to predict daily average concentrations of CO and NO_x. The sensitivity of predictions is evaluated by comparing baseline (or "nominal") and alternative inputs for meteorological, emission, and traffic allocation parameters. These comparisons include the use of four years of ambient monitoring data as well as exposure estimates predicted for both general and "vulnerable" populations in Detroit, MI. The same performance metrics as used in the core report are used to examine downwind and parallel winds, and look at day-of-week effects and season effects.

The sensitivity analyses used three sets of receptors. The first placed receptors at the near-road monitoring sites in the study domain (n=5). The second and third sets respectively represent location of a vulnerable school-age population and the general population (Figure 26). The second set used receptors that represented locations of homes (n=218) and schools (n=146; total n = 364) of children with asthma participating in the NEXUS study (called "NEXUS" receptors) (Vette et al. 2013). Approximately two-thirds of these children lived within 175 m of major roads (AADT > 75,000) at the time of enrollment into NEXUS, thus, this set oversamples near-road locations. The third set was designed to be representative of residence locations in Detroit. This set, called "Detroit residences," was created by randomly selecting (with weighting by block population) 1000 of the 2010 Census blocks in Detroit, which resulted in 543 unique blocks. Receptors were placed at the building footprint centroid of the highest occupancy occupied parcels in each selected block (U.S. Census Bureau 2015; Urban 2014).

Distances to the nearest road with AADT > 10,000 were calculated for receptors in sets 2 and 3. For the NEXUS receptors, 61% were within 200 m, 20% within 200 – 400 m, and 19% beyond 400 m; for the Detroit residences, these three groups contained 57, 29 and 13% of the population-weighted receptors, respectively. The differences between receptor sets 2 and 3 reflect the design of the NEXUS study which selected households that were near major roads (<200 m) as well as comparison households that were further away (>350 m), however, differences are somewhat diminished since many NEXUS children moved during the study period and since schools were not preferentially located. We also calculated the number of large roads within 500 m of each receptor.

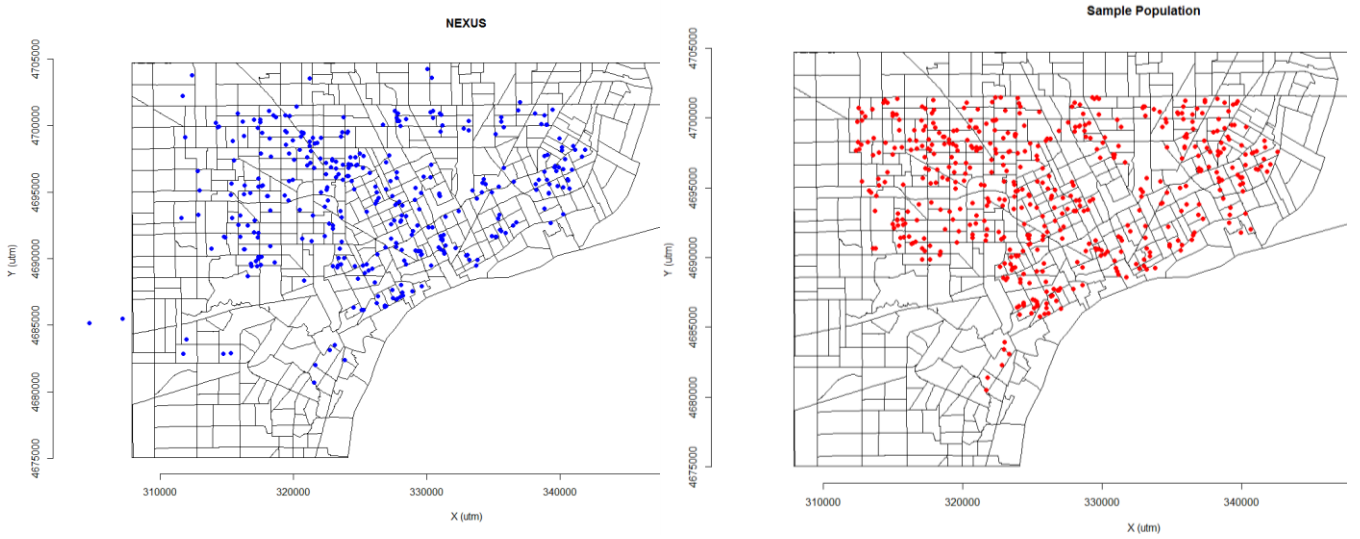

Figure 26. (Left) Locations of NEXUS receptors, representing homes and schools in the NEXUS cohort; (right) Location of Detroit residences receptors, representing a population-weighted sample in Detroit. Maps show block groups within Detroit.

REFERENCES

[Anonymous]. 2015. Air quality system (aqs) data mart.US EPA.

Aguilera I, Sunyer J, Fernández-Patier R, Hoek G, Aguirre-Alfaro A, Meliefste K, et al. 2007. Estimation of outdoor NO, NO2, and BTEX exposure in a cohort of pregnant women using land use regression modeling. Environmental science & technology 42:815-821.

Allen RW, Amram O, Wheeler AJ, Brauer M. 2011. The transferability of no and no 2 land use regression models between cities and pollutants. Atmospheric Environment 45:369.

Arunachalam S, Brantley H, Barzyk TM, Hagler G, Isakov V, Kimbrough ES, et al. 2015. Assessment of port-related air quality impacts: Geographic analysis of population. International Journal of Environment and Pollution 58:231.

Baldauf R, Thoma E, Hays M, Shores R, Kinsey J, Gullett B, et al. 2008. Traffic and meteorological impacts on near-road air quality: Summary of methods and trends from the raleigh near-road study. J Air Waste Manag Assoc 58:865-878.

Baldwin N, Gilani O, Raja S, Batterman S, Ganguly R, Hopke P, et al. 2015. Factors affecting pollutant concentrations in the near-road environment. Atmospheric Environment 115:223-235.

Banerjee S, Gelfand A, Knight JR, Sirmans C. 2004. Spatial modeling of house prices using normalized distance-weighted sums of stationary processes. Journal of Business & Economic Statistics 22:206-213.

Barzyk TM, George BJ, Vette AF, Williams RW, Croghan CW, Stevens CD. 2009. Development of a distance-to-roadway proximity metric to compare near-road pollutant levels to a central site monitor. Atmospheric Environment 43:787-797.

Barzyk TM, Isakov V, Arunachalam S, Venkatram A, Cook R, Naess B. 2015. A near-road modeling system for community-scale assessments of traffic-related air pollution in the united states. Environmental Modelling and Software 66:46.

Batterman S. 2013. The near-road ambient monitoring network and exposure estimates for health studies. EM Journal:24-30.

Batterman S, Burke J, Isakov V, Lewis T, Mukherjee B, Robins T. 2014a. A comparison of exposure metrics for traffic-related air pollutants: Application to epidemiology studies in detroit, michigan. International Journal of Environmental Research and Public Health 11:9553.

Batterman S, Chambliss S, Isakov V. 2014b. Spatial resolution requirements for traffic-related air pollutant exposure evaluations. Atmospheric Environment 94:518.

Batterman S, Ganguly R, Isakov V, Burke J, Arunachalam S, Snyder M, et al. 2014. Dispersion modeling of traffic-related air pollutant exposures and health effects among children with asthma in detroit, michigan. Transportation Research Record: Journal of the Transportation Research Board:105-113.

Batterman S. 2015. Temporal and spatial variation in allocating annual traffic activity across an urban region and implications for air quality assessments. Transportation Research Part D 41:401.

Batterman S, Cook R, Justin T. 2015. Temporal variation of traffic on highways and the development of accurate temporal allocation factors for air pollution analyses. Atmospheric Environment 107:351.

Batterman S, Cook R, Justin T. 2015a. Temporal variation of traffic on highways and the development of accurate time allocation factors for air pollution analyses Atmospheric Environment 107:351-363.

Batterman S, Ganguly R, Harbin P. 2015b. High resolution spatial and temporal mapping of traffic-related air pollutants. International Journal of Environmental Research and Public Health 12:3646.

Beelen R, Hoek G, Fischer P, van den Brandt PA, Brunekreef B. 2007. Estimated long-term outdoor air pollution concentrations in a cohort study. Atmospheric Environment 41:1343-1358.

Beelen R, Hoek G, Pebesma E, Vienneau D, de Hoogh K, Briggs DJ. 2009. Mapping of background air pollution at a fine spatial scale across the european union. Science of the Total Environment 407:1852.

Beelen R, Voogt M, Duyzer J, Zandveld P, Hoek G. 2010. Comparison of the performances of land use regression modelling and dispersion modelling in estimating small-scale variations in long-term air pollution concentrations in a dutch urban area. Atmospheric Environment 44:4614.

Beevers SD, Kitwiroon N, Williams ML, Carslaw DC. 2012. One way coupling of cmaq and a road source dispersion model for fine scale air pollution predictions. Atmospheric Environment 59:47.

Beevers SD, Kitwiroon N, Williams ML, Kelly FJ, Anderson HR, Carslaw DC. 2013. Air pollution dispersion models for human exposure predictions in London. Journal of exposure science and environmental epidemiology 23:647.

Beevers SD, Kitwiroon N, Williams ML, Kelly FJ, Ross Anderson H, Carslaw DC. 2013. Air pollution dispersion models for human exposure predictions in london. Journal of Exposure Science & Environmental Epidemiology 23:647.

Bell ML, Morgenstern RD, Harrington W. 2011. Quantifying the human health benefits of air pollution policies: Review of recent studies and new directions in accountability research. Environ Sci Policy 14:357-368.

Benson PE. 1989. A dispersion model for predicting air pollutant concentrations near roadways: Report no. Fhwa/ca/tl-84/15. Sacramento, CA:Office of Transportation Laboratory, California Department of Transportation.

Berrocal VJ, Gelfand AE, Holland DM. 2010a. A bivariate space-time downscaler under space and time misalignment. Annals of Applied Statistics 4:1942-1975.

Berrocal VJ, Gelfand AE, Holland DM. 2010b. A spatio-temporal downscaler for outputs from numerical models. Journal of Agricultural, Biological and Environmental Statistics 15:176-197.

Bliznyuk N, Paciorek CJ, Schwartz J, Coull B, others. 2014. Nonlinear predictive latent process models for integrating spatio-temporal exposure data from multiple sources. Annals of Applied Statistics 8:1538-1560.

Bornn L, Shaddick G, Zidek JV. 2012. Modeling nonstationary processes through dimension expansion. Journal of the American Statistical Association 107:281-289.

Brauer M. 2010. How much, how long, what, and where: Air pollution exposure assessment for epidemiologic studies of respiratory disease. Proceedings of the American Thoracic Society 7:111.

Briggs DJ, de Hoogh C, Gulliver J, Wills J, Elliott P, Kingham S, et al. 2000. A regression-based method for mapping traffic-related air pollution: Application and testing in four contrasting urban environments. Science of the Total Environment 253:151-167.

Brook RD, Jerrett M, Brook JR, Bard RL, Finkelstein MM. 2008. The relationship between diabetes mellitus and traffic-related air pollution. Journal of Occupational and Environmental Medicine 50:32-38.

Calder CA, Holloman C, Higdon D. 2002. Exploring space-time structure in ozone concentration using a dynamic process convolution model. Case studies in Bayesian Statistics Volume VI.

Calder CA. 2007. Dynamic factor process convolution models for multivariate space-time data with application to air quality assessment. Environmental and Ecological Statistics 14:229-247.

Calder CA. 2008. A dynamic process convolution approach to modeling ambient particulate matter concentrations. Environmetrics 19:39-48.

Canagaratna MR, Onasch TB, Wood EC, Herndon SC, Jayne JT, Cross ES, et al. 2010. Evolution of vehicle exhaust particles in the atmosphere. Journal of the Air & Waste Management Association 60:1192.

Chang JC, Hanna SR. 2004. Air quality model performance evaluation. Meteorology and Atmospheric Physics 87:167.

Chang SY, Vizuete W, Valencia A, Naess B, Isakov V, Palma T, et al. 2015a. A modeling framework for characterizing near-road air pollutant concentration at community scales. Science of the Total Environment 538:905.

Chang SY, WilliamVizuete, Valencia A, Naess B, Isakov V, Palma T, et al. 2015b. A modeling framework for characterizing near-road air pollutant concentration at community scales. Science of the Total Environment.

Chart-asa C, Gibson JM. 2015. Health impact assessment of traffic-related air pollution at the urban project scale: Influence of variability and uncertainty. Science of the Total Environment 506-507:409.

Choi J, Fuentes M, Reich BJ. 2009. Spatial-temporal association between fine particulate matter and daily mortality. Computational Statistics & Data Analysis 53:2989-3000.

Cimorelli AJ, Perry SG, Venkatram A, Weil JC, Paine RJ, Wilson RB, et al. 2004. Aermod: A dispersion model for industrial source applications. Part i: General model formulation and boundary layer characterization. Journal of Applied Meteorology.

Cressie NAC. 1993. Statistics for spatial data, 2nd edition:Wiley.

Crooks JL, Özkaynak H. 2014. Simultaneous statistical bias correction of multiple pm$_2.5$ species from a regional photochemical grid model. Atmospheric Environment 95:126-141.

Damian D, Sampson PD, Guttorp P. 2001. Bayesian estimation of semi-parametric non-stationary spatial covariance structures. Environmetrics 12:161-178.

de Hoogh K, Korek M, Vienneau D, Keuken M, Kukkonen J, Nieuwenhuijsen MJ, et al. 2014. Comparing land use regression and dispersion modelling to assess residential exposure to ambient air pollution for epidemiological studies. Environment International 73:382.

De Iaco S, Posa D. 2012. Predicting spatio-temporal random fields: Some computational aspects. Computational Geosciences 41:12-24.

Decker S, Suhrbier J, Rhoades K, Weinblat H, Brooks G, Dickson E. 1996. Use of locality-specific transportation data for the development of mobile source emission inventories. In Emissions Inventory Improvement Program (EIIP) Technical Report Series: Mobile Sources (Volume IV, Chapter 2); Cambridge Systematics, Inc: Oakland, CA, USA.

Dennis R, Fox T, Fuentes M, Gilliland A, Hanna S, Hogrefe C, et al. 2010. A framework for evaluating regional-scale numerical photochemical modeling systems. Environmental fluid mechanics 10:471-489.

Dionisio KL, Baxter LK, Burke J, Özkaynak H. 2016. The importance of the exposure metric in air pollution epidemiology studies: When does it matter, and why? Air Quality, Atmosphere & Health 9:495.

Dons E, Van Poppel M, Kochan B, Wets G, Panis LI. 2013. Modeling temporal and spatial variability of traffic-related air pollution: Hourly land use regression models for black carbon. Atmospheric Environment 74:237-246.

Dorn JG, Cooley DM, Huntley R. Epa's particulate matter augmentation tool: Autmating quality assurance and pm speciation to generate a model-ready inventory. In: Proceedings of the 12th Annual CMAS Conference, 2013. Chapel Hill, NC.

English P, Neutra R, Scalf R, Sullivan M, Waller L, Zhu L. 1999. Examining associations between childhood asthma and traffic flow using a geographic information system. Environmental Health Perspectives 107:761.

Escamilla-Nuñez M-C, Barraza-Villarreal A, Hernandez-Cadena L, Moreno-Macias H, Ramirez-Aguilar M, Sienra-Monge J-J, et al. 2008. Traffic-related air pollution and respiratory symptoms among asthmatic children, resident in Mexico City: The Eva cohort study. Respiratory Research 9:74-85.

Fanshawe TR, Diggle PJ, Rushton S, Sanderson R, Lurz PWW, Glinianaia SV, et al. 2008. Modelling spatio-temporal variation in exposure to particulate matter: A two-stage approach. Environmetrics 19:549-566.

Finkelstein MM, Jerrett M, DeLuca P, Finkelstein N, Verma DK, Chapman K, et al. 2003. Relation between income, air pollution and mortality: A cohort study. Canadian Medical Association Journal 169:397-402.

Fuentes M. 2001. A high frequency kriging approach for non-stationary environmental processes. Environmetrics 12:469-483.

Fuentes M, Smith RL. 2001. A new class of nonstationary spatial models. Raleigh, NC:North Carolina State University.

Fuentes M, Chen L, Davis JM, Lackmann GM. 2005. Modeling and predicting complex space-time structures and patterns of coastal wind fields. Environmetrics 16:449-464.

Fuentes M, Raftery AE. 2005. Model evaluation and spatial interpolation by bayesian combination of observations with outputs from numerical models. Biometrics 66:36-45.

Fujita EM, Campbell DE, Zielinska B, Chow JC, Lindhjem CE, DenBleyker A, et al. 2012. Comparison of the moves2010a, mobile6.2, and emfac2007 mobile source emission models with on-road traffic tunnel and remote sensing measurements. Journal of the Air & Waste Management Association 62:1134.

Ganguly R, Broderick BM. 2008. Performance evaluation and sensitivity analysis of the general finite line source model for CO concentrations adjacent to motorways: A note. Transportation Research Part D: Transport and Environment 13:198-205.

Ganguly R, Batterman S. 2014. Effect of geocoding errors on traffic-related air pollutant concentration estimates. submittted.

Gehring U, Cyrys J, Sedlmeir G, Brunekreef B, Bellander T, Fischer P, et al. 2002. Traffic-related air pollution and respiratory health during the first 2 years of life. European Respiratory journal 19:690-698.

Gentner DR, Jathar SH, Gordon TD, Bahreini R, Day DA, El Haddad I, et al. 2017. Review of urban secondary organic aerosol formation from gasoline and diesel motor vehicle emissions. Environmental Science & Technology 51:1074.

Giambini P, Salizzoni P, Soulhac L, Corti A. 2012. Influence of meteorological input parameters on urban dispersion modelling for traffic scenario analysis. In: Air pollution modeling and its application xxi, (Steyn DG, Trini Castelli S, eds). Dordrecht:Springer Netherlands, 453-457.

Gilani O, McKay LA, Gregoire TG, Guan Y, Leaderer BP, Holford TR. 2016. Spatiotemporal calibration and resolution refinement of output from deterministic models. Statistics in Medicine 35:2422-2440.

Grigoratos T, Martini G. 2015. Brake wear particle emissions: A review. Environmental Science and Pollution Research 22:2491.

Gryparis A, Coull BA, Schwartz J, Suh HH. 2007. Semiparametric latent variable regression models for spatiotemporal modelling of mobile source particles in the greater boston area. Journal of the Royal Statistical Society: Series C (Applied Statistics) 56:183-209.

Gurram S, Stuart AL, Pinjari AR. 2015. Impacts of travel activity and urbanicity on exposures to ambient oxides of nitrogen and on exposure disparities. Air Quality, Atmosphere & Health 8:97.

Hagler GSW, Baldauf RW, Thoma ED, Long TR, Snow RF, Kinsey JS, et al. 2009. Ultrafine particles near a major roadway in raleigh, north carolina: Downwind attenuation and correlation with traffic-related pollutants. Atmospheric Environment 43:1229-1234.

Hanna S, Chang J. 2012. Acceptance criteria for urban dispersion model evaluation. Meteorology and Atmospheric Physics 116:133.

Hannam K, McNamee R, De Vocht F, Baker P, Sibley C, Agius R. 2013. A comparison of population air pollution exposure estimation techniques with personal exposure estimates in a pregnant cohort. Environmental Sciences: Processes and Impacts 15:1562.

Health Effects Institute. 2010. Traffic-related air pollution: A critical review of the literature on emissions, exposure, and health effect. Boston, MA:HEI.

Heist D, Isakov V, Perry S, Snyder M, Venkatram A, Hood C, et al. 2013. Estimating near-road pollutant dispersion: A model inter-comparison. Transportation Research Part D: Transport and Environment 25:93-105.

Heist D, Isakov V, Perry S, Snyder M, Venkatram A, Hood C, et al. 2013. Estimating near-road pollutant dispersion: A model inter-comparison. Transport Res D-Tr E 25:93.

Henderson SB, Beckerman B, Jerrett M, Brauer M. 2007. Application of land use regression to estimate long-term concentrations of traffic-related nitrogen oxides and fine particulate matter. Environmental Science & Technology 41:2422-2428.

Higdon D. 1998. A process-convolution approach to modelling temperatures in the north atlantic ocean. Environmental and Ecological Statistics 5:173-190.

Higdon D, Swall J, Kern J. 1999. Non-stationary spatial modeling. Bayesian Statistics.

Higdon D. 2002. Space and space-time modeling using process convolutions. Quantitative Methods for Current Environmental Issues.

Hitchins J, Morawska L, Wolff R, Gilbert D. 2000. Concentrations of submicrometre particles from vehicle emissions near a major road. Atmospheric Environment 34:51-59.

Hoek G, Brunekreef B, Goldbohm S, Fischer P, van den Brandt PA. 2002. Association between mortality and indicators of traffic-related air pollution in the netherlands: A cohort study. The Lancet 360:1203-1209.

Hoek G, Beelen R, de Hoogh K, Vienneau D, Gulliver J, Fischer P, et al. 2008a. A review of land-use regression models to assess spatial variation of outdoor air pollution. Atmospheric Environment 42:7561.

Hoek G, Beelen R, de Hoogh K, Vienneau D, Gulliver J, Fischer P, et al. 2008b. A review of land-use regression models to assess spatial variation of outdoor air pollution. Atmospheric Environment 42:7561-7568.

Holland DM, Saltzman N, Cox LH, Nychka D. 1999. Spatial prediction of sulfur dioxide in the eastern united states. geoENV II - Geostatistics for Environmental Applications.

Houyoux MR, Vukovich JM, Coats CJ, Wheeler NJM, Kasibhatla PS. 2000. Emission inventory development and processing for the seasonal model for regional air quality (smraq) project. Journal of Geophysical Research 105:9079.

Hu SS, Fruin S, Kozawa K, Mara S, Paulson SE, Winer AM. 2009. A wide area of air pollutant impact downwind of a freeway during pre-sunrise hours. Atmospheric Environment 43:2541-2549.

Huang Y-L, Batterman S. 2000. Residence location as a measure of environmental exposure: A review of air pollution epidemiology studies. Journal of Exposure Analysis and Environmental Epidemiology 10:66.

Huang YL, Batterman S. 2000. Residence location as a measure of environmental exposure: A review of air pollution epidemiology studies. J Expo Anal Environ Epidemiol 10:66-85.

Huo H, Zhang Q, He K, Wang Q, Yao Z, Streets DG. 2009. High-resolution vehicular emission inventory using a link-based method: A case study of light-duty vehicles in beijing. Environmental Science and Technology 43:2394.

Hystad P, Demers PA, Johnson KC, Brook J, Van Donkelaar A, Lamsal L, et al. 2012. Spatiotemporal air pollution exposure assessment for a canadian population-based lung cancer case-control study. Environmental Health: A Global Access Science Source 11:22.

Ingebrigtsen R, Lindgren F, Steinsland I. 2014. Spatial models with explanatory variables in the dependence structure. Spatial Statistics 8:20-38.

Isakov V, Touma JS, Burke J, Lobdell DT, Palma T, Rosenbaum A, et al. 2009. Combining regional- and local-scale air quality models with exposure models for use in environmental health studies. Journal of the Air & Waste Management Association 59:461-472.

Isakov V, Arunachalam S, Batterman S, Bereznicki S, Burke J, Dionisio K, et al. 2014. Air quality modeling in support of the near-road exposures and effects of urban air pollutants study (nexus). Int J Environ Res Public Health 11:8777-8793.

Isakov V, Barzyk T, Arunachalam S, Snyder M, Venkatram A. 2016. A community-scale modeling system to assess port-related air quality impacts.385-390.

Jerrett M, Arain A, Kanaroglou P, Beckerman B, Potoglou D, Sahsuvaroglu T, et al. 2005. A review and evaluation of intraurban air pollution exposure models. Journal of Exposure Analysis and Environmental Epidemiology 15:185.

Jerrett M, Arain MA, Kanaroglou P, Beckerman B, Crouse D, Gilbert NL, et al. 2007. Modeling the intraurban variability of ambient traffic pollution in toronto, canada. Journal of Toxicology and Environmental Health, Part A 70:200.

Jerrett M, Finkelstein MM, Brook JR, Arain MA, Kanaroglou P, Stieb DM, et al. 2009. A cohort study of traffic-related air pollution and mortality in toronto, ontario, canada. Environmental Health Perspectives 117:772-777.

Karner AA, Eisinger DS, Niemeier DA. 2010. Near-roadway air quality: Synthesizing the findings from real-world data. Environ Sci Technol 44:5334-5344.

Katzfuss M. 2013. Bayesian nonstationary spatial modeling for very large datasets. Environmetrics 24:189-200.

Kendrick CM, Koonce P, George LA. 2015. Diurnal and seasonal variations of no, no2 and pm2.5 mass as a function of traffic volumes alongside an urban arterial. Atmospheric Environment 122:133-141.

Kennedy D, Bates RR. 1987. Air pollution, the automobile, and public health:National Academies Press.

Kimbrough S, Shores RC, Whitaker DA, Vallero DA. 2013. Fhwa and epa national near-road study, detroit, mi. Research Triangle Park, NC 27711

Kumar P, Ketzel M, Vardoulakis S, Pirjola L, Britter R. 2011. Dynamics and dispersion modelling of nanoparticles from road traffic in the urban atmospheric environment—a review. Journal of Aerosol Science 42:580.

Künzli N, Jerrett M, Mack WJ, Beckerman B, LaBree L, Gilliland F, et al. 2005. Ambient air pollution and atherosclerosis in los angeles. Environmental Health Perspectives 113:201-206.

Levitin J, Härkönen J, Kukkonen J, Nikmo J. 2005. Evaluation of the caline4 and car-fmi models against measurements near a major road. Atmospheric Environment 39:4439-4452.

Lindgren F, Rue Ha, Lindström J. 2011. An explicit link between gaussian fields and gaussian markov random fields: The stochastic partial differential equation approach. Journal of the Royal Statistical Society: Series B (Statistical Methodology) 73:423-498.

Lindhjem CE, Pollack AK, DenBleyker A, Shaw SL. 2012. Effects of improved spatial and temporal modeling of on-road vehicle emissions. Journal of the Air & Waste Management Association 62:471.

Lindstrom J, Szprio AA, Sampson PD, Oron AP, Richards M, Larson TV, et al. 2014. A flexible spatio-temporal model for air pollution with spatial and spatio-temporal covariates. Environmental and Ecological Statistics 21:411-433.

Lippmann M. 2013. Exposure science in the 21st century: A vision and a strategy. Journal of Exposure Science and Environmental Epidemiology 23:1.

Lobdell DT, Isakov V, Baxter L, Touma JS, Smuts MB, Ozkaynak H. 2011. Feasibility of assessing public health impacts of air pollution reduction programs on a local scale: New haven case study. Environmental Health Perspectives 119:487-493.

Madsen C, Carlsen KCL, Hoek G, Oftedal B, Nafstad P, Meliefste K, et al. 2007. Modeling the intra-urban variability of outdoor traffic pollution in oslo, norway - a ga 2 len project. Atmospheric Environment 41:7500-7511.

Matsuo T, Nychka DW, Paul D. 2011. Nonstationary covariance modeling for incomplete data: Monte carlo em approach. Computational Statistics & Data Analysis 55:2059-2073.

McMillan NJ, Holland DM, Morara M, Feng J. 2010. Combining numerical model output and particulate data using Bayesian space-time modeling. Environmetrics 21:48-65.

Michelle W, Beate R. 2005. Local variations in co and particulate air pollution and adverse birth outcomes in los angeles county, california, USA. Environmental Health Perspectives 113:1212.

Michigan Department of Environmental Quality. 2014. Michigan air emissions reporting system (maers) annual pollutant totals query.Michigan Department of Environmental Quality.

Michigan Department of Environmental Quality. 2015. Proposed sulfur dioxide one-hour national ambient air quality standard state implementation plan.Michigan Department of Environmental Quality.

Michigan Department of Environmental Quality. 2016. Meteorological data.Michigan Department of Environmental Quality.

Michigan Department of Transportation. Annual traffic volumes.Michigan Department of Transportation.

Michigan Department of Transportation. 2016. Traffic monitoring information system (tmis).Michigan Department of Transportation.

Milando C, Huang L, Batterman S. 2016. Trends in pm2.5 emissions, concentrations and apportionments in detroit and chicago. Atmospheric Environment 129:197.

Molitor J, Jerrett M, Chang CC, Molitor NT, Gauderman J, Berhane K, et al. 2007. Assessing uncertainty in spatial exposure models for air pollution health effects assessment. Environmental Health Perspectives 115:1147-1153.

Montagne DR, Hoek G, Klompmaker JO, Wang M, Meliefste K, Brunekreef B. 2015. Land use regression models for ultrafine particles and black carbon based on short-term monitoring predict past spatial variation. Environmental Science & Technology 49:8712-8720.

Morgenstern V, Zutavern A, Cyrys J, Brockow I, Gehring U, Koletzko S, et al. 2007. Respiratory health and individual estimated exposure to traffic-related air pollutants in a cohort of young children. Occupational and Environmental Medicine 64:8-16.

Myung CL, Park S. 2011. Exhaust nanoparticle emissions from internal combustion engines: A review. International Journal of Automotive Technology 13:9.

Naeher LP, Holford TR, Beckett WS, Belanger K, Triche EW, Bracken MB, et al. 1999. Healthy women's PEF variations with ambient summer concentrations of PM_{10}, $PM_{2.5}$, SO_4^{2-}, H+, and O_3. American Journal of Respiratory and Critical Care Medicine 160:117-125.

National Research C, Committee on Environmental Epidemiolgy NR, National Academy of S. 1997. Environmental epidemiology, volume 2:National Academies Press.

Neto JHV, Schmidt AM, Guttorp P. 2014. Accounting for spatially varying directional effects in spatial covariance structures. Journal of the Royal Statistical Society: Series C (Applied Statistics) 63:103-122.

North American Research Strategy for Tropospheric Ozone. 2005. Improving emission inventories for effective air quality management across north america, narsto 05-001. In: NARSTO 05-001.

Nychka D, Wikle C, Royle JA. 2002. Multiresolution models for nonstationary spatial covariance functions. Statistical Modelling 2:315-331.

Oettl D, Kukkonen J, Almbauer RA, Sturm PJ, Pohjola M, Harkonen J. 2001. Evaluation of a gaussian and a lagrangian model against a roadside data set, with emphasis on low wind speed conditions. Atmospheric Environment 35:2123-2132.

Özkaynak H, Baxter LK, Dionisio KL, Burke J. 2013. Air pollution exposure prediction approaches used in air pollution epidemiology studies. Journal of Exposure Science & Environmental Epidemiology 23:566.

Pachón JE, Saavedra C, Pérez MP, Galvis BR, Arunachalam S. 2016. Exposure assessment to high-traffic corridors in bogota using a near-road air quality model. In: Influence of ammonia emissions on aerosol formation in northern and central europe. London:Springer International Publishing,, 403-407.

Paciorek CJ, Schervish MJ. 2006. Spatial modelling using a new class of nonstationary covariance functions. Environmetrics 17:483-506.

Paciorek CJ, Yanosky JD, Puett RC, Suh HH. 2009. Practical large-scale spatio-temporal modeling of particulate matter concentrations. Annals of Applied Statistics 3:370-397.

Padró-Martínez LT, Patton AP, Trull JB, Zamore W, Brugge D, Durant JL. 2012. Mobile monitoring of particle number concentration and other traffic-related air pollutants in a near-highway neighborhood over the course of a year. Atmospheric Environment 61:253.

Pant P, Harrison RM. 2013. Estimation of the contribution of road traffic emissions to particulate matter concentrations from field measurements: A review. Atmospheric Environment 77:78.

Parrish DD. 2006. Critical evaluation of us on-road vehicle emission inventories. Atmospheric Environment 40:2288.

Patel MM, Chillrud SN, Correa JC, Feinberg M, Hazi Y, Deepti KC, et al. 2009. Spatial and temporal variations in traffic-related particulate matter at New York City high schools. Atmospheric Environment 43:4975.

Patton AP, Milando C, Durant JL, Kumar P. 2017. Assessing the suitability of multiple dispersion and land use regression models for urban traffic-related ultrafine particles. Environmental Science & Technology 51:384.

Pikhart H, Bobak M, Gorynski P, Wojtyniak B, Danova J, Celko MA, et al. 2001. Outdoor sulphur dioxide and respiratory symptoms in Czech and Polish school children: A small-area study (SAVIAH). International Archives of Occupational and Environmental Health 74:574-578.

Pintore A, Holmes CC. 2005. A dimension-reduction approach for spectral tempering using empirical orthogonal functions. Geostatistics Banff 2004.

Puett RC, Hart JE, Yanosky JD, Paciorek C, Schwartz J, Suh H, et al. 2009. Chronic fine and coarse particulate exposure, mortality, and coronary heart disease in the nurses' health study. Environmental Health Perspectives 117:1697-1701.

Querol X, Alastuey A, Ruiz CR, Artiñano B, Hansson HC, Harrison RM, et al. 2004. Speciation and origin of pm10 and pm2.5 in selected european cities. Atmospheric Environment 38:6547.

Rao ST, Sistla G, Keenan MT, Wilson JS. 1980. An evaluation of some commonly used highway dispersion models. Journal of the Air Pollution Control Association 30:239-246.

Reich BJ, Eidsvik J, Guindani M, Nail AJ, Schmidt AM. 2011. A class of covariate-dependent spatiotemporal covariance functions for the analysis of daily ozone concentration. Annals of Applied Statistics 5:2425-2447.

Reich BJ, Chang HH, Foley KM. 2014. A spectral method for spatial downscaling. Biometrics 70:932-942.

Rémy S, Verena M, Josef C, Anne Z, Olf H, Heinz-Erich W, et al. 2007. Traffic-related atmospheric pollutants levels during pregnancy and offspring's term birth weight: A study relying on a land-use regression exposure model. Environmental Health Perspectives 115:1283.

Reponen T, Grinshpun SA, Trakumas S, Martuzevicius D, Wang ZM, LeMasters G, et al. 2003. Concentration gradient patterns of aerosol particles near interstate highways in the greater cincinnati airshed. J Environ Monit 5:557-562.

Rioux CL, Gute DM, Brugge D, Peterson S, Parmenter B. 2010. Characterizing urban traffic exposures using transportation planning tools: An illustrated methodology for health researchers. Journal of urban health : bulletin of the New York Academy of Medicine 87:167.

Risser MD, Calder CA. 2015. Regression-based covariance functions for nonstationary spatial modeling. Environmetrics 26:284-297.

Rundel CW, Schliep EM, Gelfand AE, Holland DM. 2015. A data fusion approach for spatial analysis of speciated $PM_{2.5}$ across time. Environmetrics 26:515-525.

Ryan PH, LeMasters GK. 2007. A review of land-use regression models for characterizing intraurban air pollution exposure. Inhalation Toxicology 19:127.

Sahu SK, Gelfand AE, Holland DM. 2006. Spatio-temporal modeling of fine particulate matter. Journal of Agricultural, Biological, and Environmental Statistics 11:61-86.

Samaranayake S, Glaser S, Holstius D, Monteil J, Tracton K, Seto E, et al. 2014. Real-time estimation of pollution emissions and dispersion from highway traffic. Computer-Aided Civil and Infrastructure Engineering 29:546.

Sampson PD, Guttorp P. 1992. Nonparametric estimation of nonstationary spatial covariance structure. Journal of the American Statistical Association 87:108-119.

Sarnat SE, Klein M, Sarnat JA, Flanders WD, Waller LA, Mulholland JA, et al. 2010. An examination of exposure measurement error from air pollutant spatial variability in time-series studies. Journal of Exposure Science and Environmental Epidemiology 20:135.

Schmidt AM, Gelfand AE. 2003. A bayesian coregionalization approach for multivariate pollutant data. Journal of Geophysical Research: Atmospheres (1984-2012) 108.

Schmidt AM, O'Hagan A. 2003. Bayesian inference for non-stationary spatial covariance structure via spatial deformations. Journal of the Royal Statistical Society: Series B (Statistical Methodology) 65:743-758.

Schmidt AM, Guttorp P, O'Hagan A. 2011. Considering covariates in the covariance structure of spatial processes. Environmetrics 22:487-500.

Sheppard L, Burnett RT, Szpiro AA, Kim S-Y, Jerrett M, Pope Iii CA, et al. 2012. Confounding and exposure measurement error in air pollution epidemiology. Air Quality, Atmosphere & Health 5:203.

Shi JP, Khan A, Harrison RM. 1999. Measurements of ultrafine particle concentration and size distribution in the urban atmosphere. Science of the Total Environment 235:51-64.

Smith RL, Kolenikov S, Cox LH. 2003. Spatio-temporal modeling of $PM_{2.5}$ data with missing values. Journal of Geophysical Research 108.

Snyder M, Arunachalam S, Isakov V, Heist D, Batterman S, Talgo K, et al. Sensitivity analysis of dispersion model results in the nexus health study due to uncertainties in traffic-related emissions inputs. In: Proceedings of the Air & Waste Management Association Annual Conference & Exhibition, 2013 2013. June 25-28th, 2013.

Snyder M, Arunachalam S, Isakov V, Talgo K, Naess B, Valencia A, et al. 2014. Creating locally-resolved mobile-source emissions inputs for air quality modeling in support of an exposure study in detroit, michigan, USA. International Journal of Environmental Research and Public Health 11:12739.

Snyder MG, Venkatram A, Heist DK, Perry SG, Petersen WB, Isakov V. 2013. Rline: A line source dispersion model for near-surface releases. Atmospheric Environment 77:748-756.

Solomon P, Cumpler D, Flanagan JB, Jayanty RKM, Rickman JEE, Dade C. 2014. United states national pm2.5 chemical speciation monitoring networks - csn and improve: Description of networks. Journal of Air and Waste Management Association 64:1410-1438.

Son J-Y, Bell ML, Lee J-T. 2010. Individual exposure to air pollution and lung function in Korea: Spatial analysis using multiple exposure approaches. Environmental Research 110:739-749.

Southeast Michigan Council of Governments (SEMCOG). 2011. On-road mobile source emissions inventory for southeast michigan $PM_{2.5}$ redesignation request. Southeast Michigan Council of Governments.

Stedman JR, Vincent KJ, Campbell GW, Goodwin JW, Downing CE. 1997. New high resolution maps of estimated background ambient NO_x and NO_2 concentrations in the UK. Atmospheric Environment 31:3591-3602.

Stieb DM, Chen L, Hystad P, Beckerman BS, Jerrett M, Tjepkema M, et al. 2016. A national study of the association between traffic-related air pollution and adverse pregnancy outcomes in Canada, 1999–2008. Environmental Research 148:513.

Stroh E, Harrie L, Gustafsson S. 2007. A study of spatial resolution in pollution exposure modelling. International Journal of Health Geographics 6:19.

Thorpe A, Harrison RM. 2008. Sources and properties of non-exhaust particulate matter from road traffic: A review. Science of the Total Environment 400:270.

Turner JR, Allen DT. 2008. Transport of atmospheric fine particulate matter: Part 2-findings from recent field programs on the intraurban variability in fine particulate matter. Journal of the Air & Waste Management Association 58:196.

U.S. Census Bureau. 2015. Tiger/line® with selected demographic and economic data. US Census Bureau.

U.S. Environmental Protection Agency. 2000. Meteorological monitoring guidance for regulatory modeling applications epa-454/r-99-005. Research Triangle Park:Office of Air Quality Planning and Standards.

U.S. Environmental Protection Agency. 2003. User's guide to mobile6.1 and mobile6.2 mobile source emission factor model epa420-r-03-010. Washington DC.

U.S. Environmental Protection Agency. 2012. Near-road no2 monitoring technical assistance document, epa-454/b-12-002.US Environmental Protection Agency.

U.S. Environmental Protection Agency. 2013. National summary of nitrogen oxides emissions, nei 2008. Available: http://www.epa.gov/cgi-bin/broker?polchoice=NOX&_debug=0&_service=data&_program=dataprog.national_1.sas [accessed April 16 2013].

U.S. Environmental Protection Agency. 2014. National emission inventories (nei) and technical support documents.US Environmental Protection Agency.

U.S. Environmental Protection Agency. 2015a. Technical support document (TSD) for replacement of CALINE3 with AERMOD for transportation related air quality analyses., EPA-454/b-15-002. Research Triangle Park, North Carolina.

U.S. Environmental Protection Agency. 2015b. Moves 2014a user guide.US Environmental Protection Agency.

U.S. Environmental Protection Agency. 2017. Interactive map of air quality monitors. Available: https://www.epa.gov/outdoor-air-quality-data/interactive-map-air-quality-monitors 2017].

Urban N. 2014. Motor City mapping, winter 2013-14 certified results. Data Driven Detroit.

Valencia A, Venkatram A, Heist D, Carruthers D, Arunachalam S. 2018. Development and evaluation of the R-LINE model algorithms to account for chemical transformation in the near-road environment. Transportation Research Part D 59:464-477.

Van Den Hooven EH, Pierik FH, Van Ratingen SW, Zandveld PYJ, Meijer EW, Hofman A, et al. 2012. Air pollution exposure estimation using dispersion modelling and continuous monitoring data in a prospective birth cohort study in the Netherlands. Environmental Health: A Global Access Science Source 11:9.

Venkatram A, Snyder MG, Heist DK, Perry SG, Petersen WB, Isakov V. 2013. Re-formulation of plume spread for near-surface dispersion. Atmospheric Environment 77:846-855.

Vette A, Burke J, Norris G, Landis M, Batterman S, Breen M, et al. 2013. The near-road exposures and effects of urban air pollutants study (nexus): Study design and methods. Science of the Total Environment 448:38.

Wang H, Chen C, Huang C, Fu L. 2008. On-road vehicle emission inventory and its uncertainty analysis for Shanghai, China. Science of the Total Environment 398:60.

Wang M, Gehring U, Hoek G, Keuken M, Jonkers S, Beelen R, et al. 2015. Air pollution and lung function in Dutch children: A comparison of exposure estimates and associations based on land use regression and dispersion exposure modeling approaches. Environmental Health Perspectives 123:847.

Wang R, Henderson SB, Sbihi H, Allen RW, Brauer M. 2013. Temporal stability of land use regression models for traffic-related air pollution. Atmospheric Environment 64:312.

Wang YJ, Zhang KM. 2009. Modeling near-road air quality using a computational fluid dynamics model, CFD-VIT-RIT. Environmental Science and Technology 43:7778.

Wang YJ, DenBleyker A, McDonald-Buller E, Allen D, Zhang KM. 2011. Modeling the chemical evolution of nitrogen oxides near roadways. Atmospheric Environment 45:43.

Ward MH, Wartenberg D. 2006. Invited commentary: On the road to improved exposure assessment using geographic information systems. American Journal of Epidemiology 164:208.

Watkins N, Baldauf R. 2012. Near-road NO_2 monitoring technical assistance document. Research Triangle Park, NC:U.S. Environmental Protection Agency, Office of Air Quality Planning and Standards, Air Quality Assessment Division, Ambient Air Monitoring Group.

Wilson JG, Kingham S, Pearce J, Sturman AP. 2005. A review of intraurban variations in particulate air pollution: Implications for epidemiological research. Atmospheric Environment 39:6444.

Wilton D, Szpiro A, Gould T, Larson T. 2010. Improving spatial concentration estimates for nitrogen oxides using a hybrid meteorological dispersion/land use regression model in Los Angeles, CA and Seattle, WA. Science of the Total Environment 408:1120-1130.

Woodruff TJ, Parker JD, Darrow LA, Slama R, Bell ML, Choi H, et al. 2009. Methodological issues in studies of air pollution and reproductive health. Environmental Research 109:311.

Wu J, Wilhelm M, Chung J, Ritz B. 2011. Comparing exposure assessment methods for traffic-related air pollution in an adverse pregnancy outcome study. Environmental Research 111:685.

Yang B, Xu D, W., Stuart B, Deshmukh P, Snow. R, Baldauf RW, et al. 2017. On-road chemical transformation of nitrogen oxides. Submitted.

Yu CH, Fan ZH, Lioy PJ, Baptista A, Greenberg M, Laumbach RJ. 2016. A novel mobile monitoring approach to characterize spatial and temporal variation in traffic-related air pollutants in an urban community. Atmospheric Environment 141:161.

Yu H, Stuart AL. 2016. Exposure and inequality for select urban air pollutants in the Tampa Bay area. Science of the Total Environment 551-552:474.

Zhai X, Russell AG, Sampath P, Mulholland JA, Kim B-U, Kim Y, et al. 2016. Calibrating R-LINE model results with observational data to develop annual mobile source air pollutant fields at fine spatial resolution: Application in Atlanta. Atmospheric Environment 147:446-457.

Zhang K, Batterman S. 2010. Near-road air pollutant concentrations of CO and $PM_{2.5}$: A comparison of Mobile6.2/CALINE4 and generalized additive models. Atmospheric Environment 44:1740.

Zhang L-J, Zheng J-Y, Yin S-S, Peng K, Zhong L-J. 2010. Development of non-road mobile source emission inventory for the Pearl River Delta region. Huanjing Kexue/Environmental Science 31:886.

Zhang S, Wu Y, Huang R, Wang J, Yan H, Zheng Y, et al. 2016. High-resolution simulation of link-level vehicle emissions and concentrations for air pollutants in a traffic-populated eastern Asian city. Atmospheric Chemistry and Physics 16:9965.

Zheng J, Zheng Z, Zhang L, Che W, Yin S. 2009. A highly resolved temporal and spatial air pollutant emission inventory for the Pearl River Delta region, China and its uncertainty assessment. Atmospheric Environment 43:5112.

Zhu Y, Kuhn T, Mayo P, Hinds WC. 2006. Comparison of daytime and nighttime concentration profiles and size distributions of ultrafine particles near a major highway. Environ Sci Technol 40:2531-2536.

Zidek JV, Le ND, Liu Z. 2012. Combining data and simulated data for space-time fields: Application to ozone. Environmental and Ecological Statistics 19:37-56.